Fieldtrip Guidebook

Research on Arid Soils in Southern Nevada: Dust Emissions, Petrocalcic Genesis, Petrogypsic Soils and Biological Soil Crusts

Brenda J. Buck, Douglas Merkler, and Shawnalea Thai (editors)

Western Regional Cooperative Soil Survey
Western Society of Soil Science/Western Society of Crop Science
Joint Conference
Las Vegas, Nevada June 21-24, 2010

U.S. DEPARTMENT OF THE INTERIOR
BUREAU OF LAND MANAGEMENT

USDA NRCS
United States Department of Agriculture
Natural Resources Conservation Service

UNLV
UNIVERSITY OF NEVADA LAS VEGAS

NATIONAL PARK SERVICE

Valley of Fire. Photo courtesy of Doug Merkler

Welcome to the field trip. In the next 9+ hours and 180 miles, we'll explore the unique soils of this part of the Mojave Desert. From evidence of ancient climates to the activities of humans, we'll see how soils benefit, threaten, and direct current human residents of southern Nevada.

On this trip, we'll supply you with water and lunch. Feel free to bring additional snacks. Bring a hat for the sun and be prepared for short walks on easy terrain (likely in extreme heat). We hope you enjoy the trip!

Brenda J. Buck[1], Doug Merkler[2], and Shawnalea Thai[3] (editors)

[1]Professor, Dept. Geoscience, UNLV, Las Vegas NV, buckb@unlv.nevada.edu
[2] Nevada State Resource Soil Scientist, Natural Resource Conservation Service, USDA, Las Vegas NV, doug.merkler@nv.usda.gov
[3]Volunteer, UNLV & Natural Resource Conservation Service, Las Vegas NV, azn4u54@gmail.com

Cover photo: Nellis Dunes, courtesy of Rhonda Fairchild

Where we are going: Map of Fieldtrip Route

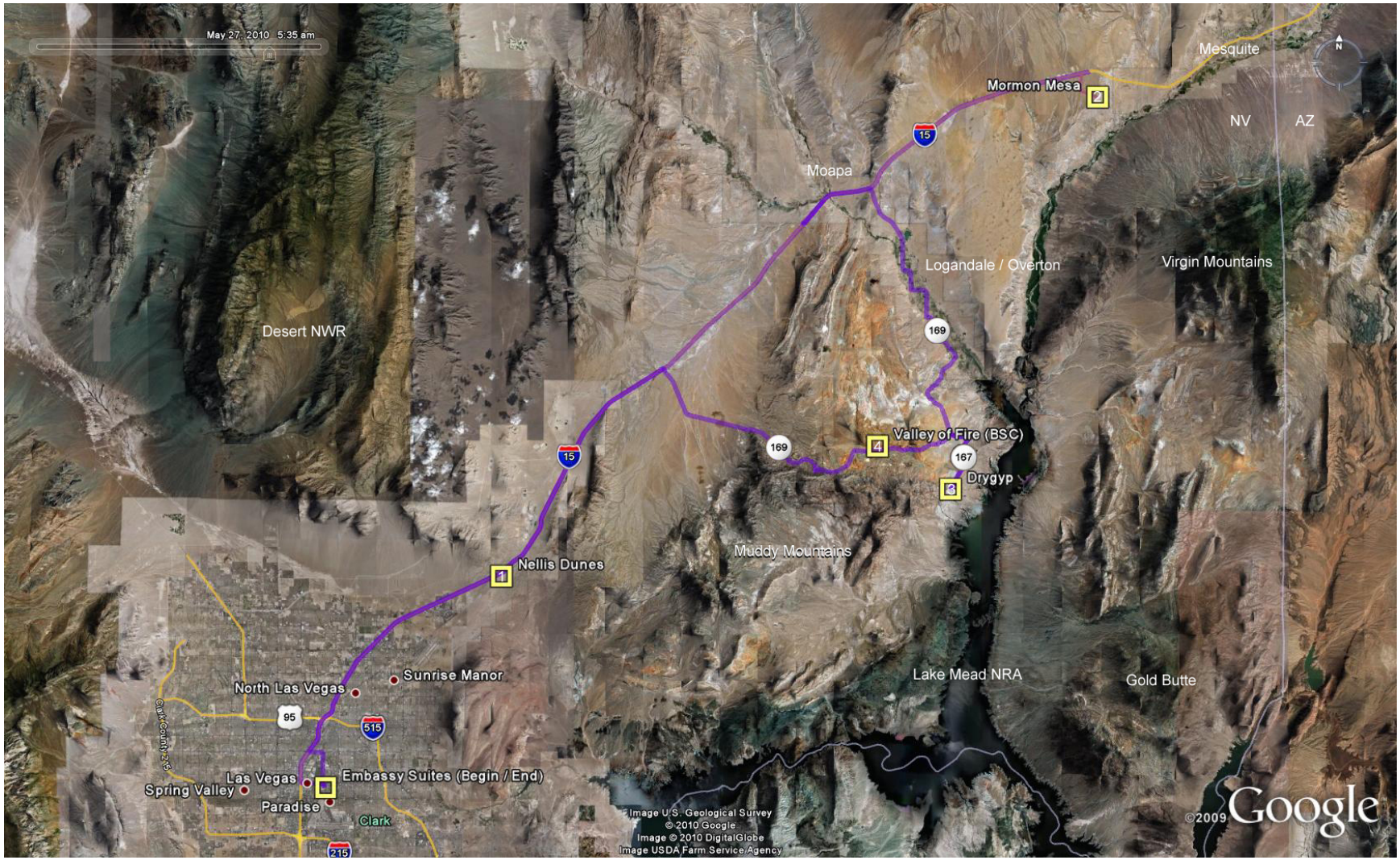

TABLE OF CONTENTS

OVERVIEW OF SCHEDULE **4**

STOP 1. NELLIS DUNES **5**

Measuring Dust Emissions, Chemistry and Mineralogy to Assess, Predict, and Manage Natural and Disturbed Land Surfaces, Nellis Dunes Recreation Area, Nevada. 5

Surficial Mapping for Managing Dust Emissions *6*

Dust Emission during ORV Driving *11*

Potential Emissions in ORV trails as Compared to Undisturbed Surfaces *14*

PM10 Concentrations over 1 year at NDRA *16*

Dust Emission and Dust Deposition by Wind Erosion *19*

Mineralogical Composition of Soil and Dust Samples, Nellis Dunes, Nevada *21*

Trace Element Chemistry of Soil and Dust Samples, Nellis Dunes, Nevada *22*

Radionuclide Characterization of Nellis Dunes Recreation Area Soils and Dust *26*

Immunotoxicological Health Effects of Acute Exposure to Dust Samples Collected from Nellis Dunes Recreational Area *27*

TRIP NOTES: WHILE DRIVING TO STOP 2 ..... **34**

Poster Child of the Mojave Desert, Creosote bush Larrea tridentata. 34

TRIP NOTES: WHILE DRIVING TO STOP 2 (CONT.) **37**

Sahara Mustard (Brassica tournefortii) 37

LOGISTICAL NOTES FOR STOP 2 ..... **38**

STOP 2. MORMON MESA **39**

Genesis of Mormon Mesa Petrocalcic Horizons: Implications for Paleoclimate and Isotopic Dating Applications 39

Appendix A: Mormon Mesa Series 53

TRIP NOTES: WHILE WAITING FOR THE NEXT SHUTTLE AT STOP 2 ..... **55**

Mediterranean grass and Red brome. 55

TRIP NOTES: WHILE DRIVING TO STOP 3 ..... **56**

Lake Mead Could Be Going Dry? 56

STOP 3: DRYGYP SOIL SERIES **58**

Drygyp Soil Series Concept: Geologic setting and source of the gypsum 58

Drygyp Soil Series: DRYGYP S04NV-003-001 ..... *60*

Drygyp Soil Series: Interpretation of Lab Data and Micromorphology 85

Edaphic Relationships of the Drygyp Soil Series: Las Vegas bearpoppy and Relict Leopard frog 90

Endolithic Cyanobacteria in Soil Gypsum: Applications for Extraterrestrial Life 93

STOP 4. VALLEY OF FIRE **100**

Biological Soil Crusts in the Mojave 100

ACKNOWLEDGMENTS **103**

Field Trip Speakers

Dr. Brenda J. Buck	Professor of Geoscience, UNLV	buckb@unlv.edu
Douglas Merkler	Resource Soil Scientist, NRCS	doug.merkler@nv.usda.gov
Dr. Dirk Goossens	Research Professor of Geosciences, UNLV	Dirk.Goossens@unlv.edu
Dr. Debra Keil	Associate Professor of Clinical Laboratory Sciences, UNLV	deborah.keil@unlv.edu
Dr. Colin Robins	Postdoc, Geosciences, UNLV	robinscolin@gmail.com
Mandy Williams	PhD Candidate, Geosciences, UNLV	willamje@unlv.nevada.edu

Our Sponsors

USDA NRCS

United States Department of Agriculture
Natural Resources Conservation Service

U.S. DEPARTMENT OF THE INTERIOR
BUREAU OF LAND MANAGEMENT

NATIONAL PARK SERVICE

UNLV
UNIVERSITY OF NEVADA LAS VEGAS

Overview of Schedule

7:15 a.m.	Find a seat on 1 of 2 buses In front of Embassy Suites		Do you have your gear for the day?
7:30 a.m.	Buses depart	Take I-15 North	
8:00 a.m.	Exit I-15 at Apex.	Turn Right (south)	Turn left into parking lot/overview of Nellis Dunes Recreation Area
8:05 a.m.	***Stop 1: Nellis Dunes***		Follow tour leaders onto mesa overlook for discussion.
9:00 a.m.	Depart Stop 1.	Continue north on I-15	See notes about sights along the drive
10:00 a.m.	Exit I-15 at east end of Mormon Mesa.	Exit bus, take shuttle buses to outcrop: Requires we break into 2 groups	
10:15 a.m.	***Stop 2: Mormon Mesa Petrocalcic***		Break into 2 groups for shuttle buses trip to outcrop
10:50 a.m.	Group 1 leave outcrop, take shuttle bus; followed by Group 2		
11:45 a.m.	Depart for Stop 3. Lunch on the buses.	Drive southwest on I-15, exit highway 169 south towards Logandale & Overton.	
12:30 p.m.	***Stop 3: Drygyp Petrogypsic***		Lake Mead National Park
12:45 p.m.	Soil pit discussion	Walk about one-third mile to soil profile. Bring water, camera, and sunglasses with you.	
1:45 pm	Walk back to buses		
2:00 p.m.	Drive north on Hw169 turn left at Valley of Fire State Park		
2:35 p.m.	Stop at Valley of Fire Visitor Center	Go straight through exhibits to back door, take the marked path uphill to lecture area for Stop 4	
2:40 p.m.	***Stop 4: Biologic Soil Crust***		Valley of Fire State Park
3:15 p.m.	Return to Buses & Depart	Take I-15 south to Las Vegas	
5:00 p.m.	Arrive	Embassy Suites	

Stop 1. Nellis Dunes

Measuring Dust Emissions, Chemistry and Mineralogy to Assess, Predict, and Manage Natural and Disturbed Land Surfaces, Nellis Dunes Recreation Area, Nevada.

Brenda J. Buck[1], Dirk Goossens[1,2], Brett McLaurin[3], Debbie Soukup[1], Deborah Keil[4], Yuanxin Teng[1], Ralf Sudowe[5], Stephen Proper[6], Margie Peden-Adams[7], Nadia Ayala[4], Jennifer Berger-Ritchie[8], Stephanie Lebahn[4], Sharon Young[9], Dirk Baron[10] and Audrey Roman[11]

[1]Deptartment of Geoscience, University of Nevada Las Vegas, Las Vegas NV, buckb@unlv.nevada.edu
[2]Department of Earth and Environmental Sciences, Katholieke Universiteit Leuven, Belgium
[3]Department of Geography and Geosciences, Bloomsburg University of Pennsylvania, Bloomsburg, PA
[4]Clinical Laboratory Sciences, University of Nevada Las Vegas, Las Vegas NV
[5]Department of Health Physics and Diagnostic Sciences & Radiochemistry Program, University of Nevada Las Vegas, Las Vegas NV
[6]School of Medicine, Michigan State University, Lansing, MI.
[7]Harry Reid Center for Environmental Studies, University of Nevada Las Vegas, Las Vegas, NV
[8]School of Community Health, University of Nevada Las Vegas, Las Vegas, NV
[9]Department of Anthropology, University of Nevada Las Vegas, Las Vegas, NV
[10]Department of Physics and Geology, California State University, Bakersfield, Bakersfield CA.
[11]Radiochemistry Program, University of Nevada Las Vegas, Las Vegas, NV

Air quality is a special concern in the Las Vegas valley, southern Nevada, USA. Las Vegas is one of the fastest-growing metropolitan areas in the United States (Lazaro et al., 2004) with approximately 1.9 million people. This year Las Vegas received a failing grade from the American Lung Association's (2010) annual "State of the Air" report. Of special concern is particulate matter, which is one of the largest problems with air quality not only in Las Vegas, but also in all desert areas worldwide.

Research into the effects of PM10 (particulates ≤ 10 microns) and PM2.5 (particulates ≤ 2.5 microns) emissions on human health increasingly show a strong link to numerous diseases and mortality including asthma, heart disease, dementia, and cancer (Besancenot et al., 1997; Lambert et al., 1999; Korenyi-Both et al., 1992; Jinadu 1995; Athar et al 1998; Komatsu et al., 2003; Ichinose et al., 2005; Griffin and Kellogg 2004; Sultan et al., 2005; Wang et al., 2008). Epidemiological studies have demonstrated that daily mortality may be attributed to cardiopulmonary and respiratory damages caused by ambient particulate matter (PM2.5; PM10) (Dockery et al., 1993; Peters et al., 1997; Laden et al., 2006). Furthermore, outdoor dust and soil are primary sources for indoor dust creating opportunities for exposure spanning infants to the elderly. In fact, studies have demonstrated a remarkable agreement between both house and outdoor dust (Fishbein 1991; Feng and Barratt 1993; Fergusson and Kim 1991; Akhter and Madany, 1993).

In addition to the negative health affects caused by the particulates, significant adverse health affects have been found to occur from airborne exposure to cadmium, lead, and arsenic (Jarup, 2003). These include cancer, hypertension, cardiovascular disease, kidney damage, diminished

intellectual capacity in children, and skeletal damage (Jarup, 2003). Naturally occurring minerals in numerous locations throughout southern Nevada contain significant quantities of these and other known hazardous elements. Therefore, dust from these sources may pose potential additional health risks beyond those induced by the particulates themselves.

In Las Vegas, large amounts of particulate matter are emitted from the desert surfaces surrounding the metropolis, either by natural processes (wind erosion) or human activities. In the city, the most dust is produced in the non-developed, but disturbed vacant lots and during construction. Also, traffic-caused re-suspension of dust accumulated on the streets is an important mechanism (Lazaro et al., 2004). Outside the city, two types of areas are known to produce dust. The first are the surfaces of dry lakes (playas) south and north of the city, which are devoid of almost any vegetation. These playas are surrounded by areas rich in sand, acting as an initiator for deflation (Shao, 2008). The second dust source near Las Vegas is Nellis Dunes Recreation Area (NDRA), a popular 36 km^2 ORV (off-road vehicle driving) destination managed by the Bureau of Land Management (BLM) that contains a dune area located just 6 km northeast of the city.

For the past forty years the NDRA has provided the only publicly accessible area in southern Nevada for legal off-road driving with annual visitors estimated at over 300,000 (Goossens and Buck, 2009a). A research project at UNLV was funded by BLM to address the concerns of how anthropogenic and natural processes at NDRA may be impacting local and regional air quality. Several manuscripts have been published or are in review (pdfs are available upon request). Currently, data show that dust emissions from NDRA are frequently blown into the Las Vegas metropolitan area, potentially affecting more than 2 million people. Listed below is only a short summary of this work:

Surficial Mapping for Managing Dust Emissions

McLaurin, Goossens, and Buck (in review)

A 1:10,000 map of the study area was produced in which units are based upon surficial characteristics that are known to affect dust emission (e.g. soil texture, rock cover, surface crusts, vegetation)(Fig. 1). This map was designed to provide a spatial dataset to use in combination with process measurements (emissions data) to better understand the distribution and controls on dust emissions. To our knowledge, this study is the first of its kind to explicitly link a detailed spatial dataset to dust emissions and dust characterization (chemistry, mineralogy, radioactivity, and health effects – see below).

Seventeen surface types were found and were grouped into 4 classes (Table 1; Fig. 1):

1. Sands and sand-affected areas: active or stabilized sands, with or without rock fragments and/or vegetation;
2. Silt/clay areas: loose and slightly stabilized silt/clay deposits, with or without rock fragments;
3. Rock-covered areas: stabilized silty or sandy silt deposits with rock fragments on top, desert pavements over a silty sublayer (Av horizon), bedrock, and/or petrocalcic horizons;
4. Drainage areas: active drainages in sand and silt areas, and gravelly drainages.

TABLE 1. GENERALIZED MAP UNIT DESCRIPTIONS

Map unit	Description	Rock fragments	Surface crust	Vegetation
Sand and sand-affected areas				
1.1	Active dunes without vegetation. Decimeter to several meters thick.	Sparse; may have exposed petrocalcic horizons	Absent	Absent
1.2	Active dunes with vegetation. Coppice dunes < 50 cm may be present.	Sparse; < 5% rock cover	Absent	Isolated shrubs
1.3	Anthropogenic disturbed sand surfaces. Typically < 2-3 cm thick loose sands overlying petrocalcic horizons or bedrock.	Common, mixed with 2-3 cm thick loose sand overlying bedrock	Absent	Absent
1.4	Patchy, shallow (1-3 cm thick), loose sand overlying silty/rocky subsoil.	Common, not interlocking, rocks in subsoil are exposed at surface.	Absent	Isolated shrubs
1.5	Very fine sand and coarse silt outcrops. Commonly badlands.	Absent	Physical	Mostly absent
Silt/clay areas				
2.1	Silt/clay outcrops with biological crust.	Sparse; < 3-4% rock cover	Biologic	Isolated shrubs
2.2	Silt/clay outcrops with gravel.	Common, < 15%, not interlocking	Physical	Usually absent
2.3	Aggregated silt deposits, Commonly badlands, aggregates < 5 mm diameter.	Absent	Physical, patchy distribution	Absent
Rock-covered areas				
3.1	Well-developed desert pavements with underlying silty Av horizon.	Abundant: Tightly interlocking rock fragments nearly 100% surface cover	Physical between rock fragments	Rare, Isolated shrubs
3.2	Rock-covered surface with silt/clay.	Many: 60-80%, poorly interlocking	Physical and biological between rock fragments	Common shrubs (10-15%)
3.3	Rock-covered surface with sandy loam.	Many: 60-80%, poorly interlocking	Physical and biological between rock fragments	Common shrubs (10-15%)
3.4	Rock-covered with encrusted sand & biological crusts.	Common: 20-30%, poorly interlocking	Biological, continuous	Common shrubs (10%)
3.5	Bedrock and/or exposed petrocalcic horizons.	Continuous rock outcrop	Absent	Rare shrubs
Active drainages				
4.1	Gravelly drainages, without fine sediment.	Abundant: 90-100%, non-interlocking gravel clasts	Absent	Absent
4.2	Gravel and sand drainages.	Abundant: 70-80% with sand mixture	Absent	Absent
4.3	Gravel and silt/clay drainages.	Common: 30-60%, poorly interlocking, with silt mixture	Physical	Common shrubs (10-30%)

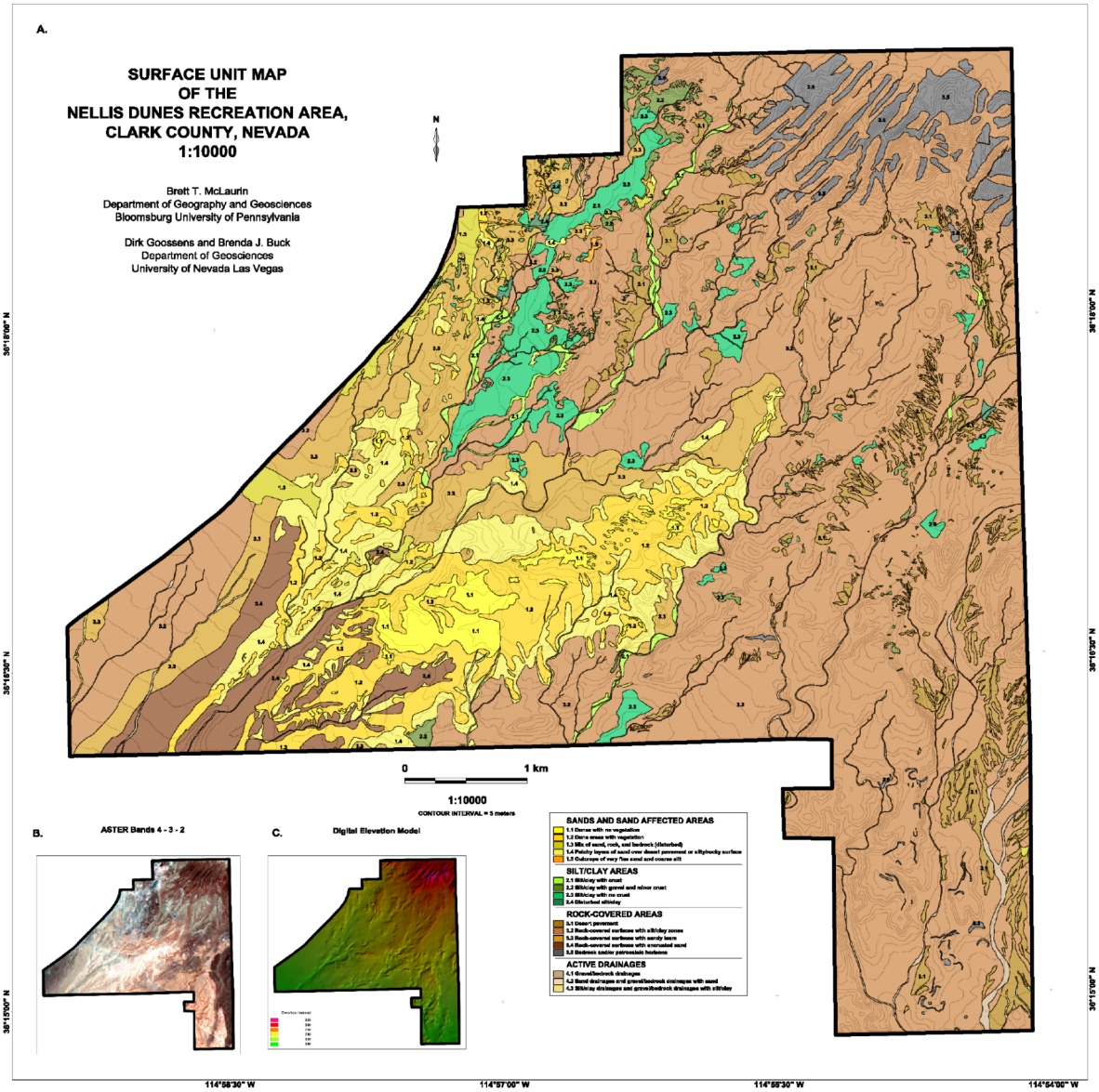

Figure. 1. Surface unit map of NDRA (McLaurin et al., in review).

Field experiments were carried out in the Nellis Dunes area to measure natural dust emissions (wind erosion) and anthropogenic dust emissions (off-road driving). These experiments are described in the next sections. Results from these studies were combined with the surface unit map to produce risk maps for natural and ORV emission in the Nellis Dunes area.

Using this data, a risk map for potential dust emission caused by natural wind erosion was created (Fig. 2). This map shows that the highest risk for dust emission due to wind erosion occurs in the sand areas (units 1.1, 1.2, 1.3, 1.4, 1.5) whereas the silt/clay areas with gravel (unit 2.2), desert pavements with Av horizons (unit 3.1), and silty drainages (unit 4.3) produce very little dust unless disturbed by human activity.

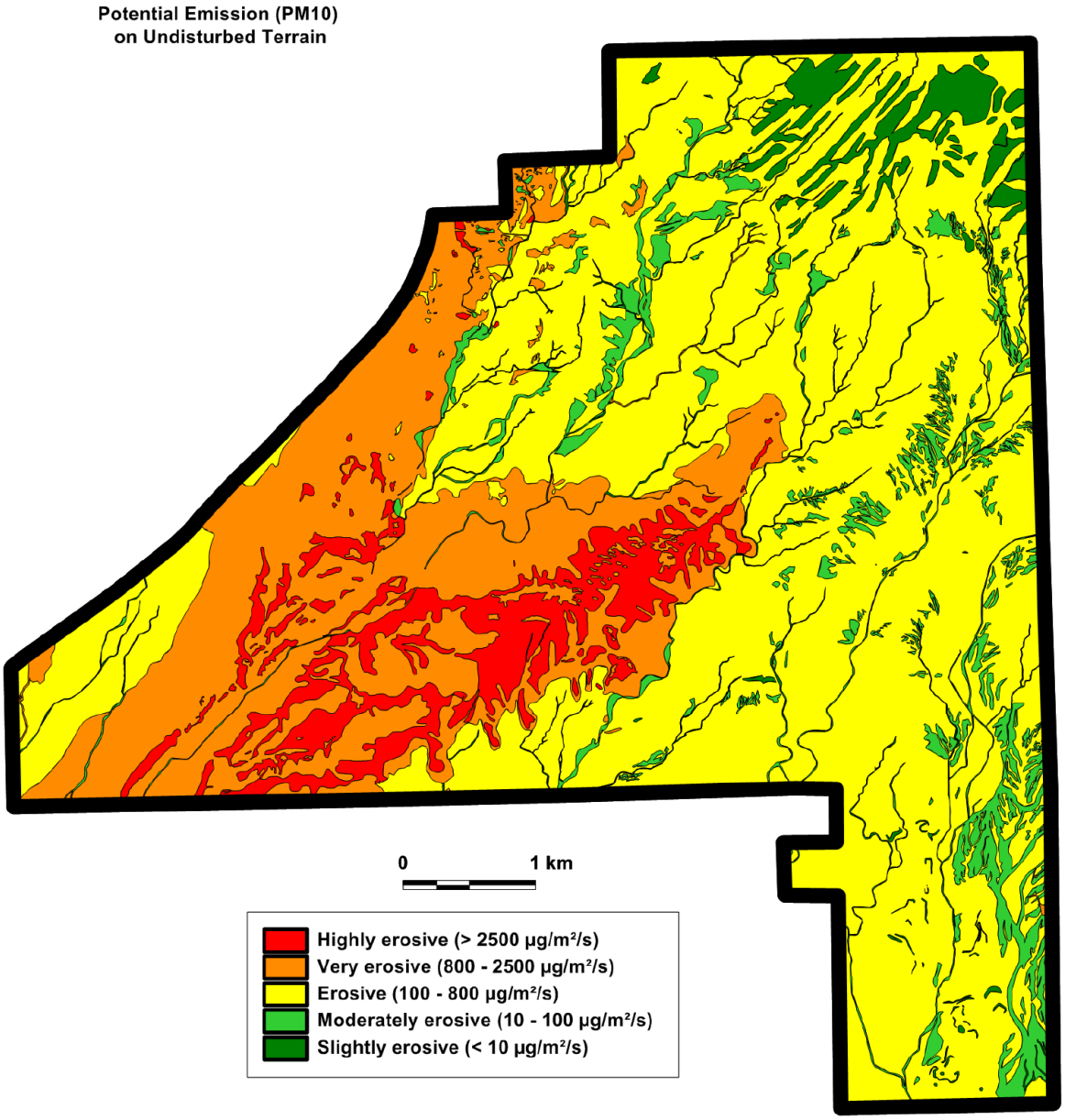

Figure. 2. Risk map for potential dust emission by wind erosion (McLauren, Goossens and Buck, unpublished map)

In contrast, a risk map for dust emission caused by ORV (Fig. 3) shows that the highest emission risk correspond to silt/clay surfaces with gravel (unit 2.2), desert pavements with Av horizons (unit 3.1) and silty drainages (unit 4.3). The least risky units are the sand areas (units 1.1, 1.2, 1.3, 1.4, 1.5, 3.4), the non-silty drainages (4.1, 4.2) and bedrock (3.5).

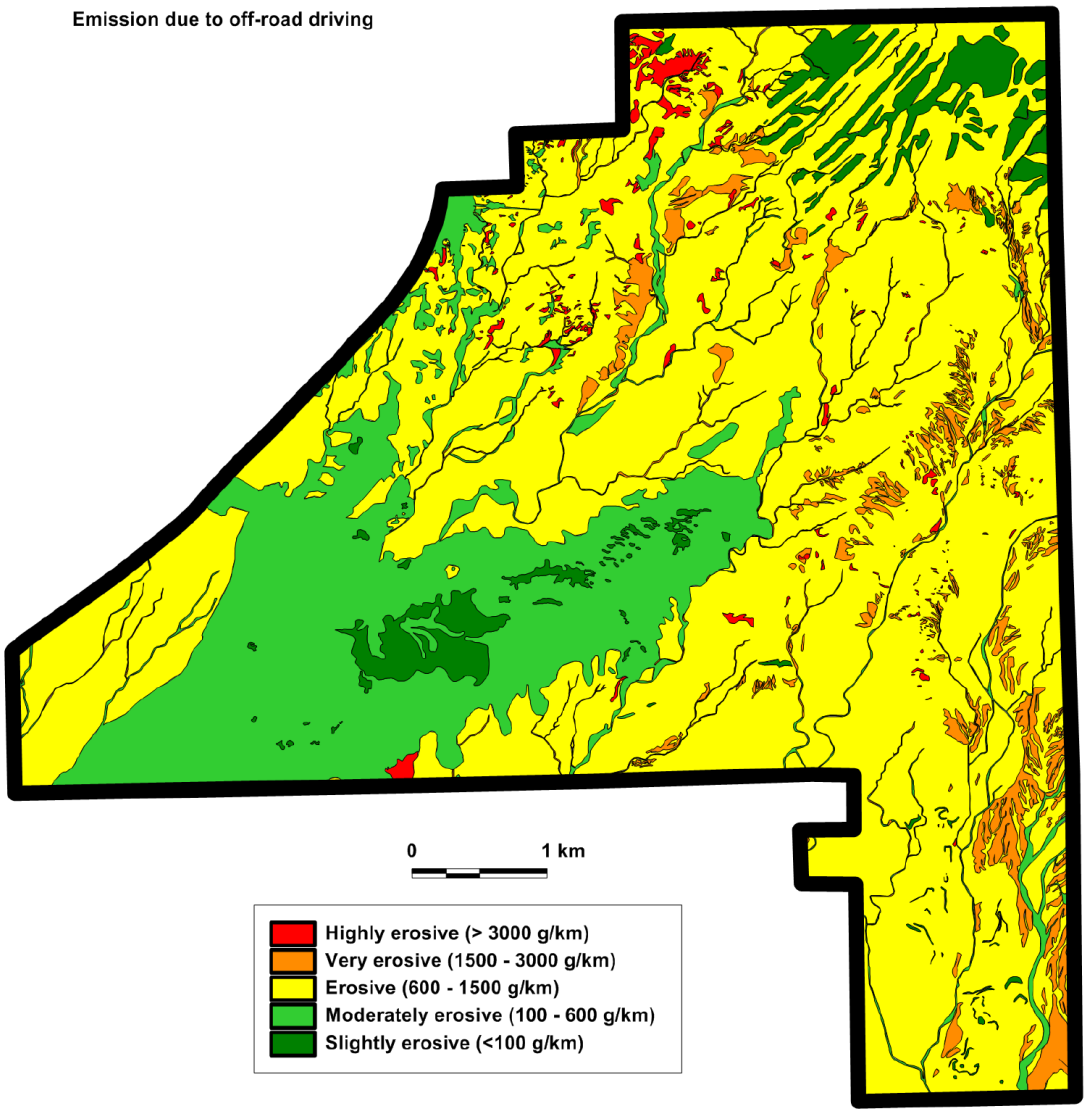

Figure. 3. Risk map for dust emission created by ORV activity (McLauren, Goossens and Buck, unpublished map)

Therefore a management plan for NDRA that addresses direct emission generated during ORV activity would need to direct ORV drivers to stay within the areas covered by sand and avoid the silt/clay areas with gravel, desert pavements, and silty drainages (units 2.2, 3.1, 4.3). Also restoration of trackways in these areas could be performed to decrease emissions from natural wind erosion in these disturbed areas.

Unit 3.2 (rock covered surfaces with silt/clay zones – i.e. a partially degraded desert pavement) contains the highest surface area of tracks in NDRA. Although limiting ORV use in this unit may be unpopular, land managers may want to significantly limit both ORV use and especially the creation of new tracks because this unit also has a fairly significant dust emission potential. Future management plans should consider both the emissivity of a surface as well as the density of trackways occurring upon it.

More datasets describing the chemical, mineralogical and biological composition of the surface units in the Nellis Dunes area are currently being composed. These datasets will be applied to the surface unit map in order to provide a better understanding of the areal distribution and controls on dust emission and its environmental impacts. This also allows a much more complete understanding of the response of specific map units to both anthropogenic disturbance (ORV) and natural wind erosion. The results of this study are critically important for land management.

Dust Emission during ORV Driving

Goossens and Buck, 2009a

Emission of dust by ORV driving was measured by a series of field experiments on three types of vehicles: 4-wheelers (quads), dirt bikes (motorcycles) and dune buggies (Fig. 4). Data were collected on all soil types at various driving speeds, and emissions were measured for a large number of grain size fractions.

Off-road driving was found to be a significant source of dust, but varies strongly depending upon type of vehicle, speed, and type of surface. For PM10 (particles <10 μm) as well as for total suspendable dust (TSP, defined here as the fraction <60 μm), the largest amounts are produced by 4-wheelers, followed by dune buggies and dirt bikes (Fig. 5). The faster the vehicles are driving, the more dust they will emit. It may be worth recalling that in many areas the dirt bike is able to drive faster than the dune buggy (and, sometimes, the 4-wheeler) and therefore can emit significant amounts of dust. Interestingly, the dust emitted by a dune buggy is somewhat finer than that emitted by a 4-wheeler or a dirt bike.

We found that off-road driving changes the characteristics of the topsoil. Dust emitted by off-road driving is finer than the parent sediment on the road surface. Off-road driving thus results in a progressive coarsening of the top layer on the road, except for silty surfaces with no, or almost no, vegetation. For these surfaces there is no substantial difference in the median grain diameter of the emitted dust compared to the road dust. Off-road driving will not alter the average grain size of these roads. Also, off-road driving destroys any surficial crust naturally present on many pristine desert surfaces.

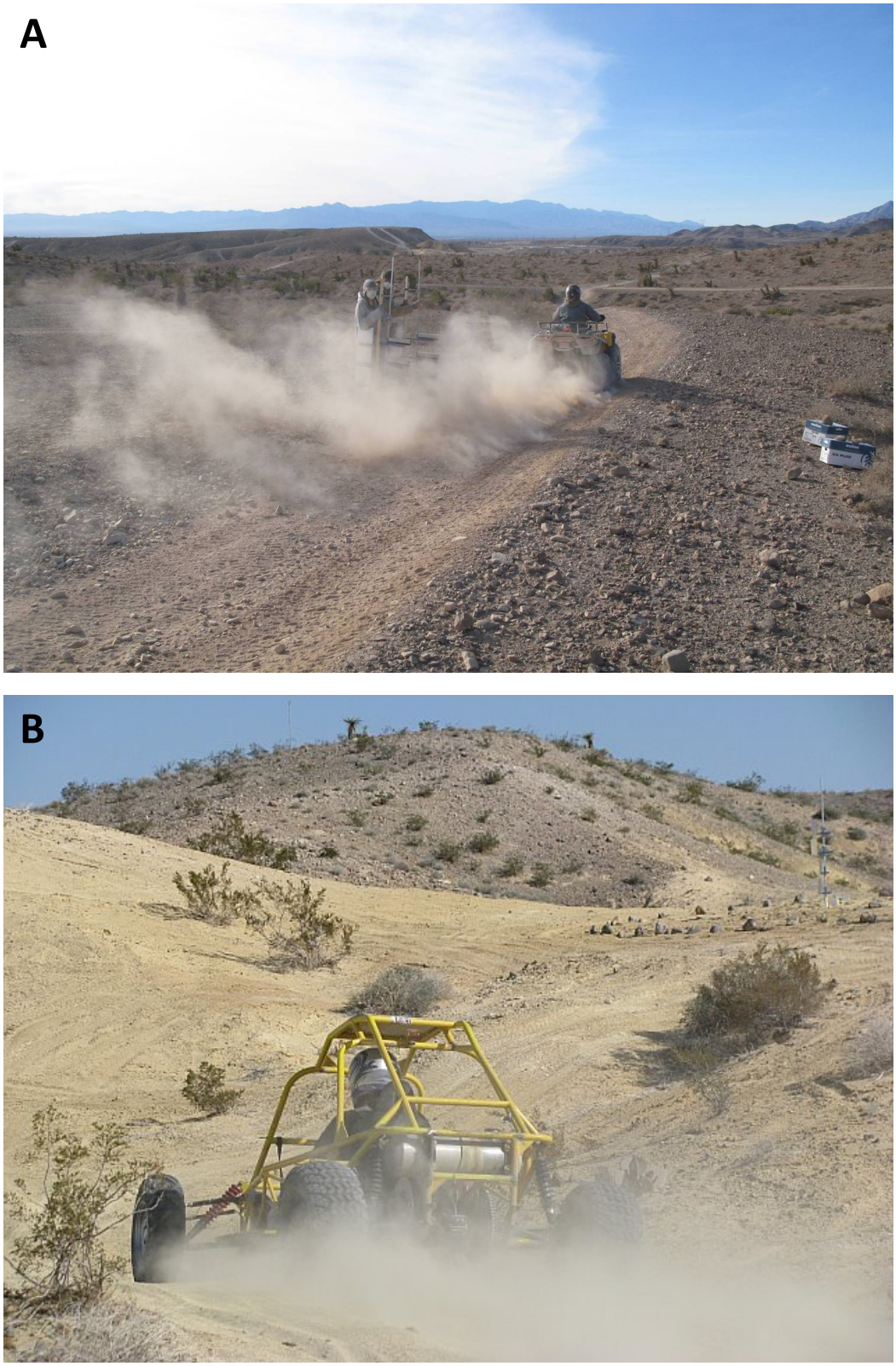

Figure. 4. Dust emission during an experiment with (a) 4-wheeler, (b) dune buggy (photos by (a) D. Goossens; (b) R. Fairchild)

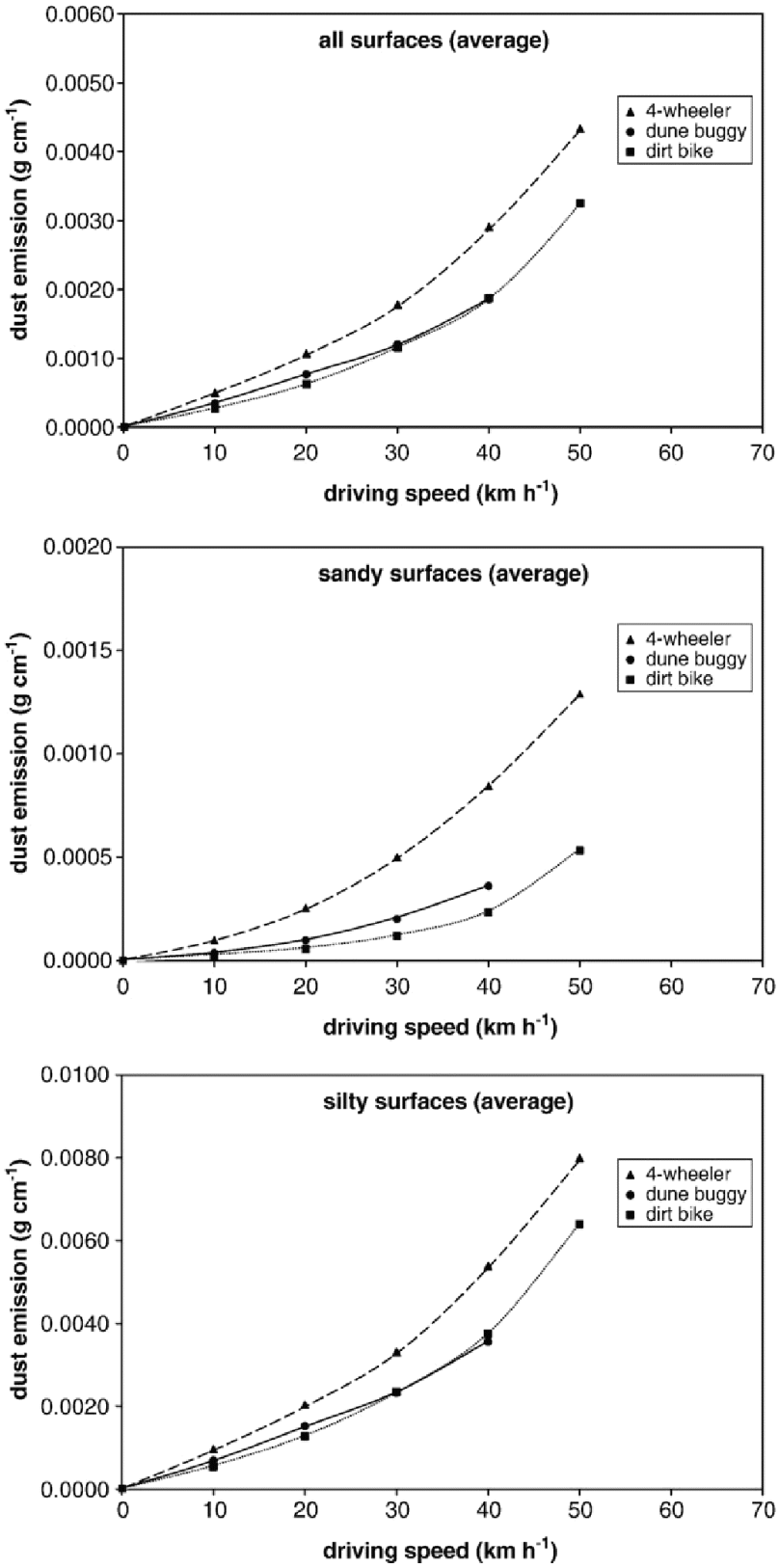

Figure. 5. PM10 emission curves for various combinations of surface type, vehicle type and driving speed (from Goossens and Buck 2009a)

A guidance document by the US EPA (AP-42, 1999) does not include vehicle speed as a parameter for estimating emissions from unpaved roads. Results from Goossens and Buck (2009a) indicate that this is problematic because in most cases the increase in emission with vehicle speed was exponential – in agreement with other studies (e.g. Etyemezian et al., 2003; Hussein et al., 2008). In addition, the US EPA formula for estimating emissions only includes a single soil parameter (% silt). Although Goossens and Buck (2009a) found that sandy soils produce less dust than silty soils, the high internal variability in surface characteristics of mapped units (rock content, presence of vegetation and/or soil crusts, contamination of the top layer with locally blown in sediment, etc.) demonstrates that a single soil parameter such as percentage of silt is insufficient to describe the effect of soil on dust emission by ORV. Field measurements remain necessary for obtaining adequate data in each specific case of soil type.

Using conservative estimates of the number of ORV drivers, length of each drive and common routes driven, we calculated the total amount of dust emitted in the Nellis Dunes area by off-road driving: 1813 tons year^{-1} (TSP) and 372 tons year^{-1} (PM10). These values are comparable to wind erosion: 1674 tons year-1 (TSP), and 394 tons year^{-1} (PM10). In areas with stabilized surfaces (areas with an undisturbed surface crust, for instance) off-road driving usually emits significantly more dust than wind erosion does. Much depends on how intensely the area is driven, how stable the undisturbed surfaces are, and what types of vehicle are used. Heavy vehicles such as cars and trucks, which were not tested in this study, produce even more dust than the vehicles used in this study.

Potential Emissions in ORV trails as Compared to Undisturbed Surfaces

Goossens and Buck, 2009b

Soil analyses and measurements with the Portable In Situ Wind Erosion Laboratory (PI-SWERL, see Fig. 6) were performed in ORV trails as well as on undisturbed terrain to investigate how ORV driving affects the vulnerability of a soil to emit PM10. The PI-SWERL measures the potential PM10 emissions of a surface by artificially creating wind shear (Etyemezian et al., 2007; Sweeney et al., 2008).

Figure. 6. The Portable In Situ Wind Erosion Laboratory or PI-SWERL (photo: D. Goossens)

Results show that the creation of new ORV trails in undisturbed terrain strongly affects the emission behavior of the soil. Although ORV activity itself always results in seriously increased emissions, adequate management in ORV regions also requires an understanding of the effect ORV driving exerts on natural emission, i.e. wind erosion. The potential PM10 production (quantified by means of the emission flux) from natural wind erosion is significantly higher in ORV trails than on undisturbed terrain (Fig. 7). Depending on the climatological conditions, vegetation cover and the intensity of ORV activities wind erosion in disturbed areas may or may not be greater than the direct emissions produced by the vehicles.

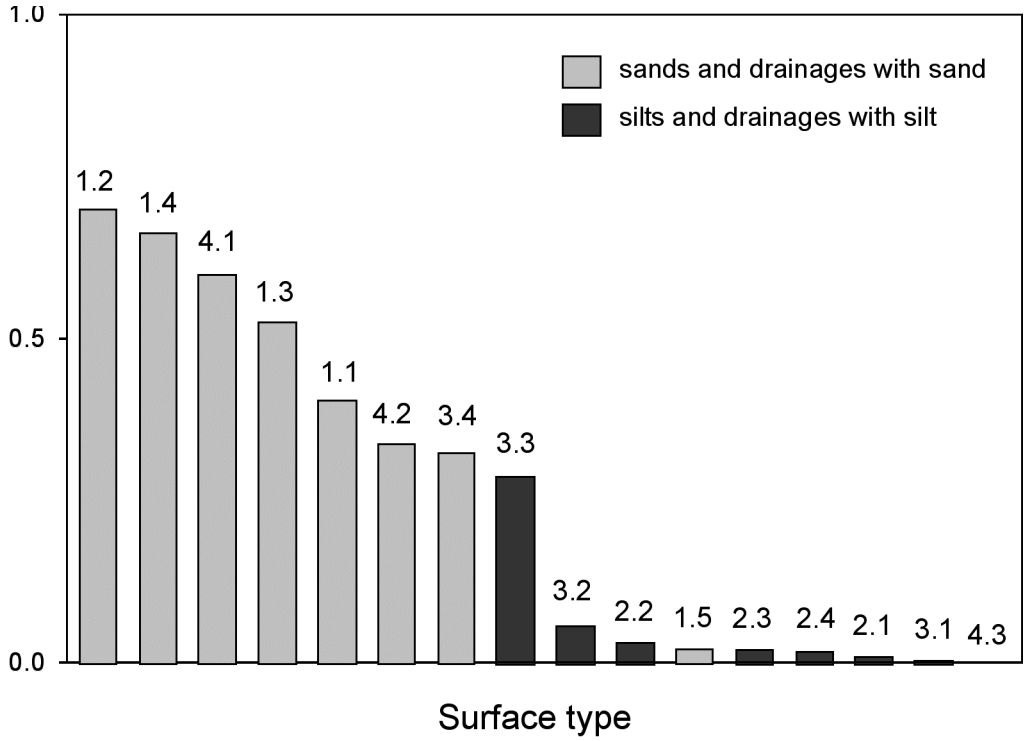

Figure. 7. Ratio of PM10 emission flux on undisturbed terrain to the emission flux in a trail, for the 17 surface units investigated (from Goossens and Buck 2009b)

Compaction and the amount of PM10 in the top layer are key factors with respect to PM10 dust production in an ORV trail. On sandy surfaces ORV driving increases the degree of compaction in the top layer, making the surface less PM10 productive. In contrast, on silty surfaces ORV driving results in the creation of a loose surficial layer of fine sediment, thus increasing emissions despite the increased compaction of the deeper soil. For ORV trails and undisturbed surfaces characterized by an equal percentage of PM10, the emissions are significantly higher in the trails. In the trails high emissions are usually associated with a high PM10 content in the top layer. This differs from the undisturbed terrain, where emissions remain small regardless of the percentage of PM10 in the top layer.

Continued ORV driving in a trail results in a gradual coarsening of the top layer (Fig. 8). The speed of coarsening is higher in trails in sand than in trails in silt. Trails in drainages coarsen even more rapidly. On sands, trail formation increases the supply limitation of the top layer, which means that the capacity of the reservoir of emission-available PM10 is reduced. On silt the supply limitation decreases; the capacity of the PM10 reservoir increases. On gravel the

reservoir does not change appreciably when new ORV trails are created. Compaction and the related binding of the grains explain this difference in behavior.

The results of this study strongly suggest that, if new ORV terrains are being planned, they should preferably be created in sandy areas. New trails on silt surfaces, or in non-gravel drainages, should be avoided.

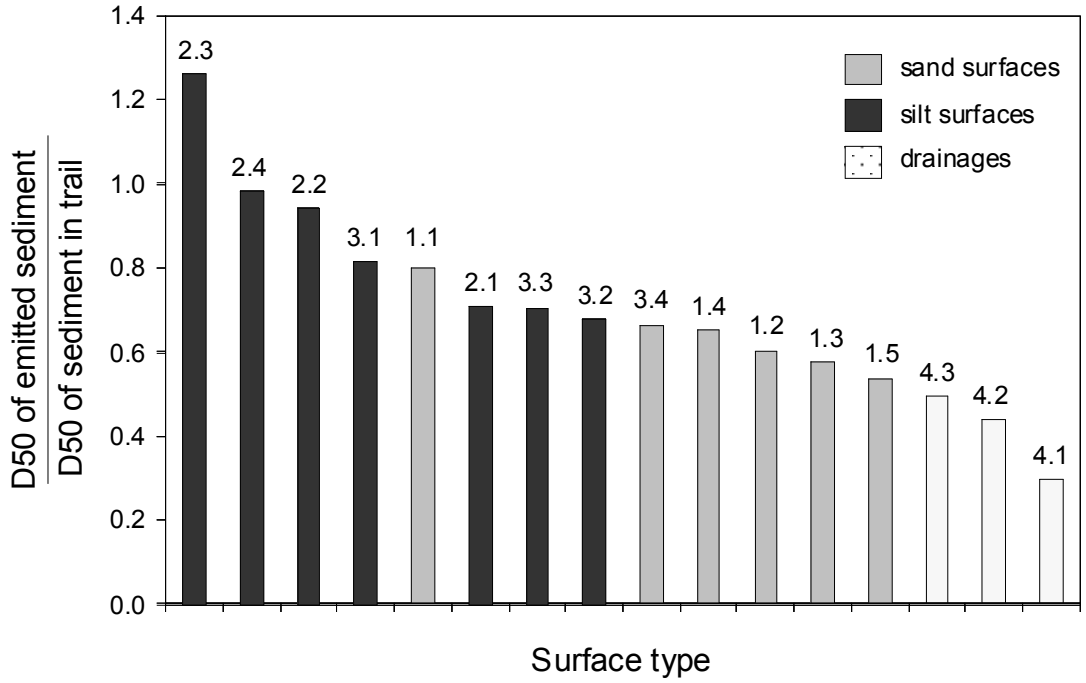

Figure. 8. Ratio of median grain diameter (D50) in ORV-emitted sediment to the median grain diameter in a trail, for the 17 surface units investigated (from Goossens and Buck 2009b)

PM10 Concentrations over 1 year at NDRA

Goossens and Buck, (in review)

PM10 concentrations were measured with a DustTrak 8520 aerosol monitor (TSI Inc., St. Paul, Michigan, USA). The instrument was installed in the center-north of NDRA, on a surface well resistant to wind erosion and well outside the areas with the greatest natural wind erosion and ORV emissions. Direct contributions, to the dust load, of local sources were thus eliminated and the dust collected can be considered sufficiently representative of the background dust created from NDRA as a whole. Grain size distribution of dust around the DustTrak was also determined by collecting sediment in BSNE collectors (Fryrear, 1986) at four levels: 25 cm, 50 cm, 75 cm and 100 cm. Wind speed and direction were measured throughout the experiment using electronic cup anemometers and a wind vane. Data were collected over one complete year, from 19 December 2007 to 17 December 2008.

At Nellis Dunes Recreation Area PM10 concentrations are highest in summer and lowest in winter (Fig. 9a). They are also higher during the day hours than at night (Fig. 9b). Short-term wind erosion events may occur all year round but are most abundant in spring. During such events PM10 concentrations can be very high, up to 1300 µg m^{-3} and more. PM10 is finer in summer than in winter. Median grain diameter in summer is around 3 µm compared to 4 µm in winter.

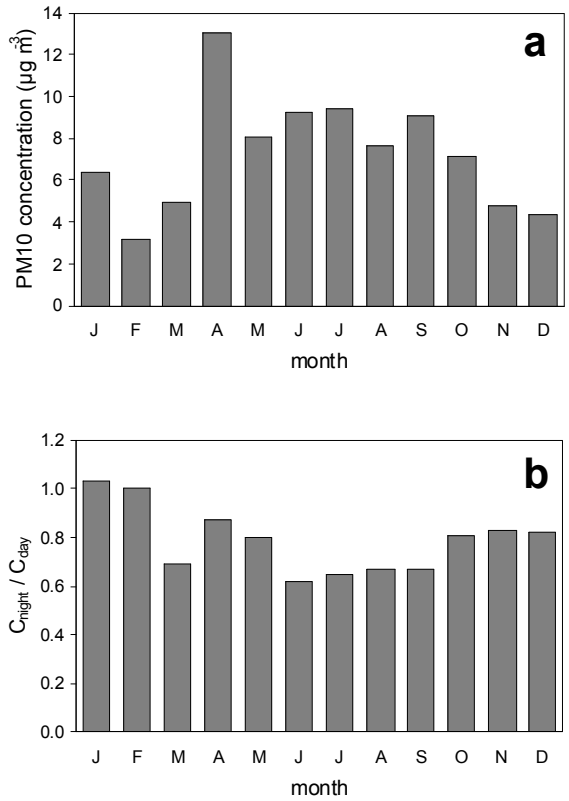

Figure. 9. (a) Monthly evolution of PM10 concentration at NDRA; (b) Ratio of dust concentration at night to dust concentration by day at NDRA. (Goossens and Buck, in review-b)

Two mechanisms of dust production occur in NDRA. Wind erosion in the sand dunes and on loose, uncompacted silty substrata in the center and west produce dust during periods of strong wind. All year round, off-road vehicular activity adds additional dust to the atmosphere. On an annual basis, the amounts of dust produced at NDRA by ORV activity and wind erosion are comparable: each produce around 0.10 tons ha^{-1} yr^{-1}, or some 380 tons yr^{-1} for NDRA as a whole for PM10, and around 0.48 tons ha^{-1} yr^{-1}, or some 1740 tons yr^{-1} for TSP

The diurnal pattern of PM10 concentration at NDRA shows a maximum in the early afternoon and a minimum in the morning (Fig. 10). In winter, a (sometimes double) secondary maximum occurs around midnight. Summer months show only one maximum, in the afternoon. Also, the duration of the time period of high concentration is shorter in the summer: from 11:00 to 18:00 as compared to 7:00 to 18:00 in winter.

No correlation was found between PM10 concentration and wind speed. High concentrations were observed at all wind speeds, and high wind speeds did not necessarily result in high PM10 concentrations. Therefore, the higher concentrations during the day are not related to local wind erosion. They are also not explained by the diurnal pattern of atmospheric stability. Highest concentrations are observed in the early afternoon, when atmosphere is unstable and mixing height and ventilation are large. Lowest concentrations are observed at night, when atmosphere is stable and mixing height and ventilation are small. Import of dust from the nearby conurbation of Las Vegas also does not explain the diurnal pattern of PM10 concentration at NDRA. No rush hour effects appear in the PM10 curves, and increase in concentration in the morning occurs well before the wind starts blowing from the city. Also, peaks in concentration occur when winds are blowing from the much cleaner northeastern sector.

Off-road vehicular activity in NDRA provides an explanation for all of the trends observed in the PM10 curves and is therefore the most plausible mechanism for generating the diurnal PM10 pattern at Nellis Dunes Recreation Area.

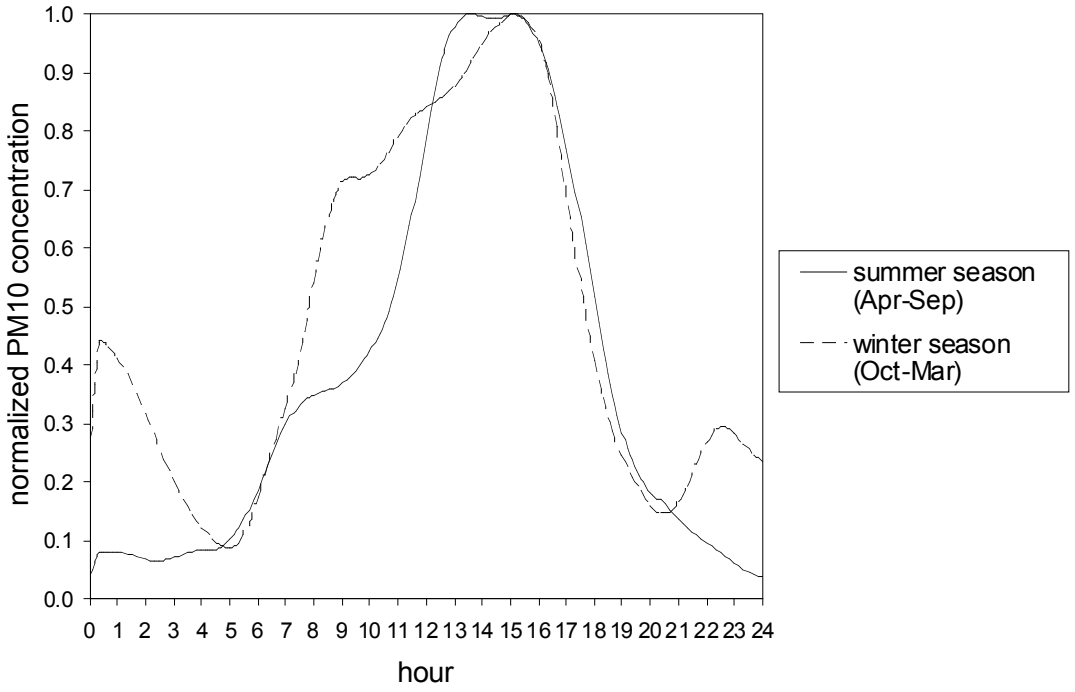

Figure. 10. Diurnal evolution of PM10 concentration at NDRA (Goossens and Buck, in review-b)

Dust Emission and Dust Deposition by Wind Erosion

Goossens and Buck, (in review)

Grain size distribution of airborne dust was determined by collecting sediment in BSNE collectors (Fryrear, 1986) on all 17 map units, at four levels: 25 cm, 50 cm, 75 cm and 100 cm for 1 complete year (19 December 2007 to 17 December 2008), with data collection every 2 weeks (Fig. 11). Wind speed, direction, and temperature data were also collected. Three 20-m wind towers and one 10-m wind tower collected these data as 1-h averages between 19 December 2007 and 16 October 2008 and as 10-min averages from 16 October 2008 to 16 December 2008. Data from the nearby Nellis Air Force Base meteorological station, which borders on the test field, were used to fill data gaps, but only after careful calibration between the wind towers and the Nellis Air Force Base station. Additional wind measurements were performed at all dust stations with a portable 3-m long wind tower containing 4 anemometers (heights: 56 cm, 121 cm, 202 cm and 259 cm) to determine the roughness length and the wind profile near each pole. In total, 396 periods of 10 min each were sampled with the portable tower. Wind speeds at all catcher levels were then calculated and linked to the data collected from the 4 wind towers. From this information it is possible to calculate the wind speeds and friction velocities required to determine erosion.

Figure. 11. Dust station with BSNE dust collectors (photo: D. Goossens)

Results show that it is necessary to distinguish gross erosion from net erosion. In contrast to net erosion, which quantifies the (eventually negative) accumulation of sediment on the surface, gross erosion measures *all* of the sediment removed from a surface over time. This distinction is not sufficiently made in the literature. At Nellis Dunes, gross deposition is less than gross erosion, thus all surfaces are net erosive. On average, for all 17 surface types, gross erosion was 235 times larger than net erosion and the coarser the particles, the greater the increase in gross erosion over net erosion (Fig. 12). Once eroded by wind, nearly all particles >40 µm settle quickly. At least 91.5% of particles in short-term suspension (25 to 70 µm) settled shortly after emission. However, a greater proportion of these particles was transported over sandy units as compared to the other units. For silt, silt/rock and drainage units, net emissions occurred for all particle sizes between 1 and 100 µm, whereas little net emission was observed for particles between 20 and 60 µm in sand units. The traditionally-accepted 70 µm grain diameter for maximum susceptibility to wind erosion only exists for net erosion – there is no such diameter between 0 and 100 µm for gross erosion. Therefore, the classic deflation curves on wind erosion are only applicable to net erosion, not to gross erosion. In addition, we found in undisturbed sandy units the particle size with the maximum susceptibility to wind erosion was 15 µm (instead of 70 µm) and in disturbed sandy units it was 25 µm. This may reflect the impacts of saltating grains. Our results show that the type of surface greatly affects the susceptibility of particles to wind erosion.

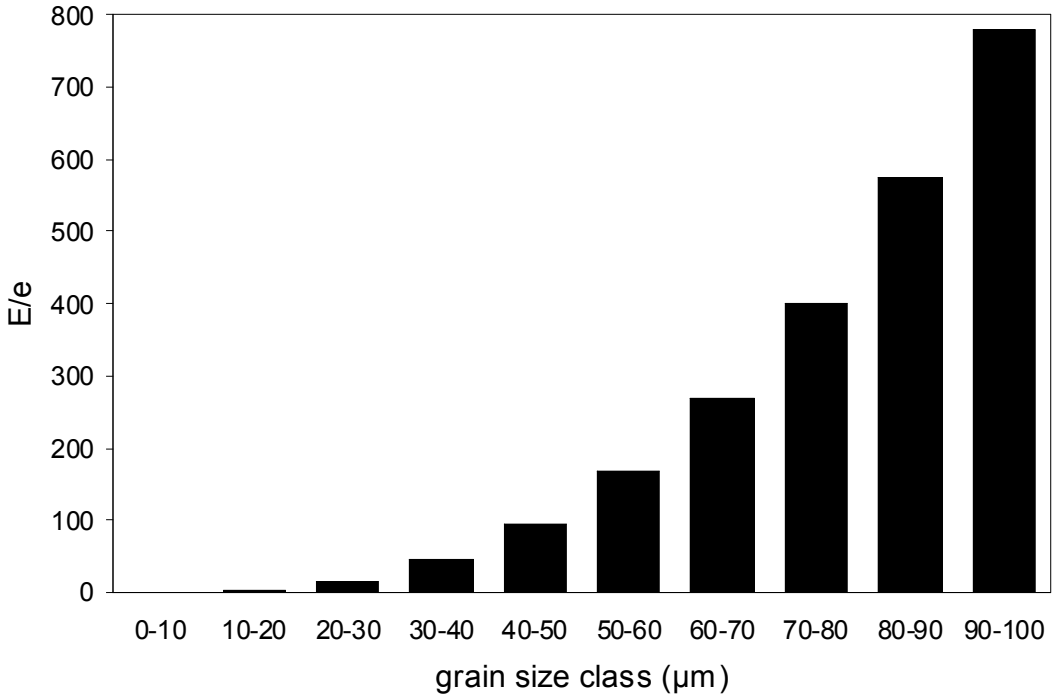

Figure. 12. Ratio of gross erosion (*E*) to net erosion (*e*) as a function of grain size. Data represents the annual average for all 17 surface units investigated. (Goossens and Buck, in review-a)

CONTINUING RESEARCH:

Mineralogical Composition of Soil and Dust Samples, Nellis Dunes, Nevada

Debbie Soukup[1], Brenda Buck[1], Dirk Goossens[1,2], Yuanxin Teng[1], Dirk Baron[3]

[1]Dept. Geoscience, University of Nevada Las Vegas, Las Vegas NV, gsoukup@bak.rr.com
[2]Department of Earth and Environmental Sciences, Katholieke Universiteit Leuven, Belgium
[3]Department of Physics and Geology, California State University, Bakersfield, Bakersfield CA.

X-ray diffraction (XRD) analyses were made on soil samples collected from 17 dust stations representing the 17 different surface types in the Nellis Dunes area. Soil samples from five parking areas were also collected for XRD analyses. The following size fractions were analyzed: <2 µm, 2-20 µm, 20-60 µm and 60-100 µm.

The mineralogical composition of the 20-60 µm and 60-100 µm fractions of the 17 dust station and 5 parking lot samples is relatively uniform, consisting mainly of quartz and calcite, with lesser amounts of plagioclase and alkali feldspars. Over one-half of the samples contain palygorskite; palygorskite is more commonly observed in the finer fractions of the samples. Several of the samples also contain amphiboles and a few contain a trace of kaolinite, gypsum, and mica/illite. Most of the gypsum that may have been present in these samples would have been removed during the distilled water rinses prior to fractionation.

The mineralogical composition of the clay (<2 µm) and silt (2-20 µm) fractions is also relatively uniform consisting mainly of smectite with lesser amounts of mica/illite, kaolinite, quartz, and calcite. Nearly all of the samples also contain chlorite, palygorskite, and plagioclase and alkali feldspars. Three of the silt samples contain amphiboles and one sample contains a 1:1 interstratified illite/smectite within the clay and silt fractions. Trace amounts of gypsum were also detected in a few of the samples, although most of the gypsum in these samples would have been removed during the distilled water rinses.

Many different minerals have been found to accumulate in lung tissue and adversely affect health (quartz, mica, gypsum, apatite, talc, rutile, pyroxene, feldspar, numerous clay and zeolite minerals) (Churg, 1983). Palygorskite is of special concern because its fibrous morphology is similar to asbestos and it has been found to induce lung cancer in rats as well as shown other deleterious health effects (Fig. 13) (Bignon et al, 1980; Rom et al., 1983; Begin et al., 1987; Wagner et al., 1987; Lemaire et al., 1989; Duzgoren-Aydin, 2008; Krewski et al., 2008). In addition to inhalation, swallowing inhaled fibrous minerals or ingesting food or beverages containing these minerals has been linked to gastrointestinal cancer, although palygorskite is believed to be much less dangerous than asbestos minerals (Reiss et al. 1980). Map units that contain palygorskite in the finest fractions (< 2 µm) include all of the sand units (1.1, 1.2, 1.3, 1.4, 1.5), all of the rock-covered surfaces (3.1, 3.2, 3.3, 3.4, 3.5), silty areas that have been disturbed (2.4), gravel and silt/clay drainages (4.3), and all 5 of the parking lot areas.

Minerals with high cation exchange capacity can pose increased risk because known carcinogens may be absorbed onto them (Nettesheim and Griesemer, 1978; Guthrie, 1997; Duzgoren-Aydin, 2008). At Nellis Dunes, smectite clay minerals in the < 2 µm fraction are found in all of the sandy and rock-covered units (1.1, 1.2, 1.3, 1.4, 1.5, 3.1, 3.2, 3.3, 3.4, 3.5), and almost all of the silt/clay and drainage units (2.2, 2.3, 2.4, 4.2, 4.3).

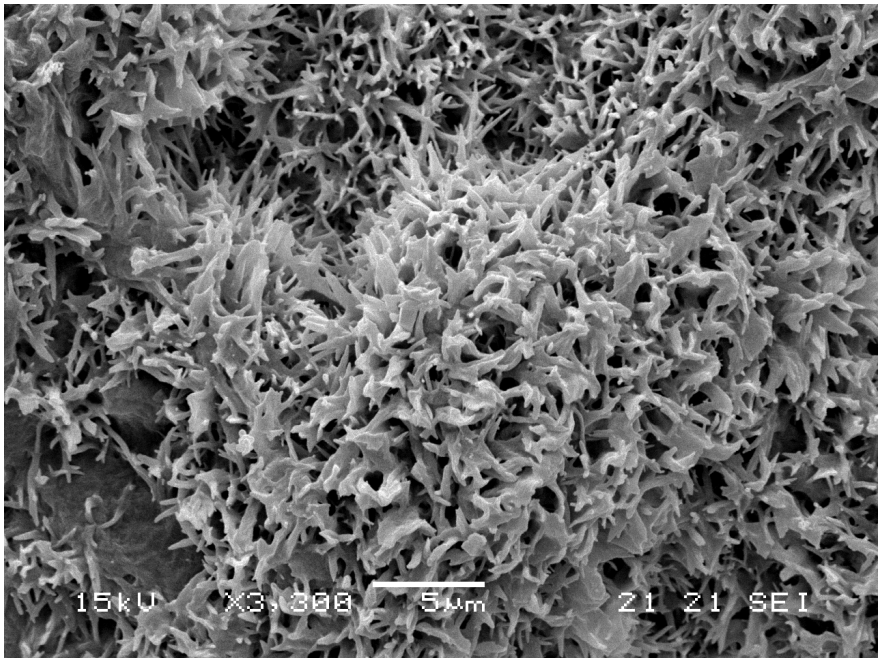

Figure 13. SEM image of authigenic palygorskite from a soil in Death Valley CA. See also this volume, Buck et al., Stop 2 for more images of the fiberous morphology of this mineral.

Trace Element Chemistry of Soil and Dust Samples, Nellis Dunes, Nevada

Debbie Soukup[1], Brenda Buck[1], Dirk Goossens[1,2], Yuanxin Teng[1], Dirk Baron[3]

[1]Dept. Geoscience, University of Nevada Las Vegas, Las Vegas NV, gsoukup@bak.rr.com
[2]Department of Earth and Environmental Sciences, Katholieke Universiteit Leuven, Belgium
[3]Department of Physics and Geology, California State University, Bakersfield, Bakersfield CA.

Soil samples collected from the 17 different surface types in the Nellis Dunes area and five parking areas were initially scanned for 66 different elements using inductively coupled plasma mass spectroscopy (ICP-MS). The purpose of the initial semi-quantitative scan was to identify potential elements of environmental concern in the samples. The <2 mm fraction of the soil samples was obtained by sieving and digested in accordance with EPA Method 3052 prior to analysis. Based on the results of the semi-quantitative scan, the following elements were identified as elements of potential concern: arsenic (As), cobalt (Co), chromium (Cr), cesium (Cs), copper (Cu), cadmium (Cd), silver (Ag), nickel (Ni), lead (Pb), strontium (Sr), uranium (U), vanadium (V), thallium (Tl), boron (B), molybdenum (Mo), antimony (Sb), and mercury (Hg). The soil and parking area samples were then re-analyzed quantitatively for these elements using ICP-MS.

Dust samples collected using the Portable In-Situ Wind Erosion Laboratory (PI-SWERL) were also analyzed for the potential elements of environmental concern. The PI-SWERL samples were collected from 16 of the 17 different surface types on both ORV trails and on undisturbed surfaces near the trails; samples could not be collected from areas of outcropping bedrock or outcropping petrocalcic horizons. PI-SWERL samples were also collected from 5 parking areas. The <10 µm and 10-60 µm size fractions were separated by sedimentation and wet sieving and digested in accordance with EPA Method 3052 prior to analysis.

Additionally, 10:1 water:soil extracts were prepared to determine the water soluble constituents in the PI-SWERL samples. The 10:1 extracts were used instead of a saturated paste because of limited sample sizes. These samples were allowed to sit overnight and were then filtered to obtain the supernatant. The supernatant was also analyzed for the potential elements of environmental concern by ICP/MS.

The pH values of the *soluble* PI-SWERL extracts were near neutral to slightly alkaline, ranging from 7.44 to 9.11. Electrical conductivity of the extracts was from 0.43 to 2.43 dS m^{-1}. The analytical results indicate elevated concentrations of As, Sr, U, V, B, and Mo in some of the samples. Arsenic concentrations ranged from 0.419 to 14.71 µg g^{-1}, Sr from 4.37 to 1344.6 µg g^{-1}, U from 0.005 to 1.168 µg g^{-1}, V from 0.30 to 10.80 µg g^{-1}, B from 2.80 to 174.4 µg g^{-1}, and Mo from 0.038 to 13.52 µg g^{-1}.

In neutral to alkaline soils impacted by sodium (Na), arsenic may be highly mobile and form soluble sodium arsenates (McBride, 1994, Matera and Le Hécho, 2001). Strontium is a relatively common trace element in the Earth's crust and is likely to be concentrated in intermediate magmatic rocks and in carbonate sediments. Strontium also behaves similarly to calcium (Ca) in the environment and is often associated with Ca in soil and sediments. Strontianite ($SrCO_3$) is easily solublized and its dissolution may be responsible for the elevated Sr concentrations (Kabata-Pendias, 2001). Under arid conditions, U forms compounds with varying solubility with oxides, carbonates, phosphates, vanates, and arsenates (Kabata-Pendias, 2001). The elevated concentrations of soluble B may result from the presence of soluble sodium borate salts, which commonly occur in alkaline soils in arid regions (McBride, 1994). Vanadium and Mo are also known to have high availability and bioavailability in oxidized soils that are neutral to alkaline.

Concentrations of Co, Cr, Cs, Tl, Sb, Sr, and Hg in the *insoluble* fraction of the soil, parking lot, and PI-SWERL samples were generally similar. However, concentrations of As, Cu, Cd, Ag, Ni, Pb, U, V, B, and Mo in the soil samples were up to one order of magnitude lower as compared to the PI-SWERL samples. These results are expected because of the larger particle size (<2 mm) of the soil samples as compared to the PI-SWERL samples (<10 µm and 10-60 µm). The XRD results demonstrated that the finer fractions of the samples are dominated by smectite minerals, which are known to be major contributors to soil CEC and therefore, affect the retention of metals in the soil (Reid-Soukup and Ulery, 2002). The amount of smectite in the dust station and parking lot soil samples is "diluted" relative to that in the PI-SWERL samples, because smectite is only present in the finest portions of these samples.

In general, the lowest elemental concentrations reported in the soil and parking lot soil samples occurred in the sand areas, particularly in Unit 1.2 (dunes with vegetation). These results are expected because the sand areas have the lowest proportion of clay and silt. As stated previously, the XRD results demonstrated that the finer fractions of the samples are dominated by smectite minerals which retain metals. The lowest reported concentrations of Pb, Sr, Mo, Sb, and Tl occurred in samples from the parking lots. The highest concentrations of most elements, as expected, occurred in samples from silt/clay areas, particularly in Units 2.2 (silt/clay with gravel) and 2.3 (aggregated silt).

In contrast, the lowest elemental concentrations in the PI-SWERL samples occurred in various units, and not within the sand areas. This may be caused by variations in clay mineral chemical composition as well as other minor mineralogical differences between samples. XRD analyses show that the mineralogical composition of the clay (<2 μm) and silt (2-20 μm) fractions of the samples is relatively uniform, and dominated by smectite minerals. The highest elemental concentrations are reported primarily in Unit 1.5, which consists of outcrops of very fine sand and coarse silt. The results of the XRD analyses show that the <2 μm and 2 to 20 μm fractions of this sample are dominated by highly crystalline smectite. The Unit 1.5 smectite may have a lower layer charge than most of the other smectites present in the Nellis Dunes area. Smectites with lower layer charge have a greater shrink-swell capacity than smectites with higher layer charge resulting in greater amounts of water, hydrated cations and organic molecules being attracted to the interlayer region (Reid-Soukup and Ulery, 2002).

The reported concentrations of elements in the soil, parking lot and PI-SWERL samples were also compared with the USEPA Region 3, 6, and 9 screening levels (SLs) for chemical contaminants in residential soils and soil concentrations considered to be protective of groundwater resources (USEPA, 2010). The SLs are developed using risk assessment guidance from the EPA Superfund program and are used for site "screening: and as initial cleanup goals, if applicable. The risk-based SLs are considered by the EPA to be protective for humans (including sensitive groups) over a lifetime. However, it should be noted that the SLs may not be applicable at a particular site and they do not address non-human health endpoints, including ecological impacts. The EPA has also established SLs for residential and industrial air which are applicable to human inhalation; these SLs are based on chemical concentrations in the air ($\mu g\ m^{-3}$). Future work includes recalculating the chemical concentrations in terms of mass per volume air (ug/m3) by combining the chemical concentrations in the soil with the emission rates measured during the ORV experiment. These results are not yet available.

The reported concentrations of As in the soil and parking lot soil samples ranged from 3.49 to 83.02 $\mu g\ g^{-1}$ or parts per million (ppm) and from 16.13 to 312 $\mu g\ g^{-1}$ in the *insoluble fraction* of the PI-SWERL samples. Arsenic concentrations in the *soluble fraction* of the PI-SWERL samples ranged from 0.601 to 7.78 $\mu g\ g^{-1}$. The arsenic concentrations in all of the samples analyzed exceed the EPA's SL of 0.39 $\mu g\ g^{-1}$ for As in residential soil. The reported concentrations of the other elements analyzed do not exceed the EPA's SLs for residential soil. The As concentrations are of concern, because inorganic arsenic is acutely toxic to humans and ingestion of large quantities causes gastrointestinal symptoms, severe cardiovascular and central nervous system disturbances, and eventually death (Järup, 2003). Studies on various populations exposed to arsenic by inhalation demonstrate an excess risk of lung cancer, with

the risk increasing with increasing exposure. Additionally, arsenic exposure may lead to hypertension and cardiovascular disease (Järup, 2003). These results are particularly concerning because of the high concentrations of arsenic in the soluble fraction.

Naturally occurring background concentrations of arsenic vary regionally because of a combination of climatic, geologic, and anthropogenic factors. Sources of As in the environment include weathering of As-bearing rocks and minerals, volcanic eruptions, fly ash from coal burning plants, smelter fumes released during the treatment of As-containing metallic ores, and application of arsenical pesticides, herbicides and corrosion inhibitors. Background concentrations of As in soil and dust often exceed the EPA SL, particularly in arid areas such as Nellis Dunes. Average background concentrations of arsenic in soils throughout the world reportedly range from 2.2 to 25 ppm, and in the United States at average concentrations ranging from 3.6 to 8.8 ppm (McBride, 1994). In a 1975 study of 21 soil samples collected in the western United States, As concentrations ranged from non-detectable to 97 ppm with an average concentration of 6.1 ppm (Connor and Shacklette, 1975). In another study, As analyses were performed on 50 soils collected throughout California. Arsenic concentrations in these soils ranged from 0.6 to 11 ppm, with an average concentration of 3.5 ppm (Bradford et al., 1996). Reheis et al. 2009 conducted a compositional study of modern dust and surface sediments in the desert southwest, United States. These investigators reported median As concentrations of 20 ppm in dust and 10 ppm in surface soil samples. Based on the results of their study, Reheis et al. (2009) also concluded that modern dust compositions in their study area have been influenced by anthropogenic sources and emissions from Owens (dry) Lake after its artificial desiccation in 1926.

The As concentrations reported in some of the Nellis Dunes samples are one order of magnitude higher than those reported in previous investigations. Some of the highest concentrations were reported in the PI-SWERL samples, which are dominated by smectite minerals. It may be possible that the As is associated with the smectite. Pascua et al. (2005) reported the occurrence of an As-rich smectite (1,500 to 4,000 ppm) in a geothermal field in Japan. These investigators found that minimal adsorption of As on smectite surfaces had occurred. Rather, the As was predominantly dissolved within the smectite or occurred within mineral occlusions.

The reported concentrations of As and Co in all of the samples exceed the EPA SLs considered to be protective of groundwater. The SL for Sb is exceeded in all samples except for the parking lot soil samples. Eight of the soil samples and nearly all of the PI-SWERL samples exceed the SL for Hg. Nearly all of the PI-SWERL samples also exceed the SL for Mo, and all of the PI-SWERL samples exceed the SL for B. Three of the PI-SWERL samples exceed the SLs for Cu and Ag, and two PI-SWERL samples exceed the SL for Cd. None of the reported concentrations of Ni, Sr, U, and V in the samples exceeded the SLs for groundwater for these elements. The EPA has not established SLs for groundwater for Cr, Cs, Tl, and Pb. Although the reported elemental concentrations in many samples exceed one or more of the EPA SLs, the potential risk to groundwater resources from leaching of these elements is considered to be minimal because of the arid climate and depth to groundwater (>100 feet below ground surface). However, the high soluble concentrations of metals in these soils are a concern for downstream contamination from runoff.

Radionuclide Characterization of Nellis Dunes Recreation Area Soils and Dust

Sudowe, R.[1,2], Roman, A.[2], Buck, B.[3], Goossens, D.[3], Teng, Y.[3]

[1]Department of Health Physics and Diagnostic Sciences, & Radiochemistry Program, University of Nevada Las Vegas, Las Vegas NV, ralf.sudowe@unlv.edu; [2]Radiochemistry Program, University of Nevada Las Vegas, Las Vegas, NV; [3]Department of Geosciences, University of Nevada Las Vegas, Las Vegas, NV

Every soil contains a variety of naturally occurring and man-made radionuclides. The presence of shorter lived man-made radionuclides in the soil is the result of fallout from atmospheric nuclear weapons tests conducted between 1945 and 1963. The resulting terrestrial radiation exposure to humans makes up for about 8% of the total average annual exposure of 360 mrem. This is exposure is due to the radiation field caused by gamma-emitting radionuclides present in the soil. The alpha-emitting nuclides present in the soil have a higher energy deposition associated with their decay; however their range is so small that they cannot penetrate the outer layer of the skin. Their contribution to the external radiation exposure is therefore insignificant.

This situation changes however drastically if radionuclides, in particular alpha emitters, are incorporated in the human body. Such incorporation can occur either through ingestion or more likely through inhalation. Radionuclides entering the body through inhalation will deposit either in the nasal passages, the tracheobronchial tree or the deep lung parenchyma. These three regions have very different characteristics for retention of aerosols that are introduced. The penetration into these regions is determined entirely by the aerodynamic properties of the particles inhaled, in particular by the particle diameter. Penetration into the deep lung parenchyma is the most important process to consider. As a result of this penetration the radioactive atom is placed in the immediate vicinity of a biologically sensitive target, such as the lung tissue. The energy resulting from the radioactive decay is completely absorbed in the tissue, given rise to an appreciable internal dose. In particular the high-energy deposition associated with the alpha decay of the radon daughters' polonium-218 and polonium-214 is of concern.

Off-road driving at NRDA will not only cause significant dust inhalation by the driver, it also has the potential to significantly increase the amount of dust generally present in the air. This will likely affect the air quality not only in the vicinity of NRDA but also in places that are downwind from the dunes. The goal of this study is to determine the concentration of radionuclides in soil and dust samples from the NDRA to assess the potential health hazard associated with the dust inhalation. The study is complemented by the mineral and chemical studies described above (Soukup et al., in prep.).

A total of seventeen samples obtained from the NDRA were assayed to determine the concentration of gamma-emitting radionuclides. The samples were measured using a Canberra Model GR3519 high-purity germanium gamma detector with a relative efficiency of 35%. A certified soil reference standard in the same sample geometry was used to perform a multi-point energy and detection efficiency calibration on the detector. The calibration was carried out in accordance with ANSI Standard N42.14-1999. A certified reference material obtained by the National Institute for Standards and Technology was measured as an unknown sample to verify

the calibration. Measurement and subsequent analysis of the soil samples was carried out using a modification of EPA Method 901.1. The samples, a blank and the detector background were all measured for 72 hours with the exception of one sample that was measured for 88 hours. All results were background corrected. The activities measured were corrected for sample mass to obtain the specific activity in picocurie per gram of soil.

The radioisotopes actinium-228 (Ac-228), lead-212 (Pb-212) and bismuth-212 (Bi-212) from the thorium decay series were found in all samples. The mother nuclide for this series, thorium-232 (Th-232) was found in seven samples. The members of the uranium decay series protactinium-234m (Pa-234m), lead-214 (Pb-214) and bismuth 214 (Bi-214) were also identified in all samples. Thorium-231 (Th-231) from the actinium decay series was found in all of the samples and protactinium-231 (Pa-231) from the same series was identified in five samples. The mother nuclide for this series, uranium-235 (U-235) was found in all samples except one. In addition the primordial isotope potassium-40 (K-40) was present in all samples. Cesium-137 (Cs-137) was also found in all samples. This isotope was deposited in the soil as a result of atmospheric testing of nuclear weapons. Future work will measure radionuclide concentration in dust samples used in the study described below.

Immunotoxicological Health Effects of Acute Exposure to Dust Samples Collected from Nellis Dunes Recreational Area

[1]Keil, D.E., [2]Proper, S., [3]Peden-Adams, M., [1]Ayala, N., [4]Berger-Ritchie, J., [1]Lebahn, S., [5]Young, S., [6]Buck, B., [6,7]Goossens, D., [6]Soukup, D., [8]Sudowe, R., [6]Teng, Y., [9]Baron, D.

[1]Clinical Laboratory Sciences, University of Nevada Las Vegas, Las Vegas NV; [2]School of Medicine, Michigan State University, Lansing, MI; [3]Harry Reid Center for Environmental Studies, University of Nevada Las Vegas, Las Vegas, NV; [4]School of Community Health, University of Nevada Las Vegas, Las Vegas, NV; [5]Department of Anthropology, University of Nevada Las Vegas, Las Vegas, NV; [6]Department of Geosciences, University of Nevada Las Vegas, Las Vegas, NV; [7]Department of Earth and Environmental Sciences, Katholieke Universiteit Leuven, Belgium; [8]Department of Health Physics and Radiochemistry, University of Nevada Las Vegas, Las Vegas NV; [9]Department of Physics and Geology, California State University, Bakersfield, Bakersfield CA.

Research into the effects of PM10 and PM2.5 emissions 5 (particulates ≤ 10 and 2.5 microns respectively) on human health increasingly show a strong link to numerous diseases and mortality including asthma, heart disease, dementia, and cancer. Epidemiological studies have demonstrated that daily mortality may be attributed to cardiopulmonary and respiratory damages caused by ambient particulate matter. However, less is known regarding the effects of dust exposure on systemic immunological parameters and disease resistance.

The Nellis Dunes Recreation Area (NDRA) is a popular off-road vehicle (ORV) driving destination managed by the Bureau of Land Management (BLM) and located just 6 km northeast of Las Vegas NV. For the past forty years the NDRA has provided the only publicly accessible area in southern Nevada for legal off-road driving with annual visitors estimated at over 300,000 (Goossens and Buck, 2009a).

To simulate the potential health impacts of a weekend exposure to dust at the NDRA, adult female B6C3F1 mice were exposed by tracheal aspiration to dust samples with a median diameter of 4 microns or less at 0, 0.1, 1.0, 100, or 1000 mg/kg/day daily for 3 days. Samples were collected from 3 different soil types in the NDRA: unit 2.2 (a silt/clay unit with some surface gravel that forms a portion of 'badlands' topography in the NDRA), unit 3.1 (a well-developed desert pavement with underlying silty Av soil horizon), and unit 3.2 (a rock-covered surface with silt/clay zones that comprises the greatest amount of surface area in the NDRA). All dust was extracted from samples taken from the uppermost cm of the topsoil using a cyclone dust separator that only collects the finest particles.

Particle size was measured with laser diffraction using a Malvern Mastersizer S particle size analyzer. Extractions and particle size analyses were performed at the Earth and Environmental Sciences Department, Katholieke Universiteit Leuven, Belgium. Total chemical composition was measured using total digestion (EPA Method 3052) and measured using ICP-MS at California State University Bakersfield. Radionuclide content of the soil was determined by gamma spectroscopy using a High-Purity Germanium detector. Soil mineralogy was determined using x-ray diffraction (XRD) at UNLV XRD laboratory. Effects on lung and systemic immunological parameters were assessed 2 days following 3 daily exposures. Preliminary data demonstrate alterations in thymus weight, T-cell populations, and cellularity, as well as changes in kidney and liver weight.

The most sensitive effects appear to affect antibody production. Significant decreases were observed in the IgM antibody plaque forming cell (PFC) response (Figure 14) beginning at 0.1 mg/kg/day dose for the 2.2 dust sample collection (ED_{50}=0.08 mg/kg/day), and 1.0 mg/kg/day for dust samples collected at sites 3.1 and 3.2 (ED_{50}= 19.5 and 5.06 mg/kg/day, respectively). Decreases in CD4+ helper T-cells occurred following exposure to all doses of the Dust 2.2 (ED50=396 mg/kg/day) and following exposure to the 1, 100, and 1000 mg/kg/day treatments of the Dust 3.1 (ED_{50}=995 mg/kg/day; Figure 15). Decreases in splenic CD4+CD8+ (double positive cells) were also noted following exposure to Dust 2.2 and 3.1 (Figure 15). Body weight was significantly decreased at the 1000 mg/kg/day following exposure to all dust collection samples demonstrating that overt toxicity was evident in the highest dose group, only.

Additional immunological and health parameters are currently under examination. Thus far, these preliminary data demonstrate significantly decreased systemic immune function following brief exposures to dust particles 2.2, 3.1 or 3.2 within the estimated human exposure range for ORV driving. With deficits evident in specific IgM responses and splenic CD4+ T-helper cells, both of which are critical to the development of pathogen specific antibodies, increased susceptibility to pathogenic disease should be investigated. Additionally, systemic or extra-thymic CD4+CD8+ cells are thought to have important roles in tumor surveillance, it would also be important to assess susceptibility to tumor growth.

As outdoor dust and soil from the greater Las Vegas area are likely primary sources for indoor residential dust, the effects of dust exposure on human health should also be evaluated with regards to the impact on occupational and residential environments.

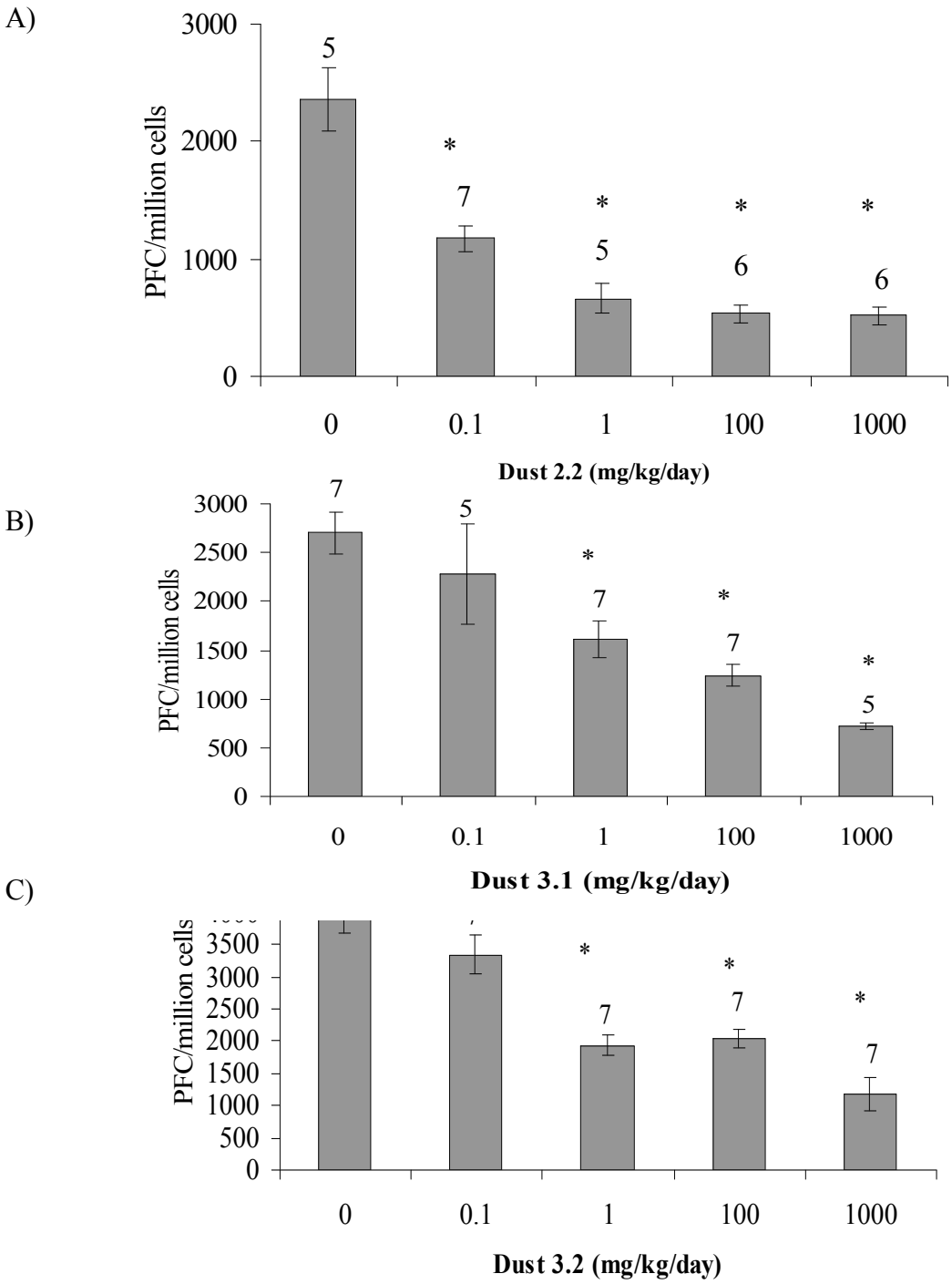

Figure 14. Sheep red blood cell-specific-IgM antibody production in adult female B6C3F1 mice following tracheal aspiration exposure to dust 2.2 (A), 3.1 (B), or 3.2 (C). Data are presented as mean ± SEM. Numbers above SEM bars indicate sample size. (*)Indicates significantly different from respective control ($p < 0.05$). Dust 2.2= dust samples collected from unit 2.2. Dust 3.1= dust samples collected from unit 3.1. Dust 3.2= dust samples collected from unit 3.2.

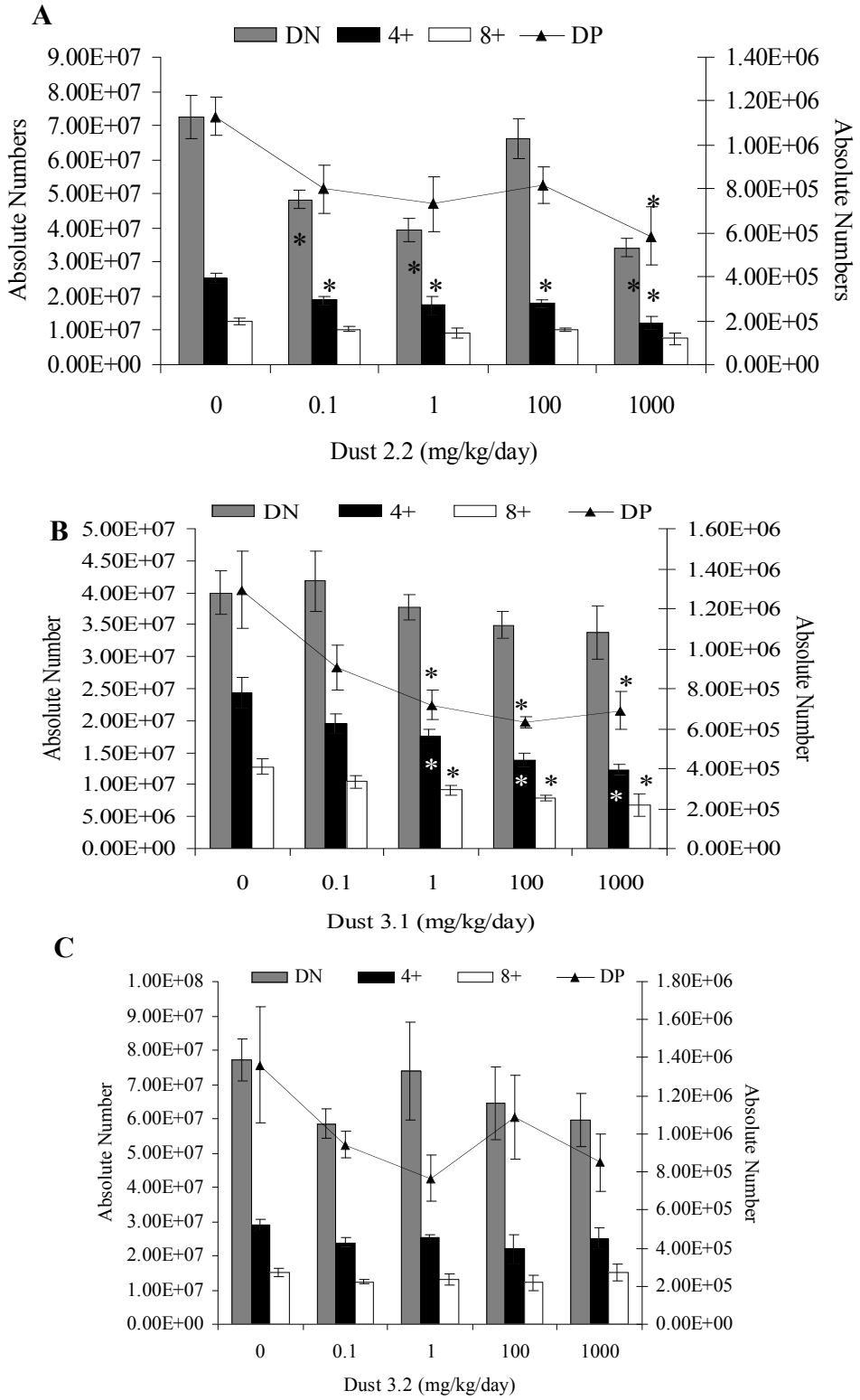

Figure 15. Splenic T-cell populations (CD4CD8) in adult female B6C3F1 mice following tracheal aspiration exposure to dust 2.2 (A), 3.1 (B), or 3.2 (C). Data are presented as mean ± SEM. Sample sizes for 0, 0.1, 1, 100, and 1000 mg/kg/day for dust 2.2 are 5, 7, 5, 6 and 6, respectively. Sample sizes for 0, 0.1, 1, 100, and 1000 mg/kg/day for dust 3.1 are 7, 5, 7, 7 and 5, respectively. Sample sizes for 0, 0.1, 1, 100, and 1000 mg/kg/day for dust 3.2 are 6, 7, 7, 7, and 7, respectively. (*)Indicates significantly different from respective control ($p < 0.05$). Double positive (DP; CD4+DC8+) cells are one the second axis. DN= Double negative cells (CD4-CD8), 4+ = CD4+CD8-, 8+ =CD4-CD8+. Dust 2.2= dust samples collected from unit 2.2. Dust 3.1= dust samples collected from unit 3.1. Dust 3.2= dust samples collected from unit 3.2.

Acknowledgements
The Federal Bureau of Land Management (BLM) funded this project through a SNPLMA Conservation Initiative, and granted permission for executing the measurements in NRDA. L. Christianson (BLM) provided administrative assistance throughout the project. D. Pepper and U. Rangegowda (College of Engineering, University of Nevada Las Vegas, Las Vegas, NV) and X. Wang (Purdue University Calumet, Hammond, IN) organized the collection of wind data from 4 permanent wind towers and performed the initial processing of the wind records. Wind data from the Nellis Air Force Base meteorological station were provided by M. EmelyPoynter (Nellis Air Force Base, Las Vegas, NV). V. Etyemezian, G. Nikolich and J. King (Desert Research Institute, Las Vegas, NV) provided a portable wind tower, processed the raw data collected from it and offered assistance during some of the PI-SWERL measurements. PM10 measuring equipment was graciously provided by D. James, College of Engineering, University of Nevada Las Vegas, Las Vegas, NV. R. Jordan (Sun Buggy Fun Rentals, Las Vegas) provided a dune buggy, a dirt bike and several of the drivers for the off-road driving experiment. A 4-wheeler was provided by S. Kingsley, and another dirt bike by B. Wilson. The Quickbird imagery used in this study was funded through the SNPLMA Round 5 550 Conservation Initiative Program as part of an interagency project with the Bureau of Land Management, 551 National Park Service, U.S. Fish and Wildlife Service, and the U.S. Forest Service. The following persons assisted in the field experiments: L. Bangen, J. Carter, R. Davis, R. Fairchild, C. Griffing, J. Morton, M. Stropky, Y. Teng and A. Williams. We also thank Tom Gill for numerous advice and suggestions.

References

Akhter, M. S; Madany, I. M., 1993, Heavy metals in street and house dust in Bahrain. Water Air Soil Pollut. 66: 111-119

Athar M., Iqbal M., Beg M.U., Al-Ajmi D., Al-Muzaini S., 1998. Airborne dust collected from Kuwait in 1991-1992 augments peroxidation of cellular membrane lipids and enhances DNA damage. Environment International 24, 205-212.

American Lung Association, 2010, The American Lung Association State of the Air 2010, American Lung Association National Headquarters, Washington DC, www.longusa.org.

Begin, R., Masse, S., Rola-Pleszczynski, M., Geoffroy, M., Martel, M., Desmarais, Y., and Sebastien, P., The lung biological activity of American attapulgite. Environmental Research 42:328-339.

Besancenot J.P., Boko M., Oke P.C. 1997. Weather conditions and cerebrospinal meningitis in Benin (Gulf of Guinea, West Africa). European Journal of Epidemiology 13, 807-815.

Bignon, J., Sebastien, E, Gaudichet, A., and Jaurand, M. C. (1980). Biological effects of attapulgite. *In* "Biological Effects of Mineral Fibers" (J. C. Wagner, Ed.), Vol. 1. IARC Scientific Publication No. 30, IARC, Lyon.

Bradford, G.R., A.C. Chang, A.L. Page, D. Bakhtar, J.A. Frampton, and H. Wright. 1996. Background concentrations of trace and major elements in California soils. Kearney Foundation of Soil Science Special Report, p. 20.

Churg, A., Nonasbestos pulmonary mineral fibers in the general population. Environmental Research, 31:189-200.

Connor, J.J. and H. T. Shacklette. 1975. Background geochemistry of some rocks, soils, plants, and vegetables in the conterminous United States. Geological Survey Professional Paper 574-F, United States Government Printing Office, p. F27.

Dockery, D., Pope III, C., Xu, X., Spengle, R.J., Ware, J., Fay, M., Ferris, B., Speizer, F., 1993. An association between air pollution and mortality in six US cities. N. Engl. J. Med. 239, 1753–1759.

Duzgoren-Aydin, N., 2008, Health effects of atmospheric particulates: a medical geology perspective. Journal of Environmental Science and Health Part C, 26:1-39.

Etyemezian, V., Nikolich, G., Ahonen, S., Pitchford, M., Sweeney, M., Purcell, R., Gillies, J., Kuhns, H., 2007. The Portable In Situ Wind Erosion Laboratory (PI-SWERL): a new method to measure PM10 windblown dust properties and potential for emissions. Atmospheric Environment 41, 3789–3796.

Etyemezian, V., Kuhns, H., Gillies, J., Green, M., Pitchford, M.,Watson, J., 2003. Vehicle based road dust emission measurement: I — methods and calibration. Atmospheric Environment 37, 4559–4571.

Feng, Y. and Barratt, R. 1993, An assessment of data of trace elements in indoor and outdoor dusts. Int. L Environ. Health Res. 3: 18-31

Fergusson, J.E. and Kim, N.D. 1991, Trace elements in street and house dusts: sources and speciation. Sci. Total Environ. 100: 125-150.

Fishbein, L. 1991, Indoor environments: the role of metals. In: Merian, E., ed. Metals and their compounds in the environment. Weinhelm, Germany: VCH Verlagsgesellschaft mbH; 287-309; 1991

Fryrear D.W., 1986. A field dust sampler. Journal of Soil and Water Conservation 41, 117–120.

Goossens, Dirk, and Buck, Brenda, 2009a*,* Dust emission by off-road driving: Experiments on 17 arid soil types, Nevada, USA, *Geomorphology* 107, 118-138 doi:10.1016/j.geomorph.2008.12.001

Goossens, Dirk, and Buck, Brenda J., 2009b*,* Dust dynamics in off-road vehicle trails: Measurements on 16 arid soil types, Nevada, USA, *Journal of Environmental Management* 90, 3458-3469

Goossens, Dirk, and Buck, Brenda, *in review-a,* The characteristics of gross erosion, net erosion and gross deposition of dust by wind. Field data from 17 types of desert surfaces, *Earth Surface Processes and Landforms*

Goossens, Dirk, and Buck, Brenda**,** *in review-b,* Effects of wind erosion, off-road vehicular activity, atmospheric conditions and the proximity of a metropolitan area on PM10 characteristics in a recreational site near Las Vegas, USA, *Atmospheric Environment*

Griffin, D.W., and Kellogg C.A. 2004. Dust storms and their impact on ocean and human health: Dust in Earth's atmosphere. EcoHealth 1, 284-295.

Husar, R.B., Tratt, D.B., Schichtel, B.A., Falke, S.R., Li, F., Jaffe, D., Gasso, S., Gill, T., Laulainen, N.S., Lu, F., Reheis, M.C., Chun, Y.,Westphal, D., Holben, B.N., Gueymard, C., McKendry, I., Kuring, N., Feldman, G.C., McClain, C., Frouin, R.J., Merrill, J., DuBois, D.,Vigonola, F., Sugimoto, N., Malm, W.C., 2001. Asian dust events of April 1998. J. Geophys. Res. 106, 18316–18330.

Hussein, T., Johansson, C., Karlsson, H., Hansson, H.C., 2008. Factors affecting nontailpipe aerosol particle emissions from paved roads: on-road measurements in Stockholm, Sweden. Atmospheric Environment 42, 688–702.

Ichinose, T., Nishikawa, M., Takano, H., Sera, N, Sadakane, K., Mori, I., Yanagisawa, R., Odae, T., Tamura, H., Hiyoshi, K., Quan, H., Tomura, S., and Shibamoto, T., 2005, Pulmonary toxicity induced by intratracheal instillation of Asian yellow dust (Kosa) in mice. Environmental Toxicology and Pharmacology 20, 48–56

Järup, L., 2003, Impact of environmental pollution on heath: balancing risk. British Medical Bulletin 68, 167-182. doi: 10.1093/bmb/ldg032.

Jinadu B.A. 1995. Valley Fever Task Force Report on the control of Coccidioides imitis. Kern County Health Department, Bakersfield, CA.

Krewski, D., Yokel, r., Nieboer, E., Borchelt, D., Cohen, J, Harry, J., Kacew, S., Lindsay, J., Mahfouz, A., and Rondeau, V., 2007, Human health risk assissment for aluminum, aluminium oxide, and aluminium hydroxide, Journal of Toxicology and Envionronmental Health, Part B, 10:1-269.

Komatsu K., Vaz V., McRill C., Colman T., Comrie A., Sigel K., Clark T., Phelan M., Hajjeh R., Park B. 2003. Increase in coccidioidomycosis – Arizona, 1998-2001. Journal of the American Medical Association 289, 1500-1502.

Korenyi-Both A.L., Korenyi-Both A.L., Molnar A.C., Fidelus-Gort R. 1992. Al Eskan disease/ Desert Storm pneumonitis. Military Medicine 157, 452-462.

Laden, F., Schwartz, J., Speizer, F., Dockery, D., 2006, Reduction in fine particulate air pollution and mortality: extended follow-up of the Harvard six cities study. Am J. Respir. Crit Care Med 173:667-672.

Lambert, A.L., Dong, W., Winsett, D.W., Selgrade, M.K., Gilmour, M.I., 1999, Residual Oil Fly Ash Exposure Enhances Allergic Sensitization to House Dust Mite. Toxicology and Applied Pharmacology 158**,** 269–277.

Lazaro, M.A., Chang, Y.-S., Kuiper, J.A., Kotamarti, V.R., James, D.E., Brazao, R., and Pulugurtha, S., 2004, Cumulative Las Vegas Valley air quality modeling assessment of ongoing Bureau of Land Management (BLM) federal land disposition actions within the BLM Disposal Boundary: University of Chicago and University of Nevada Las Vegas, Report prepared for the Bureau of Land Management (BLM).

Lemaire, I., Dionne, P., Nadeau, D., and Dunnigan, J., 1989, Lung reactivity to natural and man-made fibrous silicates following short-term exposure. Environmental Research 48: 193-210.

McBride, M.B. 1994. Environmental Chemistry of Soils. Oxford University Press, New York, New York, pp. 327-328.

McLaurin, B., Goossens, D., and Buck, Brenda, *in press,* Combining surface mapping and process data to assess, predict, and manage dust emissions from natural and disturbed land surfaces, *Geosphere*

Pascua, C., J. Charnock, D.A. Polya, T. Sato, S. Yokoyama, and M. Minato. 2005. Arsenic-bearing smectite from the geothermal environment. Mineralogical Magazine, 69:897-906.

Peters, A., Wichmann, H., Tuch, T., Heinrich, J., Heyder, J., 1997. Respiratory effects are associated with the number of ultrafine particles. Am. J. Resp. Crit. Care Med.155,1376–1383.

Reheis, M.C., J.R. Budahn, P.J. Lamothe, and R.L. Reynolds. 2009. Compositions of modern dust and surface sediments in the desert southwest, United States. J. Geophysical Research, 114:FO1028.

Reid-Soukup, D.A. and A.L. Ulery. 2002. Smectites. In: J.B. Dixon and D.G. Schulze (eds.). Soil Mineralogy with Environmental Applications. Soil Science Soc. Of America, Madison, WI. pp. 467-499.

Reiss, B., Millette, J., and Williams, G., 1980, The activity of environmental samples in a cell culture test for asbestos toxicity. Environmental Research 22:315-321.

Rom, W.N., Casey, K. R., Parry, W.T., Mjaatvedt, C.H., and Moatamed, F., 1983, Heath implications of natural fibrous zeolites for the intermountain West. Environmental Research 30:1-8.

Rom, W., Casey, K., Parry, W., Mjaatvedt, C., Moatamed, F., 1983, Health implications of natural fibrous zeolites for the intermountain West. Environmental Research, 30:1-8.

Shao Y., 2008. Physics and Modelling of Wind Erosion (2nd Ed.). Springer Science + Business Media B.V., Dordrecht.

Sultan B, Labadi K, Guegan JF, and Janicot S (2005) Climate drives the meningitis epidemics onset in West Africa. PLoS Med 2(1): 43-49.

Sweeney, M., Etyemezian, V., Macpherson, T., Nickling, W., Gillies, J., Nikolich, G., McDonald, E., 2008. Comparison of PI-SWERL with dust emission measurements from a straight-line field wind tunnel. Journal of Geophysical Research 113, F01012. doi:10.1029/2007JF000830.

United States Environmental Protection Agency Regions 3, 6, and 9. (April 10, 2010). Regional Screening Levels for Chemical Contaminants at Superfund Sites. http://www.epa.gov/reg3hwmd/risk/human/rb-concentration_table/index.htm

US EPA, 1999. Compilation of air pollutant emission factors. Vol. I: stationary point and area sources. Report No. AP-42. US Environmental Protection Agency, Research Triangle Park, North Carolina, USA.

Wagner, J.C., Griffiths, D.M., Munday, D.E., 1987, Experimental studies with palygorskite dusts. British Journal of Industrial Medicine, 44:749-763.

Wang, K., You, D., Balakrishna, S., Ripple, M., Ahlert, T., Fahmy, B., Becnel1, D., Daly, M., Subra, W., McElduff, J.S., Lomax, L.G., Troxclair, D., and Cormier, S.A., 2008, Sediment from Hurricane Katrina: Potential to Produce Pulmonary Dysfunction in Mice. Int J Clin Exp Med 1, 130-144

Field Trip Schedule

9:00 a.m.	Depart Stop 1.	Continue north on I-15	See notes below on information about sights along the drive

Trip Notes: while driving to stop 2

Within minutes of leaving stop 1, as we drive north on I-15 you'll see an industrial park to your left (north). This industrial park continues through the intersection of I-15 and Hw 93. This is the Apex Industrial Park and is a large complex currently composed of four plants. Chemical Lime Company produces a variety of lime, such as chlorinated lime and unslaked lime as well as plant fertilizers, nutrients and herbicides. Georgia-Pacific Corporation is the worlds leading manufacturer of paper products, from tissue paper, to packing products as well as building construction supplies, such as sheet rock. US Avestor LLC is a battery manufacturing plant. It produces batteries ranging from the most basic alkaline battery to the less known fluorescent ballast battery units. Nevada Power Company is in the construction phase of a new power plant, which will implement the usage of two natural gas, fired combustion turbine generators as well as two Nooter Erickson HRSGs, one GE steam turbine, and a water-cooled condenser.

Throughout this portion of the drive, you'll note that the landscape is dominated by creosote.

Poster Child of the Mojave Desert, Creosote bush Larrea tridentata.

Douglas Merkler

The establishment and growth of desert plants are largely limited by the availability and distribution of water in soils, or the water supplying capacity of the landscape and its components. The ability of individual plants to utilize this soil moisture depends on the depth, lateral spread, and degree of overlap of their root systems (Casper and Jackson 1997). If there is a plant that represents the arid adaptation of a successful plant species in the southwest deserts, it might be the creosote bush, *L. tridentata.* Creosote bush is the most abundant and widely distributed shrub in the warm deserts of North America; in fact, its distribution is used to delineate the boundaries of the individual deserts.

The genus *Larrea* has four species *(L. divaricata, L. cuneifolia, L. nitida, L. ameghinoi*) in South America and one (*L. tridentata*) in North America. Work conducted by Kim Hunter at the UNLV Department of Biological Sciences in 2001 (Hunter et al. 2001) provided insight into a classic biogeographic pattern of the alignment of diploid, tetraploid and hexaploid races

of creosote bush (*Larrea tridentata*) across the Chihuahuan, Sonoran and Mojave Deserts of western North America. The ploidy of an organism or type of organism is a measure of how many copies of its basic chromosome set it contains. Three morphologically cryptic ploidy levels have been identified in *L. tridentate*: diploid (2n = 26) in the Chihuahuan Desert, tetraploid (4n= 52) in the Sonoran Desert and hexaploid (6n= 78) in the Mojave Desert.

This analysis led to the generalization that a different ploidy level is associated with each desert, and that increasing ploidy levels are aligned along a south–east to north–west gradient of increasing summer aridity and heat load. A plausible hypothesis is that polyploidy evolved as creosote bush encountered areas with progressively drier/hotter summers as it migrated from summer-wet areas of Mexico into higher latitudes of the southwestern United States. These early hypotheses about polyploid formation and shifting distributions were inspired by packrat midden evidence that pinyon–juniper woodlands, and not creosote bush, covered what are now desert elevations (300–1500 m) during the last glacial period.

Hunter's work involved a measurement on the geometry (area) of the guard cells adjacent to the stomata which correlated to the ploidy of the individual plant. By using fossil leaves extracted from packrat middens and radiocarbon dates (^{14}C) from the associated material in the midden, the story of the temporal migration of creosote bush into the southwestern deserts was told (Figure 1). At present, there is insufficient evidence to determine the exact timing or climatic circumstances for creosote bush migration from South to North America. The most likely time for the migration was during one or more Quaternary glaciations (the last 1.5 million years). During glaciations, the American tropics experienced drier episodes that probably closed the distance between semiarid habitats in the Andean highlands and Central American lowlands to less than 2000 km (e.g. Bradbury, 1997; Hooghiemstra & Van der Hammen, 1998; Harris & Mix, 1999).

Hypothetically, the hexaploid race could have evolved as creosote bush encountered hot, summer-dry areas at the northwestern limits of its range during either a glacial or interglacial period. Summer-dry areas would have been most extensive in Mexico and the southwestern United States during glacial periods (Bradbury, 1997). Stable isotopic analysis of soil carbonates and megafaunal tooth enamel, however, indicate considerable C_4 grass biomass, and at least moderately wet summers, along the Mexico-United States borderlands during the last glacial (Liu et al., 1996; Connin et al., 1998; Monger et al., 1998). Hence, if expansion into areas with dry summers drove the evolution of the hexaploid race, the most likely locus would have been one from central Baja California, the lower Colorado River basin and/or the present Mojave Desert. It is interesting to realize that most of the developed soils within the Mojave Desert are quite a bit older than the relative new arrival, creosote bush, which may have arrived in the Mojave as recently as 3,500 to 5,500 years ago.

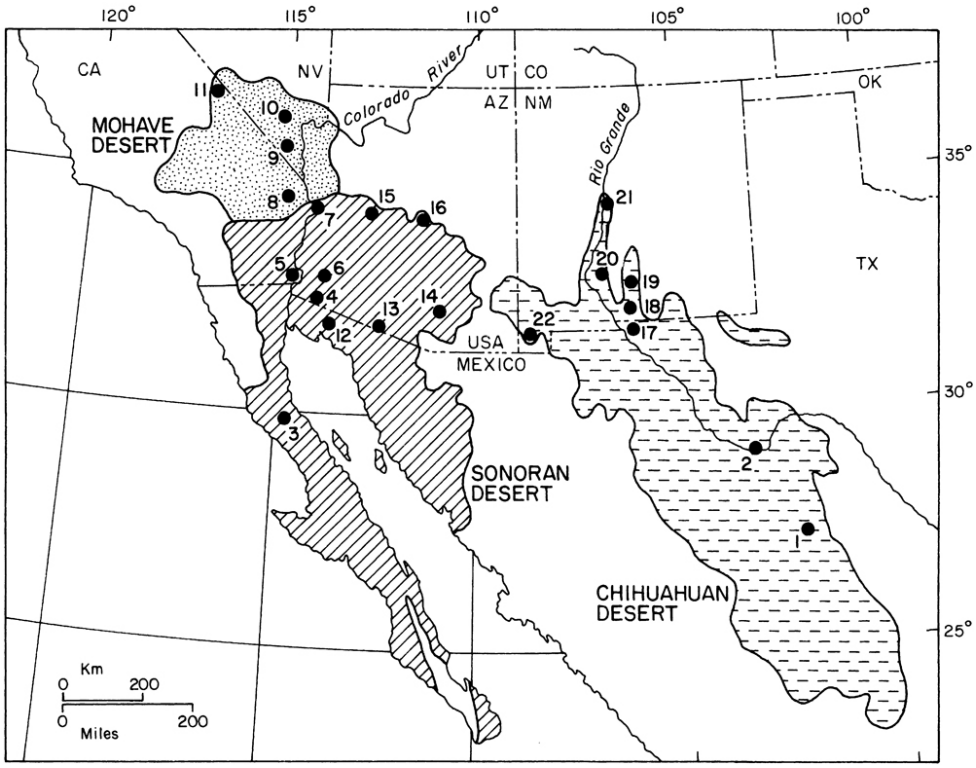

Fig. 1 Map of the arrival dates for Chihuahuan: 26 – 10 ^{14}C kyr BP, Sonoran: 8.5 - 6.4 ^{14}C kyr BP, and Mojave Deserts: 5.6 - 3.9 ^{14}C kyr BP, of North America. Ages are arrival dates given in 1,000's of ^{14}C years before present. The distribution of *Larrea tridentata* generally coincides with the boundaries of all three hot deserts. After Hunter et al., 2001

References:

Bradbury, J.P. (1997) Sources of glacial moisture in Mesoamerica. *Quaternary International*, 43/44, 97–110.

Casper, B.B., and R.B. Jackson, 1997. Plant competition underground. Annual Review of Ecology and Systematics 28:545-570.

Harris, S.E. & Mix, A.C. (1999) Pleistocene precipitation balance in the Amazon Basin recorded in deep sea sediments. Quaternary Research, 51, 14–26.

Hooghiemstra, H. & Van der Hammen, T. (1998) Neogene and Quaternary development of the neotropical rain forest: the forest refugia hypothesis, and a literature overview. Earth Science Reviews, 44, 147–183.

Hunter K. L. J. L. Betancourt B. R. Riddle T. R. Van Devender K. L. Cole W. G. Spaulding 2001 Ploidy race distributions since the last glacial maximum in the North American desert shrub, *Larrea tridentata*. *Global Ecology & Biogeography* 10: 521-533

Liu, B., Phillips, F.M. & Campbell, A.R. (1996) Stable carbon and oxygen isotopes of pedogenic carbonates, Ajo Mountains, southern Arizona: implications for palaeoclimatic change. Palaeogeography,Palaeoclimatology and Palaeoecology, 124, 233–246.

Monger, H.C., Cole, D.R., Gish, J.W. & Giordano, T.H. (1998) Stable carbon and oxygen isotopes in Quaternary soil carbonates as indicators of ecogeomorphic changes in the northern Chihuahuan Desert. Geoderma, 82, 137–172.

Trip Notes: while driving to stop 2 (cont.)

Stay on I-15 north, continue past exit 75 for highway 169 (Valley of Fire exit). Notice outcrops of Muddy Creek Formation (badlands exposures) as we continue northeast on I-15. More information on the Muddy Creek Formation can be found in Buck et al., Stop 2 (this volume).

Continue past exit 93 for Logendale & Overton (HY 169). Notice interstate climbs steeply upward to flat-topped Mesa. This surface is Mormon Mesa. Note thick petrocalcic horizons exposed in road cut. As we cross Mormon Mesa, note the eolian sand deposits (especially visible to the south).

Eolian sand covering Mormon Mesa. Photo by Doug Merkler.

Sahara Mustard (Brassica tournefortii)

by Douglas Merkler & Shawnalea Thai

Sahara mustard (*Brassica tournefortii*) is one of the top exotic invasive plants spreading through the southwestern deserts of North America. Sahara mustard is probably native to North Africa and Central Asia. In the Mojave Desert, it is common on roadsides, large washes, sand dunes, and disturbed areas. Sahara mustard germinates before many of the native annuals and as a result it has a competitive advantage over soil nutrients and moisture. As a winter annual, Sahara mustard seeds germinate after winter rainfall and population densities fluctuate as a function of available soil moisture and soil type.

Work by Suazo et al. 2008, has shown the depth of Sahara mustard seed in the soil seed bank may be greater than 5 cm and soil disturbance events may aid germination by bringing seeds to the soil surface where seeds have a better chance of emergence. Since 2004 studies have been conducted to draw attention to the spread of Sahara mustard through the Mojave Desert as well as to garner proposals for methods of control. Sahara Mustard is a coarse annual, which favors gravelly or sandy lowland desert regions, but has been found as high as 3,000 ft. Under optimum conditions Sahara Mustard leaves can grow as long as 50 cm, making it one of the largest desert herbaceous.

Chemical control can be an effective method of control if it applied early enough in the season and goats have even been considered for grazing control methods. However, *Brassica tournefortii* biotypes are resistant to acetolactate synthase (ALS)-inhibiting herbicides due to their possession of an ALS enzyme with decreased sensitivity to these herbicides, Boutsalis et al. 1999.

Boutsalis P., Karotam J., Powles S., 1999, Molecular basis of resistance to acetolactate synthase-inhibiting herbicides in *Sisymbrium orientale* and *Brassica tournefortii*, Pest Management Science, Volume 55 Issue 5, Pages 507 – 516.

Suazo, A.A., J.E. Spencer, and S.R. Abella. Response of Sahara mustard (*Brassica tournefortii*) to soil disturbance and water addition in the eastern Mojave Desert. Poster presentation at the Ecological Society of America 93rd annual meeting, Milwaukee, WI. 6 August 2008.

10:00 a.m.	Exit I-15 at east end of Mormon Mesa.	Unmarked exit at edge of mesa	Exit bus, take shuttle buses to Stop 2.

Logistical Notes for Stop 2

The two shuttles can haul only half of our group at a time. So, while the first shuttle group hears the talk at Stop 2, the shuttles will go back to pick up the other half of our group. When the shuttles return to Stop 2, the second group will then hear the talk for the stop while the shuttles return the first group back to the buses.

10:15 a.m.	**Stop 2** for first half of our group.	***Mormon Mesa Petrocalcic***	15 min. talk followed by time at the outcrop
10:25 a.m.	*Shuttles return to buses and pick up second half of our group.*		
10:35 a.m.	**Stop 2** for second half of our group	***Mormon Mesa Petrocalcic***	15 min. talk followed by time at the outcrop
10:50 a.m.	*Shuttles begin return trips to buses (group 1)*		
11:10 a.m.	*Shuttles pick up group 2 to return to buses*		
11:30 a.m.	Everyone is back at the buses. Depart for Stop 3.	Drive southwest on I-15 (returning towards Las Vegas), exit highway 169, south towards Logandale & Overton.	
	Lunch on the buses.		

Stop 2. Mormon Mesa

Genesis of Mormon Mesa Petrocalcic Horizons: Implications for Paleoclimate and Isotopic Dating Applications

Brenda J. Buck[1], Amy L. Brock[2], Colin Robins[1]

[1]Dept. Geoscience, University of Nevada Las Vegas, Las Vegas NV buckb@unlv.nevada.edu;
[2]Dept. Geology, University of Tennessee at Chattanooga, Chattanooga, TN

The soil on Mormon Mesa, NV, may be the oldest, continuously forming, petrocalcic soil on Earth. It is certainly one of Earth's rare and endangered soils, forming on a geomorphic surface that is millions of years old. Because of this, Lower Mormon Mesa is being considered for designation by the Las Vegas District BLM as an Area of Critical Environmental Concern, ACEC. If accepted, this will be the first instance of a special management area being established as the result of a unique and rare soil (i.e. Drohan and Farnham, 2006).

Soils developed in arid and semiarid regions accumulate pedogenic calcium carbonate over time. The carbonate forms from a combination of Ca^{2+} ions (primarily brought in from dust), water from rainfall, and CO_2 from plant respiration (Gile et al., 1966; Rech et al., 2003). Over time, as calcium carbonate accumulates in the soil a change in soil morphology occurs – from Stage I through Stage VI morphology (Gile et al., 1966; Bachman and Machette, 1977) (Fig. 1).

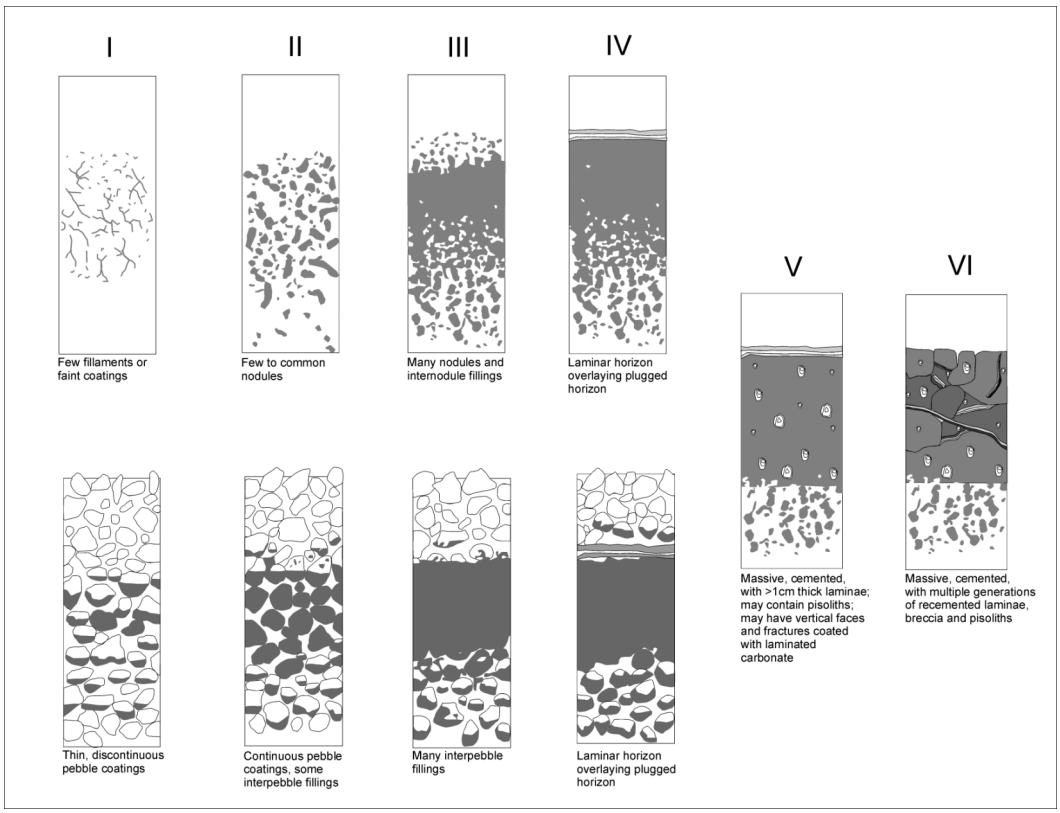

Figure 1. Stages of pedogenic calcium carbonate morphology after Gile et al., 1966 and Bachman and Machette, 1977. Figure by Amy Brock.

Although late-stage petrocalcic horizons can be found in numerous areas, we still lack a full understanding of the processes that occur in the later stages of carbonate morphology worldwide (Hay and Reeder, 1978; Arakel, 1979; Calvet and Julia,1983; Machette,1985; Dhir et al., 2004; Hirmas and Allen, 2007; Francis et al., 2007).

The definitions of Stage V and VI carbonate morphology includes the possible presence of pisoliths, which were described by Bachman and Machette (1977) as rounded (0.5-10 cm) fragments of pedogenic carbonate with enveloping concentric laminae that may also contain interiors of broken or disrupted laminae (Fig. 2).

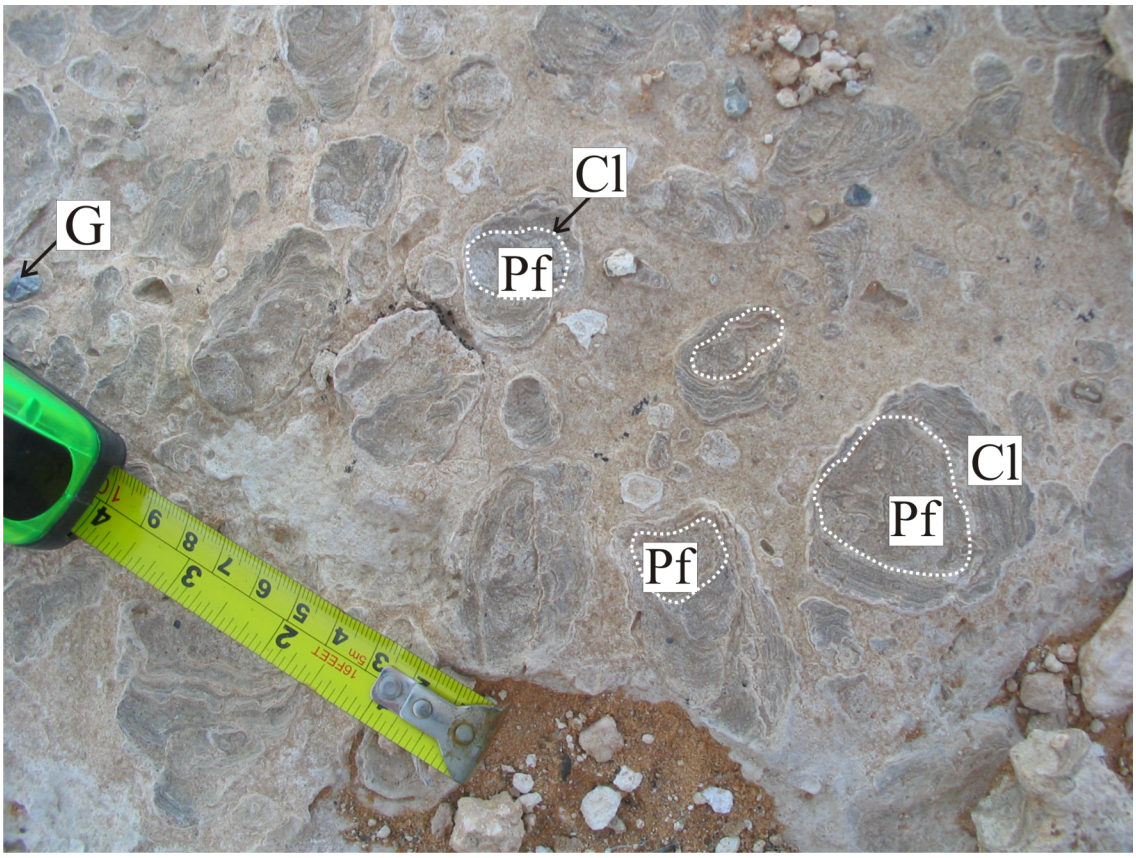

Fig. 2. Pisoliths in plan view. Pf = petrocalcic fragment nuclei. Cl = concentric lamina. G = gravel clast. From Brock and Buck, 2009.

Although pisoliths are used in the definitions of Stage V and VI carbonate morphology, how these pisoliths form and what they indicate about former (or current) soil processes was unknown previous to our study. Therefore, we began our research of the Mormon Mesa petrocalcic horizons in an attempt to better understand the genesis of Stage VI petrocalcic horizons, their pisoliths, and associated authigenic minerals including palygorskite and sepiolite. Because of the location of Mormon Mesa, this research also provides information for the timing of the incision of the lower Colorado River and formation of the Grand Canyon, as well as providing information to help interpret other highly developed petrocalcic horizons worldwide.

Mormon Mesa lies approximately 100 km northeast of Las Vegas Nevada (Fig. 3). This flat-topped mesa stands ~ 200 m above the Virgin River to the east and the Muddy River and Meadow Valley wash to the west. The top of the mesa is capped by a series of petrocalcic horizons, overlain by eolian sediments of various thicknesses. Underlying the petrocalcic horizons is the Miocene to early Pliocene Muddy Creek Formation (Kowallis and Everett, 1986).

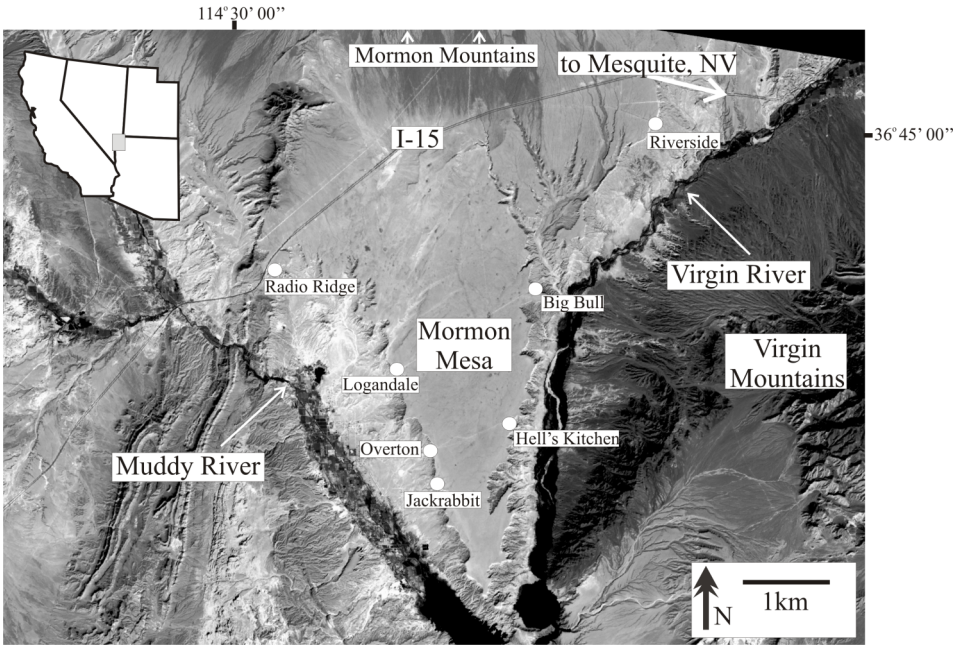

Fig 3. Location of Mormon Mesa and petrocalcic soil profiles. From Brock and Buck, 2009.

The Muddy Creek Formation has been dated from 11 to 5 Ma using fossils and absolute dating of volcanic deposits. It is composed of interbedded fluvial sand and gravel, lacustrine gypsum and travertine, eolian sand, and numerous paleosols. The Muddy Creek Formation was deposited in a series of structurally-controlled basins that, although interconnected during the Miocene, were internally-drained prior to integration of the Colorado River system (Pederson, 2008). Although still controversial (Polyak et al., 2008a; Pederson et al., 2008; Pearthree et al., 2008; Polyak et al., 2008b), much data exists to support the conclusion that incision of the Grand Canyon began approximately 6 to 5 Ma. Evidence for a thorough-flowing river system includes Colorado River sediment in the Gulf of California at 5.3 Ma (Dorsey et al., 2007) and a series of lakes south of present-day Lake Mead between ~5.6 and 4 Ma (House et al., 2005). Lava flows that are mixed with river gravels occur within ~ 110 m of current river elevation in the western end of the Grand Canyon (Howard and Bohannon, 2001). These indicate that the vast majority of the Grand Canyon incision had occurred by 4.7-4.4 Ma. Soil development on Mormon Mesa was initiated when incision of the Colorado River and associated tributaries (Virgin and Muddy rivers) focused fluvial processes away from this now-topographically higher area. At what time this occurred depends upon how fast the Virgin and Muddy rivers responded to incision along the Colorado River and/or local tectonics that could have affected base level. As calcic and petrocalcic horizons developed in the soil capping the mesa, it became more and more resistant to erosion, and is now a prominent part of the landscape.

The petrocalcic horizons capping Mormon Mesa were characterized and interpreted by Brock (2008) and Brock and Buck (2009). The following information is summarized from those publications. The Mormon Mesa soil consists of 4 distinct petrocalcic horizons (transitional, laminar, massive, and brecciated) overlain by a set of soil horizons formed in unconsolidated eolian sediments that vary greatly in thickness and type across the landscape (Fig. 4) (Brock, 2008; Brock and Buck, 2009). The total thickness of only the 4 petrocalcic horizons ranges from 175 to 405 cm.

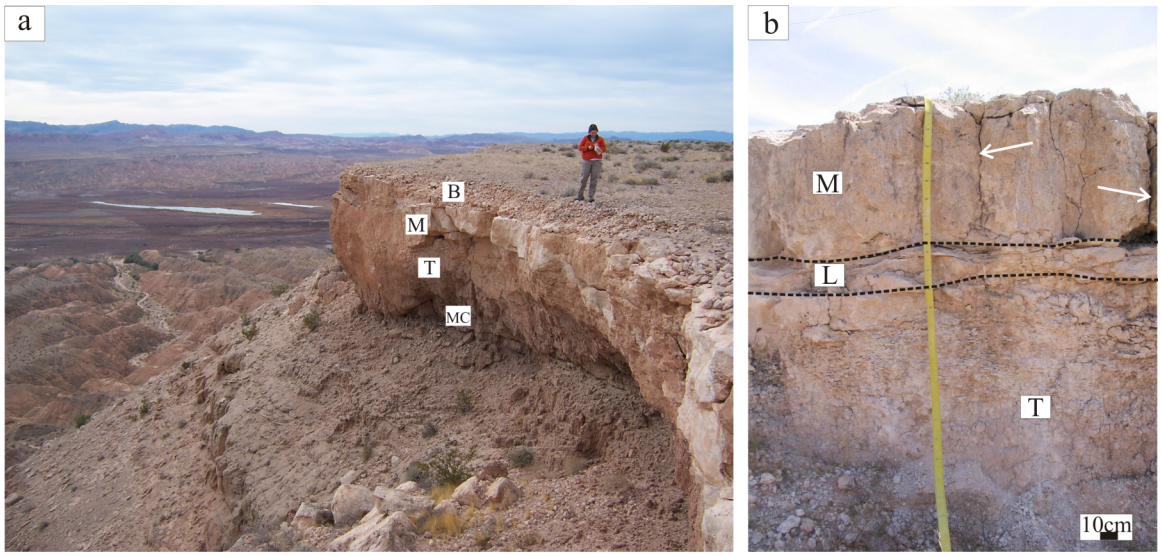

Figure 4. (a) Soil profile at Stop 2. From base to top: Muddy Creek Formation (MC) with Transitional horizon (T) formed in upper part, Massive horizon (M) with overlying Brecciated horizon (B) at surface. The laminar horizon is missing at this site. Dr. Brock for scale. (b) Radio Ridge profile (see Fig X) showing Transitional horizon (T), with overlying Laminar horizon (L) (marked with dotted lines), and Massive horizon (M). The Brecciated horizon is eroded at this location. White arrows point to open vertical cracks (from Brock and Buck, 2009).

The lowermost petrocalcic horizon is the transitional horizon, which is formed within the uppermost deposits of the Muddy Creek Formation. The transitional horizon ranges in thickness from 60-275 cm, and grades from stage II carbonate nodules, calcified root casts, and clasts with pendants at the base to a strongly indurated stage III petrocalcic horizon at the top.

In most locations on the mesa a laminar horizon, 10-35 cm thick, lies above the transitional horizon *(note: the laminar horizon is not present at the fieldtrip site – stop 2).* The laminar horizon is composed of 1-2 mm thick individual laminae, and often contains ooids and/or pellets (Hay and Wiggins, 1980).

The massive horizon is present everywhere on the mesa and ranges in thickness from 45 to 165 cm, with bulk densities that range from 2.2 to 2.8 g/cm^3. The massive horizon is characterized by well-rounded sand-sized eolian quartz grains cemented in the calcium carbonate matrix and abundant soil pisoliths (0.2 to 5.5 cm diameter). The pisoliths have nuclei of rounded petrocalcic fragments, chert clasts, and chert clasts with rotated pendants (Figs 5, 6). In plan view, the nuclei are enveloped with multiple, concentric, calcium carbonate laminae – which lead to their original description as pisoliths by Bachman and Machette (1977). However, when

viewed in cross-section, the nuclei of the pisoliths have pendant laminae extending vertically from their base (i.e. Brock and Buck, 2005) (Fig. 5, 6). ***Therefore, these pisoliths are the remnants of pendants and their presence in an otherwise fine-grained stage V or VI petrocalcic horizon is an indication that coarse fragments with pendants once existed in the profile***. In many cases the original coarse-grained clasts are no longer present because they have been dissolved thorough pressure solution (see discussion at the end of this paper). In the massive horizon, most of the pendant laminae that emanate from the pisoliths are vertical. However, commonly there are two distinct directions of pendant laminae (Fig. 6) and in some cases, there are more than two sets of pendant laminae extending in multiple directions from a single nucleus.

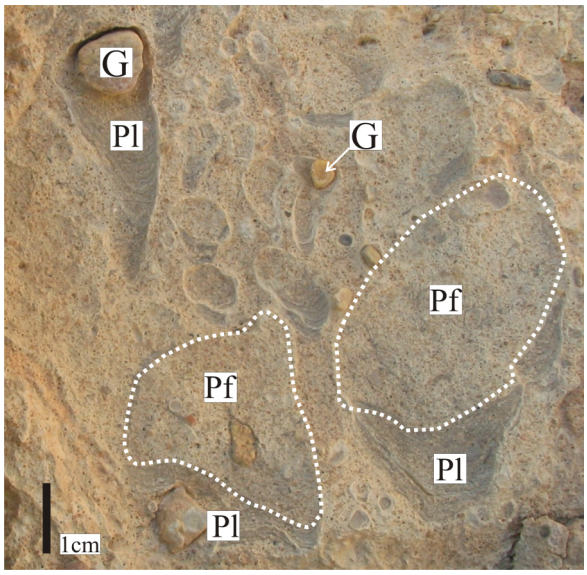

Figure 5. Viewed in cross-section, pisoliths are pendants. Gravel nuclei (G) with pendant lamina (Pl), Petrocalcic fragment nuclei (Pf) with pendant lamina (Pl) (from Brock and Buck, 2009).

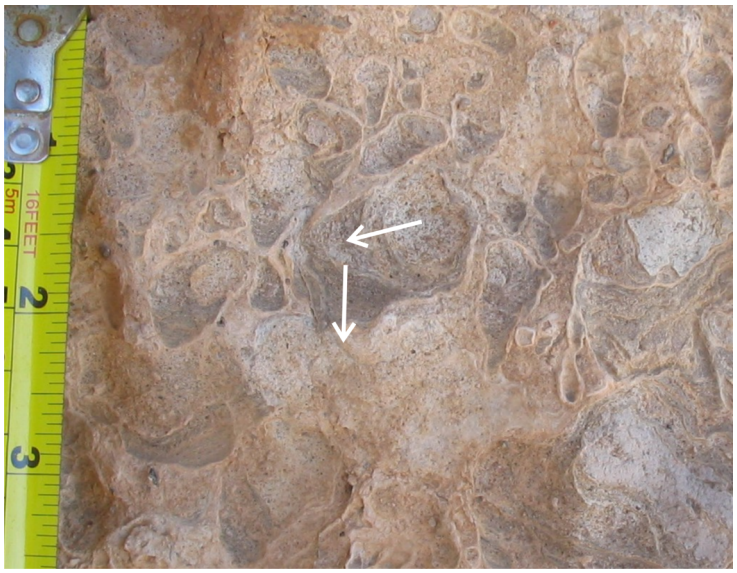

Figure 6. Two distinct directions of pendant laminae from pisoliths in the Massive horizon (from

Brock and Buck, 2009).
The brecciated horizon is the uppermost petrocalcic horizon. It is composed of brecciated blocks of stage VI petrocalcic fragments mixed with unconsolidated eolian sediments. Pendant laminae are present underneath most blocks and the blocks themselves are composed of multiple re-cemented petrocalcic fragments with multiple directions of pendant laminae. The unconsolidated eolian materials overlying the petrocalcic horizons have been described by NRCS soil survey and classified as a loamy, carbonatic, thermic, shallow Calcic Petrocalcid (see Appendix A).

Vertical cracks, up to 12 cm wide, commonly extend from the top of the massive horizon through to the underlying transitional horizon (Fig. 4b). These cracks can be completely or partially filled with calcium carbonate lamina and/or eolian sediment. When exposed at the surface, these cracks form a meter-scale polygonal pattern similar to large desiccation cracks found in salt-indurated soils in the Atcama Desert (Buck et al., 2006).

Brock and Buck (2009) interpreted the genesis of these horizons as follows (Fig. 7):

- Soil formation begins because of Colorado River incision some time after ~ 6 Ma but likely before ~ 4 Ma
- Initial soil formation in upper Muddy Creek sediments form stage II nodules in transitional horizon. (Coincides with pre-3.2 Ma 'wetter' middle-late Pliocene climate (Smith et al., 1993) = increased depth of wetting).
- Formation of stage III carbonate morphology at top of transitional horizon forms because of decreased depth of wetting caused by increased aridity and/or as a result of eolian deposition at surface which moves the depth of wetting and zone of carbonate accumulation upward. (Correlated to general trend of increasing aridity from 3.2 to 2.8 Ma (Smith et al. 1993).
- Estimated time for entire transitional horizon formation ~ > 1 Ma.

- Significant erosional event occurs – likely caused by shift to a more arid climate at ~ 2.8 Ma (Winograd et al., 1985; Ruddiman and Kutzback, 1989; Smith et al., 1993; Wakabayashi and Sawyer, 2001).
- Transitional horizon is exposed and fragments of its petrocalcic horizon, and stage II pendants are strewn across surface as finer material is removed.
- Significant eolian depositional event occurs – may have been after or concurrent with erosion of the transitional horizon. Result is eolian sands mixed with petrocalcic fragments, and stage II pendants derived from underlying transitional horizon.

- A period of soil formation and surface stabilization occurs (~ 2.8 to 2.0 Ma). Depth of wetting in most locations reaches underlying transitional petrocalcic horizon, resulting in formation of laminar horizon.
- Presence of biological features indicates rooting. Coarse petrocalcic fragments and stage II pendants are well-mixed in eolian material indicating bioturbation.
- Depth of wetting decreases – either through increased aridity or continued eolian deposition on surface. Vertical pendants form underneath coarse clasts (petrocalcic fragments and previous generation of state II pendants).
- Continued soil formation eventually indurates eolian sand and petrocalcic fragments and pendants. Massive horizon formed.

- Significant erosional event occurs. Upper portion of massive horizon exposed, broken into fragments.
- Significant eolian depositional event occurs – mixing new eolian sand with petrocalcic blocks from underlying massive horizon.
- Soil stabilization occurs. Pedogenic carbonate forms pendants on undersides of petrocalcic fragments. Continued soil formation re-cements petrocalcic blocks in multiple orientations.
- Repeat of erosion/deposition/soil formation & re-cementation multiple times – forms the brecciated horizon. Repeated cycles likely reflect Pleistocene glacial/interglacial cycles.

The processes explained above (erosion, deposition, depth of wetting for carbonate precipitation) are not uniform across the landscape nor through time. Therefore, the characteristics of each petrocalcic horizon vary spatially.

Implications for future isotopic dating:
The relative ages of pedogenic features from oldest to youngest:

1. Stage II nodules at the base of the transitional horizon
2. Pendant lamina under gravels in the mid- to upper transitional horizon and pendant lamina in rotated pisoliths of the massive horizon (which were derived from the transitional horizon).
3. Stage III petrocalcic material in the upper transitional horizon and petrocalcic fragments that are nuclei of pisoliths in the massive horizon.
4. Fragments of stage IV laminar pieces in center of pisoliths in the massive horizon (derived from rare laminae formed on top of transitional horizon).
5. Vertical pendants extending from pisoliths in the massive horizon and/or laminar horizon (oldest lamina at bottom and youngest at top).
6. Calcium carbonate that cements pisoliths in the massive horizon (matrix carbonate).
7. Calcium carbonate that cements fragments of previously eroded massive horizon, now present in brecciated horizon & oldest pendants on these fragments
8. Youngest pendants on petrocalcic blocks in brecciated horizon.

Dr. Colin Robins, using diamond blade saw to obtain samples of Mormon Mesa Petrocalcic horizon.

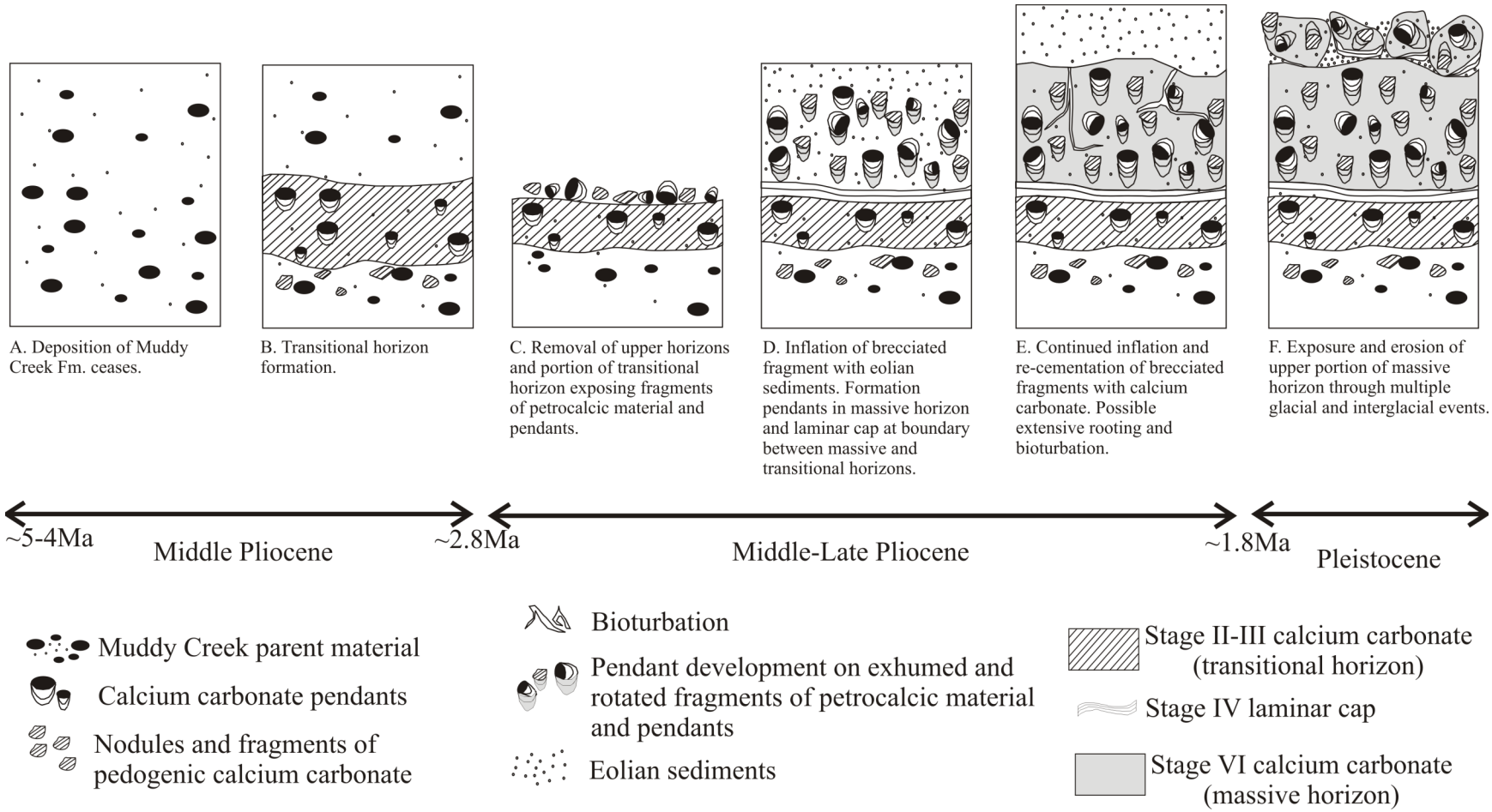

Figure 7. Model for genesis of Mormon Mesa petrocalcic horizons (from Brock and Buck, 2009).

Genesis of authigenic clays: Palygorskite & Sepiolite

Force of crystallization (Weyl, 1959) acting in tandem with fluctuating soil solution chemistry describes a process which partially or entirely fractures, dissolves, and replaces engulfed primary grains and rock fragments in stage II carbonate pendants, stage III-VI petrocalcic soils, and some near-surface, alkaline diagenetic environments. Also called pressure solution, this process has been previously described for calcic and petrocalcic environments (Bachman & Machette, 1977; Watts, 1978; Hay & Wiggins 1980; Watts 1980; Reheis, 1988; Monger & Daugherty, 1991a; Monger & Kelly, 2002; Brock & Buck, 2005) including Mormon Mesa, Nevada (Brock, 2007; Brock & Buck, 2009). This process is well known in the geologic literature as an important process of diagenesis and was recognized as early as the mid 1800's (i.e. Sorby 1863, 1865; Trurnit, 1968; McClay, 1976; Rutter, 1983; Etheridge et al., 1984; Lehner and Bataille, 1985; Lehner, 1995; Bresme and Camara, 2006).

In soils, pressure solution can only occur if grain displacement is prevented because the material is confined. This can occur in any hardpan or within well-cemented areas. In calcic soils this occurs in stage III-VI petrocalcic horizons and within stage II pendants. Under such conditions, when a fluid enters a pore space, it becomes confined between the rigid walls of the hardpan. Depending upon the chemical potential of the solution and that of the solid crystal pore walls, crystallization of a new mineral can occur. The force of crystallization is the force exerted upon the pore walls by this growing crystal. Dissolution of the primary grains (i.e. pore walls) occurs because of differences in chemical potential in a thin solution film as a new crystal precipitates out of solution (i.e. Robin, 1978; Kim and Myerson, 1996; Chatterji and Thaulow, 1997; Steiger, 2005a,b). Even minerals generally considered the most stable (i.e. quartz) are dissolved through this process. Dissolution of the primary grains can only occur when a solution is present because the solid material is removed by diffusive transport through the thin solution film (Raj, 1982; Maliva and Siever, 1988; Lehner and Bataille, 1984/1985; Lehner, 1995; Spiers and Schutjens, 1999). There is some evidence that pressure solution is increased when clay minerals are present because their presence results in a higher chemical potential and drives dissolution (Aharonov and Katsman, 2009).

Dissolution of silicate grains during the force of crystallization process releases complexes of Si^{4+} (e.g. H_2SiO_4), Al^{3+} (e.g., Al_2OH_3), and other ions into the soil solution. In addition, the high pH of petrocalcic soil environments permits unusually high Si and Al activities as compared to other soils. Amorphous silica phases are especially soluble above pH 9 (Drees et al., 1989), however, some researchers report that silanol groups start to ionize at or above pH 7 (Yariv & Cross, 2002). Aluminum solubility is comparable to that of Si under highly alkaline conditions (Velde, 1992), and may especially increase above pH 8.5 (Hay & Wiggins, 1980). These conditions are easily met within the Mormon Mesa petrocalcic horizons, where pH values approach or exceed 10 (Brock, 2008; Robins, 2010). Other soil environmental factors, including common ion effects and the presence of organic matter, can also catalyze grain dissolution (Drees et al., 1989). Once released to solution, Si^{4+} and Al^{3+} complexes can directly fuel the precipitation of pedogenic palygorskite and sepiolite clays (Weaver & Beck, 1977; Watts, 1980; Verrecchia & Le Coustumer, 1996; Singer, 1989; Monger & Daugherty, 1991a&b; Singer et al., 1995).

Palygorskite, $Si_8Mg_5O_{20}(OH)_2(OH_2)_4 \bullet 2H_2O$ (Singer, 1984), and sepiolite, $Si_{12}Mg_8O_{30}(OH)_4(OH_2)_4 \bullet 8H_2O$ (Brauner & Preisinger, 1956; Singer, 1984; García-Romero et al., 2007) are fibrous, high-magnesium phyllosilicates that are relatively rare in terrestrial sediments, yet fairly typical of late-stage petrocalcic soils (i.e. Jones & Galan, 1988; Monger and Daugherty, 1991b). In fact, both palygorskite and sepiolite can each comprise nearly 100 % of the non-carbonate clay-sized particle fraction of certain petrocalcic profiles (Watts, 1980; Jones & Galan, 1988; Francis et al., 2007). The predominance of these clays in calcic soils may also indicate that they eventually replace other, detrital phyllosilicate species such as smectite or illite.

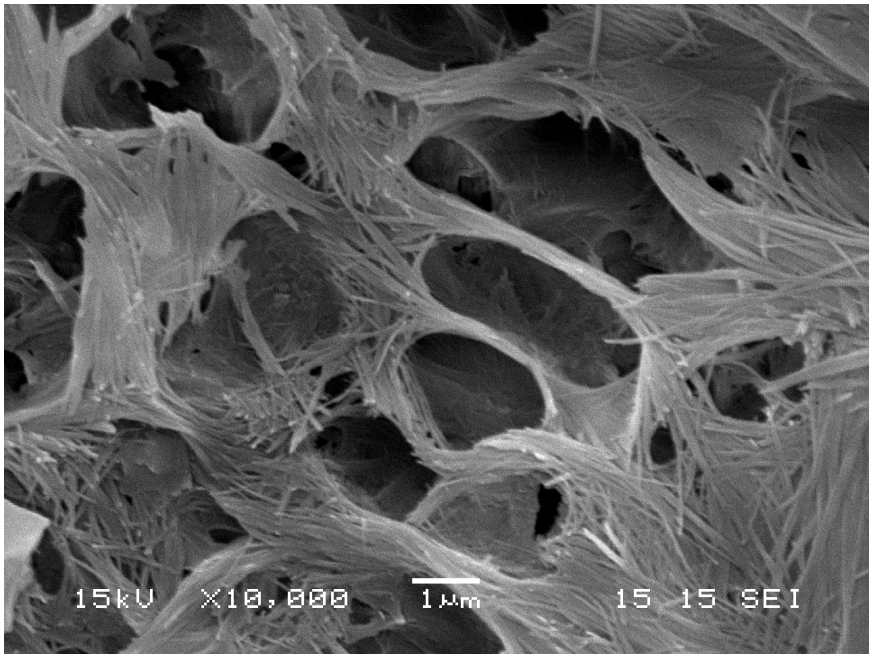

Fig. 8. Fibrous phyllosilicates (sepiolite and/or palygorkskite) can occur as a porous meshwork of crystallites, commonly intergrown with pedogenic carbonate and other secondary mineral phases. It is speculated that pores or void spaces in this image may once have been filled by carbonate rhombs, which have subsequently dissolved and left behind the meshwork of fibrous silicate clays.

The minerals that compose the petrocalcic horizons at Mormon Mesa are the product of chemical feedbacks and thresholds operating across geological timescales and significant climatic changes. Once the pedogenic carbonate becomes indurated, continued precipitation of calcite leads to dissolution of primary silicate grains through the force of crystallization causing pressure solution. Calcite crystallization also changes the partial pressure of CO_2 and increases the activity of Mg^{2+} relative to Ca^{2+} (Watts, 1980; Reheis 1988; Deocampo, 2005). As stated above, the Si and Al ion complexes produced by silicate dissolution may combine with Mg^{2+}, OH^-, and other ions to generate fibrous phyllosilicates or, in Mg-poor solutions, amorphous silica (Weaver & Beck, 1977; Watts, 1980; Reheis, 1988; Singer, 1989; Monger & Daugherty, 1991a; Singer et al., 1995; Verrecchia & Le Coustumer, 1996). It is generally accepted that palygorskite forms at higher Al^{3+} activities, whereas sepiolite precipitates instead during low Al^{3+} conditions (Hay & Wiggins, 1980; Jones, 1983; Jones & Galan, 1988; Singer, 1989). However, intergrowths of the two clays are possible and reflect oscillating soil solution chemistry.

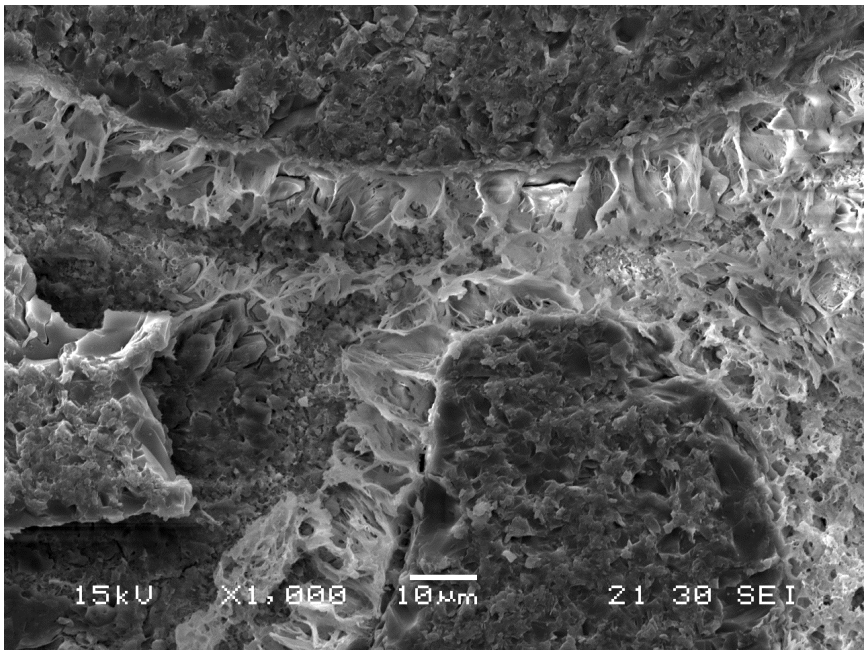

Fig. 9. Fibrous phyllosilicates (Palygorskite or Sepiolite) surround and radiate outward perpendicularly from rounded quartz grains (top and bottom, darker regions) engulfed by pedogenic carbonate in the massive horizon of the Mormon Mesa soil (the quartz grains "float" in a carbonate matrix in what is sometimes called K-fabric). This morphology can be interpreted to reflect the close association between dissolution of primary silicates by calcite force of crystallization, and precipitation of sepiolite or palygorskite clays from evaporative soil solutions in micropores adjacent to primary silicate grains.

Amorphous silica can precipitate when there is insufficient Mg for sepiolite growth, when soil chemical thresholds (e.g., pH) are crossed, and/or when local soil solutions are reduced to a gel-like state by progressive evaporation and mineral growth (Hay & Wiggins, 1980). Silica spheroids have been found crystallized upon the tips of palygorskite and sepiolite fibers in petrocalcic soils (Brock, 2007) and in some alkaline diagenetic environments (Weaver & Beck, 1977). Thus, it is likely that silica most often precipitates just before total solution evaporation, but after calcite and/or magnesian clay. Saline conditions or high contents of dissolved CO_2 may also influence silica and phyllosilicate precipitation (Watts, 1980; Jones & Galan, 1988; Deocampo, 2005). Completing the feedback cycle, formation of magnesian phyllosilicates decreases Mg^{2+} soil solution activity relative to Ca^{2+} (Weaver & Beck, 1977; Watts, 1980) and creates an environment conducive to renewed calcite growth and primary grain dissolution, given continued influx or reserves of soil solution, Ca^{2+}, and dissolved CO_2. Palygorskite may also adsorb Mg^{2+} preferentially over Ca^{2+}, further forcing conditions favorable to calcite crystallization (Weaver & Beck, 1977). Precipitation of palygorskite and sepiolite is especially favored in zones of textural contrast, whether along soil horizon contacts or within soil micropores, where water is more likely to be present (Yaalon & Wieder, 1976; Bouza et al., 2007; Duniway et al., 2007).

Conceptual models depicting this complex cycle of mineral genesis within the context of Quaternary climate oscillations have been described by Robins (2010). These models will be presented in detail in future publications with Brenda Buck and Amy Brock.

Acknowledgements
Funding for this research was provided by NSF-SGER, Geological Society of America, American Association of Petroleum Geologists, Sigma Xi Research Society, the Jack and Fay Ross Family Fellowship, UNLV Graduate Professional Student Association, and UNLV Presidential Fellowship. Thank you to Doug Merkler, Debbie Soukup, Mike Howell, Jan Brock, Curtis Monger, Caroline Sauvage-Robins, Mandy Williams, and numerous UNLV students who assisted in various aspects of this study.

References

Aharonov, E., and Katsman, R., 2009, Interaction between pressure solution and clays in stylolite development: insights from modeling. American Journal of Science. 309:607-632.

Arakel, A.V., 1979. Genesis of calcrete in Quaternary soil profiles, Hutt and Leeman lagoons, Western Australia. J. Sediment. Petrol. 521, 109–125.

Bachman, G.O., Machette, M.N., 1977. Calcic Soils and Calcretes in the Southwestern United States., USGS: Open-File Report 77–797, 163p.

Bresme, F., and Camara, L.G., 2006, Computer simulation studies of crystallization under confinement conditions. Chemical Geology. 230:197-206.

Bouza, P.J., Simón, M., Aguilar, J., del Valle, H., and Rostagno, M., 2007. Fibrous-clay mineral formation and soil evolution in Aridisols of northeastern Patagonia, Argentina. Geoderma, 139: 38-50.

Brauner, K. and Preisinger, A., 1956. Estruktur und Enstehung des sepiolits. Tschermaks Mineralogische und petrographisches Mitteilungen, 6:120-140.

Brock, A.L., 2008. Characterization of stage VI petrocalcic horizons: S. Nevada and N.W. Arizona, PhD dissertation, Univ. of Nevada, Las Vegas. 148 pp.

Brock, A. L., and Buck, B. J., 2009, Polygenetic development of the Mormon Mesa, NV petrocalcic horizons: Importance for future application of absolute dating techniques, Catena (1), p. 65-75.

Brock, A.L., Buck, B.J., 2005. A new formation process for calcic pendants from Pahranagat Valley, Nevada, USA, and implication for dating Quaternary landforms. Quaternary Research 63, 359–367.

Buck, B.J., Rech, J., Howell, M., Prellwitz, J., Brock, A., 2006. A new formation process for patterned ground, Atacama Desert, Chile. Geol. Soc. Am. Abstr. Prog. 38 (7), 520.

Calvet, F., Julia, R., 1983. Pisoids in the caliche profiles of Tarragona N.E. Spain. In: Peryt, T.M. (Ed.), Coated Grains. Springer, Berlin–Heidelberg–NewYork, pp. 456–473.

Chatterji, S., and Thaulow, N., 1997, Unambiguous demonstration of destructive crystal growth pressure. Cement and Concrete Research. 27:6:811-816.

Deocampo, D., 2005. Evaporative evolution of surface waters and the role of aqueous CO2 in magnesium silicate precipitation: Lake Eyasi and Ngorongoro Crater, northern Tanzania. South African Journal of Geology, 108: 493-504.

Dhir, R.P., Tandon, S.K., Sareen, B.K., Ramesh, R., Rao, T.K.G., Kailath, A.J., Sharma, N., 2004. Calcretes in the Thar desert: genesis, chronology and palaeoenvironment. Earth Planet. Sci. Let. 113, 473–515.

Dorsey, R., Fluette, A., McDougall, K., Housen, B., Janecke, S., Axen, G., and Shirvell, C., 2007, Chronology of Miocene-Pliocene deposits at Split Mountain Gorge, Southern California: a record of regional tectonics and Colorado River evolution. Geology. 35:1:57-60. doi: 10.1130/G23139A.1

Drees, L.R., Wilding, L.P., Smeck, N.E. and Senkayi, A.L., 1989. Silica in soils: Quartz and disordered silica polymorphs. In: Dixon, J.B. and Weed, S.B., eds., Minerals in soil environments, 2nd edition. SSSA Book Series 1. Madison, Soil Science Society of America: 913-974.

Drohan, P. and Farnham, T., 2006, Protecting life's foundation, Soil Science Society of America Journal, 70:2086-2096

Duniway, M.C., Herrick, J.E., and Monger, H.C., 2007, The high water-holding capacity of petrocalcic horizons. Soil Science Society of America Journal, 71:3:812-819.

Etheridge, M., V. Wall, S. Cox, and R. Vernon (1984), High fluid pressures during regional metamorphism and deformation: implications for mass transport and deformation mechanisms, J. Geophys. Res., 89(B6), 4344-4358.

Francis, M.L., Fey, M.V., Prinsloo, H.P., Ellis, F., Mills, A.J., and Medinski, T.V., 2007. Soils of Namaqualand: Compensations for aridity. Journal of Arid Environments, 70: 588-603.
García-Romero, E., Suárez, M., Santarén, J., and Alvarez, A., 2007. Crystallochemical characterization of the palygorskite and sepiolite from the Allou Kagne deposit, Senegal. Clays and Clay Minerals, 55 (6): 606-617.
Gile, L.H., Peterson, F.F., Grossman, R.B., 1966. Morphological and genetic sequences of carbonate accumulation in desert soils. Soil Sci. 1015, 347–360.
Hay, R.L., Reeder, R.J., 1978. Calcretes of Olduvai Gorge and the Ndolanya Beds of Northern Tanzania. Sedimentology 25, 649–673.
Hay, R.L., Wiggins, B., 1980. Pellets, ooids, sepiolite and silica in three calcretes of the Southwestern United States. Sedimentology 27, 559–576.
Hirmas, D.R., and Allen, B.L., 2007, Degradation of pedogenic calcretes in west Texas. Soil Science Society of America Journal. 71:6:1878-1888.
House, P.K., Pearthree, P.A., Howard, K., Bell, J.W., Perkins, M.E., and Brock, A.L., 2005, Birth of the lower Colorado River – stratigraphic and geomorphic evidence for its inception near the conjunction of Nevada, Arizona, and California. IN Pederson, J., and Dehler, C.M., eds. Interior Western United States Geological Society of America Field Guide 6, p. 357-387.
Howard, K.A. and Bohannon, R.G., 2001, Lower Colorado River; Framework, Neogene deposits, incision, and evolution, in Young, R.A., and Spamer, E.E., eds., The Colorado River: Origin and evolution: Grand Canyon, Arizona, Grand Canyon Association Monograph 12, p. 101–105.
Jones, B.F. and Galan, E., 1988. Sepiolite and palygorskite. Reviews in Mineralogy, 19(1): 631-674.
Jones, B.F., 1983. Occurrence of clay minerals in surficial deposits of southwestern Nevada. Sciences Géologiques Mémoires (Strasbourg), 72: 81-92.
Kim, S., and Myerson, A.S., 1996, Metastable solution thermodynamic properties and crystal growth kinetics. Ind. Eng. Chem. Res. 35:1078-1084.
Kowallis, B.J., Everett, B.H., 1986. Sedimentary environments of the Muddy Creek Formation near Mesquite, Nevada. Sed. Assoc. Pub. 15, 69–75.
Lehner, F., 1995, A model for intergranular pressure solution in open systems. Tectonophysics. 245:153-170.
Lehner, F.K. and Bataille, J., 1984/85. Nonequilibrium thermodynamics of pressure solution. Pure Appl. Geophys., 122:53 85.
Machette, M.N., 1985. Calcic soils of the Southwestern United States. Geol. Soc. Am. Spec. Paper 203, 1–21.
Maliva, R. and Siever, R., 1988, Diagenetic replacement controlled by force of crystallization. Geology 16:688-691.
McClay, K.R., 1976, Pressure solution. Nature. 264(5586):511-512.
Monger, H.C. and Daugherty, L.A., 1991a. Pressure solution: Possible mechanism for silicate grain dissolution in a petrocalcic horizon. Soil Science Society of America Journal, 55: 1625-1629.
Monger, H.C. and Daugherty, L.A., 1991b. Neoformation of palygorskite in a southern New Mexico aridisol. Soil Science Society of America Journal, 55: 1646-1650.
Monger, H.C. and Kelly, E.F., 2002. Silica minerals. In: Dixon, J.B. and Schulze, D.G., eds. Soil mineralogy with environmental applications. SSSA Book Series No.7. Madison, Soil Science Society of America: 611-636.
Pearthree, P., Spencer, J., Faulds, J., and House, P.K., 2008, Comment on "Age and evolution of the Grand Canyon revealed by U-Pb dating of water table-type speleothems". Science. 321:1634c. DOI: 10.1126/science.1158862.
Pederson, J.L., 2008. The mystery of the pre-Grand Canyon Colorado River—results fromthe Muddy Creek Formation. GSA Today 18 (3), 4–10.
Pederson, J., Young, R., Lucchitta, I., Beard, S., Billingsley, G., 2008, Comment on "Age and evolution of the Grand Canyon revealed by U-Pb dating of water table-type speleothems". Science. 321:1634b. DOI: 10.1126/science.1158019.
Polyak, V., Hill, C., and Asmerom, Y., 2008a, Age and evolution of the Grand Canyon revealed by U-Pb dating of water table-type speleothems. Science. 319:1377. DOI: 10.1126/science.1151248.
Polyak, V., Hill, C., and Asmerom, Y., 2008b, Response to Comments on the "Age and Evolution of the Grand Canyon Revealed by U-PB dating of water table-type speleothems", Science. 321:1634d. DOI: 10.1126science.1159762.
Raj, R., 1982. Creep in polycrystalline aggregates by matter transport through a liquid phase. J. Geophys. Res., 87(B6):4731 4739.
Rech, J.A., Quade, J., Hart,W.S., 2003. Isotopic evidence for the origin of Ca and S in soils gypsum, anhydrite, and calcite in the Atacama Desert, Chile. Geochim. Cosmochim. Acta 67, 575–586.

Reheis, M., 1988. Pedogenic replacement of aluminosilicate grains by CaCO3 in Ustollic Haplargids, south-central Montana, U.S.A. Geoderma, 41: 243-261.
Robin, P.F., 1978, Pressure solution at grain-to-grain contacts. Geochimica et Cosmochimica Acta. 42:1383-1389.
Robins, C.R., 2010. Micromorphology, chemistry and phyllosilicate mineralogy of the Mormon Mesa petrocalcic soil, Nevada, USA: Genetic implications. In: Phyllosilicate mineralogy, 40Ar/39Ar geochronology, and genesis of petrocalcic soils in the southwest U.S.A. Ph.D. dissertation. University of Nevada Las Vegas, Department of Geoscience: 94-174.
Ruddiman, W.F., Kutzbach, J.E., 1989. Forcing of Late Cenozoic northern hemisphere climate by plateau uplift in southern Asia and the American west. J. Geophys. Res. 94D15, 18,409–18,427.
Rutter, E.H., 1983, Pressure solution in nature, theory and experiment. J. Geol. Soc. London. 140:725-740.
Schutjens, P.M., and Spier, C.J., 1999, Intergranular pressure solution in NaCl: Grain-to-grain contact experiments under the optical microscope. Oil & Gas Science and Technology – Rev. IFP. 54:729-750.
Singer, A., 1989. Palygorskite and sepiolite group minerals. In: Dixon, J.B. and Weed, S.B., eds., Minerals in soil environments, 2nd edition. SSSA Book Series No. 1. Madison, Soil Science Society of America: 829-872.
Singer, A., Kirsten, W., and Bühman, C., 1995, Fibrous clay minerals in the soils of Namaqualand, South Africa: Characteristics and formation. Geoderma, 66: 43-70.
Smith, G.A., Wang, Y., Cerling, T.E., Geissman, J.W., 1993. Comparison of a paleosol– carbonate isotope record to other records of Pliocene–early Pleistocene climate in the western United States. Geology 21, 691–694.
Sorby, H. C. 1863. On the direct correlation of mechanical and chemical forces. Proc. R. Soc. London, 12,538-50.
Sorby, H.C., 1865. On impressed limestone pebbles, as illustrating a new principle in chemical geology. West Yorks. geol. Soc. v. 14, p, 458-461.
Steiger, M., 2005a. Crystal growth in porous materials - I: The crystallization pressure of large crystals. Journal of Crystal Growth, 282: 455-469.
Steiger, M., 2005b, Crystal growth in porous materials – II: Influence of crystal size on the crystallization pressure. Journal of Crystal Growth. 282:470-481.
Trurnit, P. (1968), Pressure Solution Phenomena in Detrital Rocks, Sediment. Geol. 2, 89-114.
Velde, B., 1992. Introduction to clay minerals: Chemistry, origins, uses and environmental significance. New York, Chapman & Hall. 198 pages.
Verrecchia, E.P. and Le Coustumer, M.-N., 1996. Occurrence and genesis of palygorskite and associated clay minerals in a Pleistocene calcrete complex, Sde Boqer, Negev Desert, Israel. Clay Minerals, 31: 183-202.
Wakabayashi, J., Sawyer, T.L., 2001. Stream incision, tectonics, uplift, and evolution of topography of the Sierra Nevada, California. J. Geol. 109, 539–562.
Watts, N.L., 1978. Displacive calcite: Evidence from recent and ancient calcretes. Sedimentology Research Laboratory, 6: 699-703.
Watts, N.L., 1980. Quaternary pedogenic calcretes from the Kalahari (southern Africa): mineralogy, genesis and diagenesis. Sedimentology, 27: 661-686.
Weaver, C.E. and Beck, K.C., 1977. Miocene of the S.E. United States: A model for chemical sedimentation in a peri-marine environment. Sedimentary Geology, 17: 1-234.
Weyl, P.K., 1959. Pressure solution and the force of crystallization - A phenomenological theory. Journal of Geophysical Research, 64(1): 2001-2025.
Williams, V.S., Bohannon, R.G. and Hoover, D.L., 1997. Geologic map of the Riverside Quadrangle, Clark County, Nevada, Geologic Quadrangle Map GQ-1770.
Winograd, I.J., Szabo, B.J., Coplen, B.J., Riggs, A.C., Kolesar, P.T., 1985. Two-million-year record of deuterium depletion in Great Basin groundwaters. Science 227, 519–521.
Yaalon, D.H. and Wieder, M., 1976. Pedogenic palygorskite in some arid brown (calciorthid) soils of Israel. Clay Minerals, 11 (1): 73-80.
Yariv, S. and Cross, H., eds., 2002. Organo-clay complexes and interactions. New York, Marcel Dekker, Inc.

Appendix A: Mormon Mesa Series

MORMON MESA SERIES: The Mormon Mesa series consist of shallow over petrocalcic, well drained soils that formed in material influenced by calcareous loess over mixed alluvium from predominantly limestone sources. The Mormon Mesa soils are on summits of fan remnants and mesas. Slope ranges from 0 to 15 percent. The mean annual precipitation is about 5 inches and the mean annual temperature is about 65 degrees F.
TAXONOMIC CLASS: Loamy, carbonatic, thermic, shallow Calcic Petrocalcids
TYPICAL PEDON: Mormon Mesa fine sandy loam, rangeland and wildlife habitat. (Colors are for dry soil unless otherwise stated.)

A--0 to 2.5 inches; light reddish brown (5YR 6/4) fine sandy loam, reddish brown (5YR 4/3) moist; moderate medium and thin platy structure; slightly hard, friable, nonsticky and slightly plastic; few fine roots; many very fine interstitial and many fine vesicular pores; violently effervescent; moderately alkaline (pH 8.2); abrupt smooth boundary. (2 to 5 inches thick)

Bk1--2.5 to 10 inches; light reddish brown (5YR 6/4) fine sandy loam, reddish brown (5YR 4/3) moist; weak medium and fine granular structure; slightly hard, very friable, nonsticky and nonplastic; few fine roots; few fine tubular and many very fine interstitial pores; few fine prominent very pale brown (10YR 8/2) calcium carbonate coatings in root channels; violently effervescent; moderately alkaline (pH 8.4); clear wavy boundary.

Bk2--10 to 16 inches; reddish brown (5YR 5/4) fine sandy loam, reddish brown (5YR 4/4) moist; massive; slightly hard, very friable, nonsticky and nonplastic; few fine roots; many very fine interstitial pores; many very fine and fine prominent white (10YR 8/1) calcium carbonate masses; violently effervescent; strongly alkaline (pH 8.5); abrupt wavy boundary. (Combined thickness of the Bk horizons is 8 to 18 inches.)

2Bkm--16 to 60 inches; white and pink (7.5YR 8/4 and 7.5YR 8/1) indurated hardpan, light brown (7.5YR 6/4) moist; massive; very rigid, very rigid; the upper 2 inches have many very fine laminae; violently effervescent; moderately alkaline (pH 8.4).

TYPE LOCATION: Clark County, Nevada; on Mormon Mesa about 3 miles northeast on U.S. Highway 91 from junction with Nevada State Highway 12 to 1/2 mile south of highway; approximately 800 feet north and 1,300 feet east of the southwest corner of section 28, T. 13 S., R. 69 E., Mount Diablo base line and meridian.

RANGE IN CHARACTERISTICS: Soil moisture - Usually dry, moist in some part during winter and spring and intermittingly moist in the upper part following summer convection storms; typic aridic soil moisture regime. **Soil Temperature** - 59 to 72 degrees F. **Depth to calcic horizon** 2 to 6 inches. **Depth to petrocalcic horizon** - 10 to 20 inches. **Control section** - Clay content: 5 to 15 percent. **Rock fragments:** Averages 0 to 20 percent, predominantly gravel or cobble size pan fragments, with 20 to 35 percent in any given subhorizon. **Profile reaction:** Moderately alkaline or strongly alkaline. **Calcium carbonate equivalent** in the fine earth fraction: 40 to 60 percent. **A horizon** - Hue: 5YR or 7.5YR. **Value:** 6 or 7 dry, 4 or 5 moist. **Chroma:** 2 through 4 dry and moist. **Bk horizons** - Hue: 5YR or 7.5YR. **Value:** 6 through 8 dry, 4 through 6 moist. **Chroma:** 2 through 4 dry and moist. **Clay content:** 5 to 15 percent. **Texture:** Fine sandy loam or sandy loam. **Rock fragments:** Averages 0 to 35 percent, predominantly gravel or cobble size pan fragments. **Structure:** Massive or subangular blocky. **Consistence:** Soft or slightly hard, friable or very friable, nonsticky or slightly sticky. **Secondary carbonates:** When rock or pan fragments are present in the profile, clasts may contain many to common

calcium carbonate coats and pendants on the vertical and undersides of fragments. Common very thin or thin calcium carbonate coats, filaments and seams. **2Bkm horizon** - Hue: 7.5YR or 10YR. **Value:** 7 or 8 dry, 6 through 8 moist. **Chroma:** 0 through 4. **Thickness:** Ranges from 4 feet to more than 20 feet.

COMPETING SERIES: These are the Bard (NV), Crossen (TX), Upton (TX, NM), Woda (NV) series. Bard soils have less than 4 foot thick Bkm (petrocalcic) horizons. Crossen soils have 3 to 20 inch thick petrocalcic horizons. Upton soils form in calcareous materials and contain 15 to 30 percent clay in the control section. Woda soils contain 20 to 30 percent clay in the control section.

GEOGRAPHIC SETTING: Mormon Mesa soils are on summits of fan remnants and mesas. Slope ranges from 0 to 15 percent. These soils formed in material influenced by calcareous loess over mixed alluvium from predominantly limestone sources. Elevations are 1,800 to 3,000 feet. The climate is low latitude desert, with mild winters and very hot summers. Precipitation is greatest in the winter with a lesser secondary peak in summer, typical of the Mojave Desert. The mean annual rainfall is 4 to 7 inches. The mean annual temperature is 57 to 70 degrees F.; average January temperature is 45 degrees F., and average July temperature is 83 degrees F. The frost free season is 220 to 300 days.

GEOGRAPHICALLY ASSOCIATED SOILS: These are the Arizo, Flattop, St. Thomas, Tonopah, and Toquop soils. Arizo and Tonopah soils are very deep and have sandy-skeletal control sections.Flattop soils have prismatic, sodium-affected clay loam Bt horizons. St. Thomas soils are very shallow or shallow over limestone and have loamy-skeletal control sections. Toquop soils are very deep sandy soils. **DRAINAGE AND PERMEABILITY:** Well drained; very high runoff; moderately rapid permeability. **USE AND VEGETATION:** These soils are used for rangeland and wildlife habitat. The vegetation is scattered white bursage, yucca, and creosotebush with some big galleta and Indian ricegrass. Many annuals grow in areas with sandy A1 horizons. **DISTRIBUTION AND EXTENT:** Mojave Desert of southern Nevada and northwestern Arizona; MLRA 30. These soils are extensive. **MLRA OFFICE RESPONSIBLE:** Davis, California **SERIES ESTABLISHED:** Clark County (Virgin River Area), Nevada, 1939.

REMARKS: Diagnostic horizons and features recognized in this pedon: **Ochric epipedon** - 0 to 2 1/2 inches. (A horizon). **Calcic horizon** 10 to 16 inches. (Bk1 and Bk2 horizons). **Petrocalcic horizon** - 16 to 60 inches. (2Bkm horizon). **Particle size control section** 10 to 16 inches. (Bk2 horizon).

Data from: Soil Survey Staff, Natural Resources Conservation Service, United States Department of Agriculture. Official Soil Series Descriptions [Online WWW]. Available URL: "http://soils.usda.gov/technical/classification/osd/index.html" [Friday, May 28, 2010]. USDA-NRCS, Lincoln, NE

Trip Notes: while waiting for the next shuttle at stop 2

Mediterranean grass and Red brome.

Mediterranean grass *Schismus arabicus (S. barbatus)*

Red brome *Bromus madritensis (B. rubens)*

Mediterranean grass is a native of Eurasia that has carved out a niche in the Mojave desert. Mediterranean grass prefers loose sandy soil, roadsides and rocky desert slopes. Red brome is an annual grass that is capable of germinating at lower rainfall and temperature levels than native species. Red brome grows best where there is little competition from other annual grasses and has become a member of the creosote–black bush communities. According to the California Exotic Pest Plant Council, Red brome is listed as an A-1: Most invasive pest plant. Other commons names for Red brome are: Foxtail chess, Compact brome and Spanish brome. Both Mediterranean grass and Red brome are described as weeds and they compete heavily with native plant species. Mediterranean grass and Red brome collectively contribute to fire hazards and have created short fire cycle seasons in areas that previously had none. Invaders that alter fire regimes are widely recognized as some of the most important system-altering species on the planet (Vitousek PM. 1990. *Biological invasions and ecosystem processes: Toward an integration of population biology and ecosystem studies.* Oikos 57:7–13.). Disturbance regimes affect ecosystem properties such as the rates of soil erosion or formation and the pathways and temporal patterns of nutrient cycling and energy flow. Disturbance regimes can also act as a selective force affecting the lifehistory traits of individual species and the composition, structure, and emergent properties of entire groups of organisms (Brooks M.L. et al. 2004, *Effects of Invasive Alien Plants on Fire Regimes*, BioScience July 2004, Vol. 54, No. 7, Pages 677–688).

Field Trip Schedule

11:45 a.m.	Depart for Stop 3.	Drive southwest on I-15 (returning towards Las Vegas)
		Exit highway 169, drive south past Logandale & Overton, continue on Hw 169 south

Trip Notes: while driving to stop 3

Note as we drive through and past the towns of Logandale and Overton, you can see Mormon Mesa to your left (east) and two prominent geomorphic surfaces to your right (west). The highest surface to your right is the Overton geomorphic surface and the lower one is the Lost City. As we continue towards stop 3, we'll climb up a steep mesa with numerous camper RV's parked on it. This is the Overton surface and if you look back towards the east, you'll see that Mormon Mesa is topographically higher. As we drive past mining operations on your right (Silica Mine, which is described below), you'll see a very high surface on the horizon. This is called Baseline Mesa, but is the same geomorphic surface as Mormon Mesa. The Overton surface lies below it. A younger surface that lies below the Overton, but is not preserved near the road, has been named the Underton by Doug Merkler. This surface has a stage IV petrocalcic horizon.

Note: Silica Mine to the West. The Overton Silica Production facility has been owned and operated by the Simplot Mining and Manufaturing Company since 1955. The mine was originally discovered in the 1920's and is known the world over for its purity at 99.5% silica. The facility produces about 700,000 tons of silica each year, of which 80% goes towards glass manufacturing.

Lake Mead Could Be Going Dry?

Douglas Merkler

We will be driving by Lake Mead, the vast reservoir for the Colorado River water that sustains the fast-growing cities of Phoenix and Las Vegas. This reservoir system could lose water faster than previously thought and run dry within 13 years, according to a new study by scientists at the Scripps Institution of Oceanography. Lake Mead, which serves as a reservoir for the Colorado River and sustains fast-growing cities in the Southwest, has a 50 percent chance of becoming unusable by 2021, researchers say. The lake has a 50 percent chance of becoming unusable by 2021, the scientists say, if the demand for water remains unchanged and if human induced climate change follows climate scientists' moderate forecasts, resulting in a reduction in average river flows.

Demand for Colorado River water already slightly exceeds the average annual supply when high levels of evaporation are taken into account, the researchers, Tim P. Barnett and David W. Pierce, point out. Despite an abundant snowfall in Colorado this year, scientists project that snowpacks and their runoffs will continue to dwindle. If they do, the system for delivering water across the Southwest would become increasingly unstable. "We were really sort of stunned," Professor Barnett said in an interview. "We didn't expect such a big problem basically right on our front doorstep. We thought there'd be more time." He added, "You think of what the implications are, and it's pretty scary." The two researchers used data on river flows and reservoir levels from the federal Bureau of Reclamation, the agency that manages the lower Colorado River and the reservoirs of Lake Mead and Lake Powell. Terry Fulp, manager of the bureau office for the lower Colorado River, said he disagreed with the paper's assumption that global climate models were sensitive or refined enough to forecast regional effects (Barnett, T. P., and D. W. Pierce, 2008, When will Lake Mead go dry? *Water Resour. Res.*, doi:10.1029/2007WR006704).

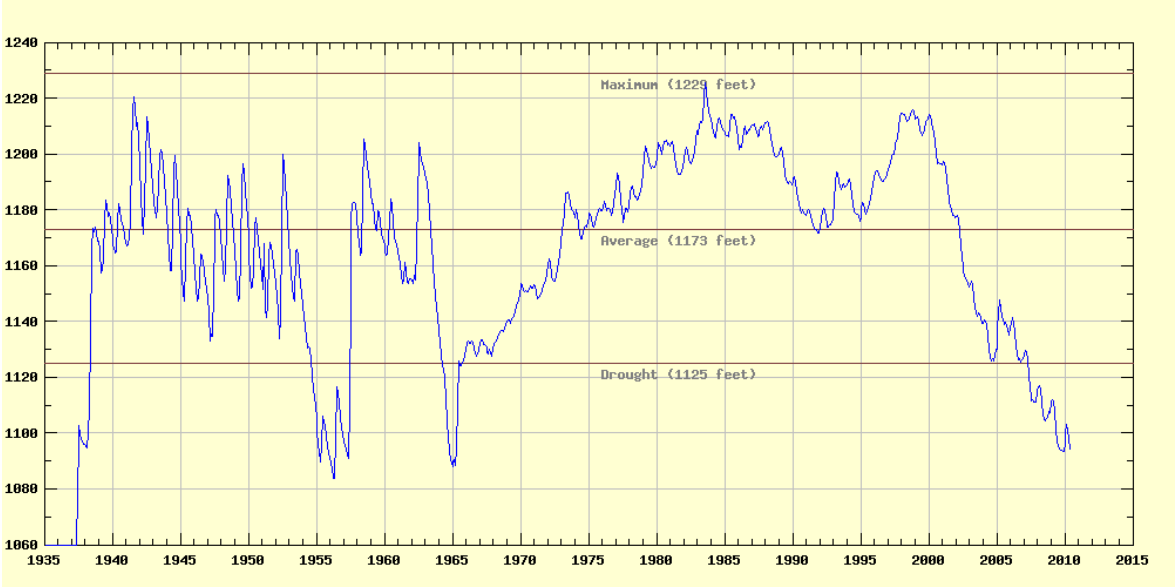

Data from Federal Bureau of Reclamation records, Merkler -2010

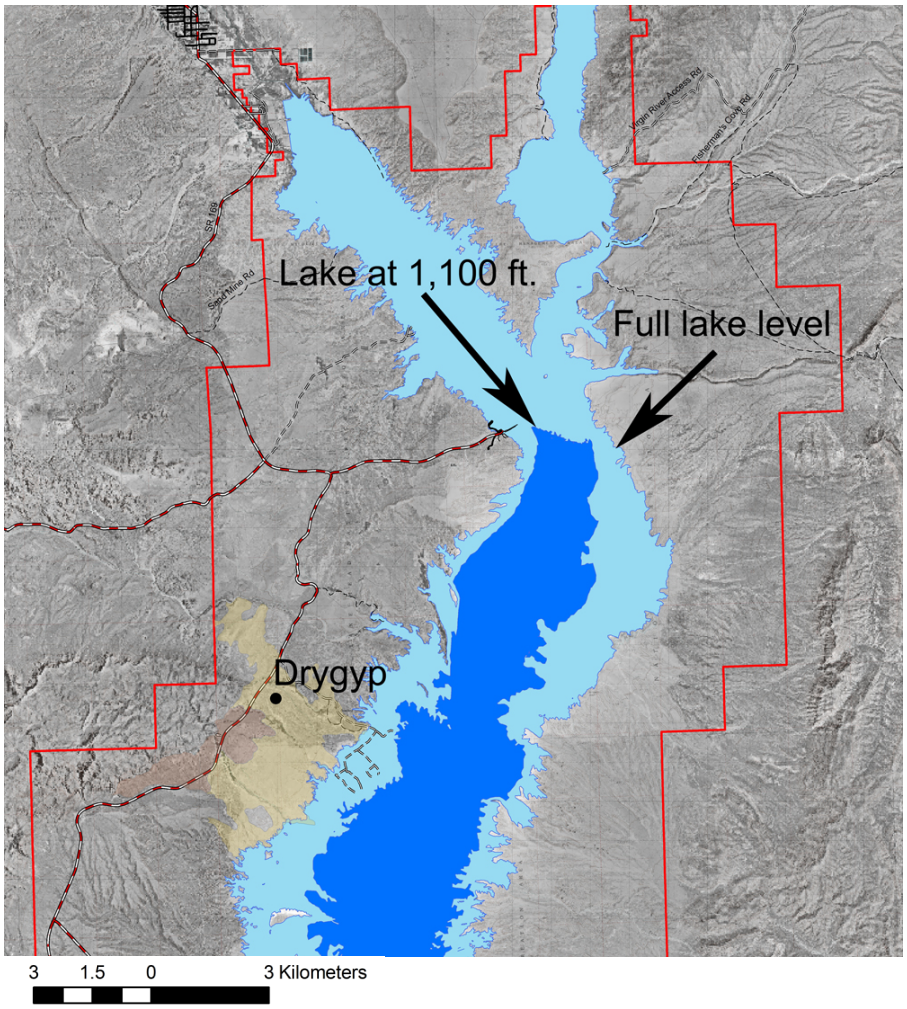

Comparison of current lake levels to historic 'topped off' levels. Merkler – 2010

Field Trip Schedule

12:30 p.m.	**Stop 3**	***Drygyp Petrogypsic***	We'll walk about one-third mile to a soil profile. Bring water, camera, and sunglasses with you.
12:45 p.m.	Soil pit discussion		
1:45 pm	Walk back to buses		

Stop 3: Drygyp Soil Series

Drygyp Soil Series Concept: Geologic setting and source of the gypsum

Douglas Merkler

Nevada State Resource Soil Scientist, Natural Resource Conservation Service, USDA, Las Vegas NV, doug.merkler@nv.usda.gov

In the Lake Mead region, the Muddy Creek Formation makes up a widespread sedimentary unit that was deposited in closed basins during the development of the Basin and Range province (Bohannon, 1984, p. 58). Between Las Vegas Wash and the Virgin River, the most common rocks in the unit are mudstone, siltstone, and fine-grained sandstone. Gypsum is present as bedded deposits or as disseminated accumulations in the mudstone, siltstone, and sandstone.

Rogers Spring and other springs in the "North Shore Complex" comprise one of the terminal discharge areas for the regional carbonate-rock aquifer system of eastern Nevada and western Utah, (Prudic et al., 1993). The source of the water to this spring and other regional carbonate-rock aquifer springs is uncertain. The prevailing theory suggests that much of the recharge water that enters the carbonate-rock aquifer occurs in the high mountain ranges around Ely, Nevada, located 250 miles north of Lake Mead. As this ground water flows south through the carbonate rocks, it encounters several faults along the way, including the Rogers Spring Fault, which has caused the older carbonate rocks (primarily limestone and dolomite) to be displaced against younger evaporite deposits of the Muddy Creek and Horse Spring formations. As the water flows through these formations (Fig. 1), it dissolves gypsum and halite from the evaporate deposits and from the sedimentary deposits that contains these minerals (Laney and Bales, 1996).

The transmissive properties of these rocks are low, forcing water to emerge at the surface in the springs along the fault trace. Most of the surface flow is at Rogers Spring and Blue Point Spring, but unknown quantities of seepage diffuse upward through the fine-grained sedimentary rocks east of the fault and are discharged by seeps and small springs and by evapotranspiration. Preferential movement of the ground water may be along faults and fractures. About 3,200 acres of land surface east of Rogers Spring and Blue Point Spring is underlain by surficial materials that consist largely of impure gypsum and other precipitated salts. In a number of places, the coarsely crystalline gypsum conforms to the local surface topography suggesting deposition at the land surface by springs and seeps over a long period.

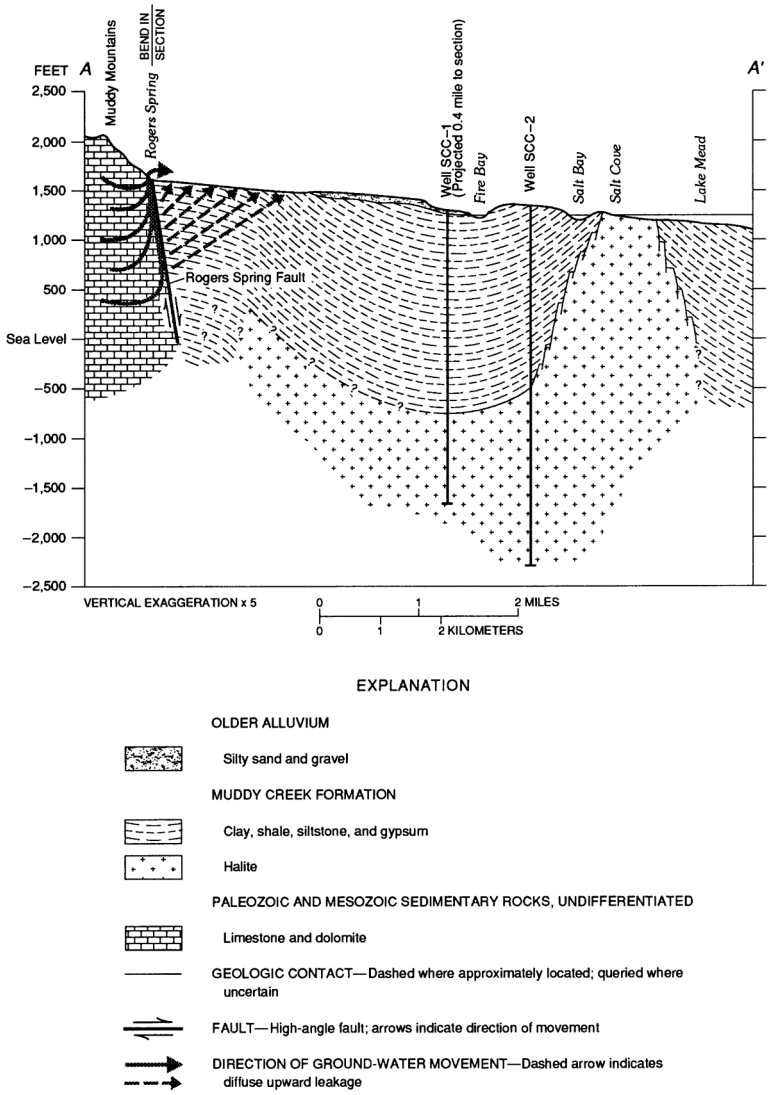

Figure 1. Generalized geologic cross-section between the Muddy Mountains and Lake Mead, from Laney and Bales, 1996.

Rogers Spring and Blue Point Spring both share a colorful history. One story involves a 1903 project to build a canal to divert water from both springs to 500 acres of farmland located several miles south of St. Thomas. During this effort, several industrious men used a horse team, scraper, homemade ditcher and shovels to construct a channel to connect both springs. They tested the channel and discovered that the water flowed only a short distance before soaking in. Undaunted, they lined the ditch with clay to prevent leakage, and when that failed, they borrowed $3,000 and took several months mixing cement by hand and again lining the ditch. Eventually, they were successful in transporting the water to the intended land. However, the project ultimately failed due to economic reasons. The men involved evidently drank the spring water while working on the project. Unfortunately, this water acted as a natural laxative, and these individuals lost a considerable amount of weight. Subsequently, the channel

discharging water from Blue Point Spring became known as “Slim Creek.” Several other projects have been attempted in association with Rogers Spring and Blue Point Spring, including a waterfowl refuge construction project that was initiated from 1938 through 1943 but never completed, and a tropical fish hatchery that operated at Blue Point Spring during the mid 1950s.

All totaled ground water discharge from springs along the Rogers Spring Fault totals approximately 1,000 gallons per minute. Due to the importance of these springs from both an ecological and recreational standpoint, the National Park Service remains vigilant in protecting these water features from potential adverse effects associated with nearby, large-scale ground water pumping from the regional carbonate-rock aquifer.

Drygyp Soil Series: DRYGYP S04NV-003-001

The Drygyp series was proposed in 1998 as part of the progressive soil survey of the Lake Mead National Recreation Area and was established in 2006 with the publication of the Soil Survey of Clark County, Nevada. In arid and semiarid environments gypsum can be a major soil component and this is the case for this Drygyp series concept, (90% gypsum within <20 cm). Drygyp is classified as a fine-gypseous, hypergypsic, hyperthermic, shallow Typic Petrogypsid and is to date the only soil series in the country in this family, with one other petrogypsid, the thermic Corvus series in the White Sands Missile Range of New Mexico. The climate of Drygyp is that of a low-latitude desert, with mild winters and very hot summers. Precipitation is greatest in the winter with lesser secondary peak in the summer, with a total of 3 to 5 inches a year, typical of the Mojave Desert transitional to Sonoran Desert. The pedon of Drygyp we will observe is not the type locality, but a different pedon sampled for full characterization by the Soil Survey Laboratory (SSL), Lincoln, NE, as soil survey sample number S04NV-003-001 (pedon # 04N0770).

Pedon Note: 38 percent surface covered with cryptogamic communities.
Classification: Fine-gypseous, hypergypsic, hyperthermic, shallow Typic Petrogypsids
Existing Vegetation: *Fremont's dalea, Parry's sandpaper plant, catclaw acacia, desert trumpet*
Parent Material: gypsum sedimentary rock
Particle Size Control Section: 0 to 18 cm.
Description origin: NASIS Description database: NSSL

A-- 0 to 1 centimeters; fine sandy loam; moderate very thick platy structure; few very fine roots; few very fine tubular and common very fine interstitial pores; abrupt irregular boundary. Lab sample # 04N04374

Byy (previously Bky)--1 to 18 centimeters; very pale brown (10YR 8/2) gypseous fine sandy loam, very pale brown (10YR 7/4) moist; 65 percent sand; moderate very thick platy structure; very friable, slightly hard; few fine roots and few medium roots and few very fine roots; few fine tubular and common very fine interstitial and few very fine tubular pores; 30 percent medium prominent platy moderately cemented 10YR 8/3, moist, gypsum masses with clear boundaries in matrix; abrupt wavy boundary. Lab sample # 04N04375

Byym1—(previously Bym1) 18 to 47 centimeters; very pale brown (10YR 8/2) cemented fine gypsum material, very pale brown (10YR 8/4), moist; 65 percent sand; strong very thick platy structure; slightly rigid, rigid; few very fine and fine roots; few very fine tubular and common very fine interstitial pores; 30 percent medium prominent platy moderately cemented 10YR 8/3, moist, gypsum masses with clear boundaries in matrix; 70 percent very strongly cemented, very weak cemented is slightly hard and friable.; gradual wavy boundary. Lab sample # 04N04376

Byym2—(previously Bym2) 47 to 90 centimeters; very pale brown (10YR 8/2) cemented fine gypsum material, very pale brown (10YR 7/3), moist; moderate very thick platy structure; firm, hard; few very fine interstitial pores; 30 percent medium prominent platy moderately cemented 10YR 8/3, moist, gypsum masses with clear boundaries in matrix; clear wavy boundary. Lab sample # 04N04377

Byy1—(previously By1) 90 to 151 centimeters; very pale brown (10YR 8/2) gypseous fine sandy loam, light gray (10YR 7/2) moist; weak coarse subangular blocky structure; firm, hard; few very fine interstitial and tubular pores; 30% of the horizon is moderately cemented, very friable and effervescent; clear wavy boundary. Lab sample # 04N04378

Byy2—(Previously By2) 151 to 178 centimeters; gypseous fine sandy loam; strong coarse subangular blocky structure; friable, slightly hard; few very fine interstitial pores; 5 percent selenite crystals, slightly moist. Lab sample # 04N04379

***NOTE: Horizon designations on characterization data (following pages) have not been updated to reflect revisions in the 11th edition of Soil Taxonomy.**

Acknowledgements
We greatly appreciate the help of Brenda Buck, Brian Hedlund, Assistant Professor, Biological Sciences, University of Las Vegas, Las Vegas, NV, Patrick Drohan Assistant Professor, Department of Crop and Soil Sciences, Pennsylvania State University who assisted with field sample collection on the Drygyp soil. Additional field assistance with soil characterization, classification and laboratory analyses of the Drygyp pedon were provided by Joe Chiaretti, Robert Engel and Rebecca Burt of the National Soil Survey Center in Lincoln, NE. A sincere thanks to Kent Turner and his Resources Division staff with Lake Mead National Recreation Area for their assistance, interest and progressive attitude with this project.

References
Bohannon, R.G., 1983, Geologic map, tectonic map and structure sections of the Muddy and Northern Black Mountains, Clark County, Nevada: U.S. Geological Survey Miscellaneous Investigations Map 1-1406, 2 sheets.
Laney, R.L. and J.T. Bales. 1996. Geohydrologic reconnaissance of Lake Mead National Recreation Area; Las Vegas Wash to Virgin River, Nevada: U.S. Geological Survey Water-Resources Investigations Report 96-4033.
Prudic, D.E., J.R. Harrill, and T.J. Burbey. 1993. Conceptual evaluation of regional ground-water flow in the carbonate-rock province of the Great Basin, Nevada, Utah, and adjacent States: U.S. Geological Survey Open-File Report 93-170, 103 p.
Soil Survey Staff 2010, National Soil Survey Characterization Data, Soil Survey Laboratory, National Soil Survey Center, USDA-NRCS - Lincoln, NE., Sunday, June 06, 2010.

*** Primary Characterization Data ***

Pedon ID: S04NV-003-001 (Clark, Nevada) Print Date: May 19 2010 6:12PM

Sampled as on Apr 13, 2004 : Drygyp ; Loamy, gypsic, hyperthermic, shallow Typic Petrogypsid

Revised to SSL on Mar 09, 2006 : Drygyp ; Loamy, gypsic, hyperthermic, shallow Typic Petrogypsid

United States Department of Agriculture

Natural Resources Conservation Service

National Soil Survey Center

Soil Survey Laboratory

Lincoln, Nebraska 68508-3866

SSL - Project C2004USNV132 IUSS Tour

- Site ID S04NV608069-DM Lat: 36° 23' 10.60" north Long: 114° 25' 43.50" west NAD83 MLRA: 30
- Pedon No. 04N0770
- General Methods 1B1A, 2A1, 2B

Layer	Horizon	Orig Hzn	Depth (cm)	Field Label 1	Field Label 2	Field Label 3	Field Texture	Lab Texture
04N04374	A		0-1	S04NV-003-001-1			FSL	L
04N04375	Bky		1-18	S04NV-003-001-2			GYP-FSL	FSL
04N04376	Bym1		18-47	S04NV-003-001-3			CEM-FSL	FSL
04N04377	Bym2		47-90	S04NV-003-001-4			CEM-FSL	L
04N04378	By1		90-151	S04NV-003-001-5			GYP-FSL	L
04N04379	By2		151-178	S04NV-003-001-6			GYP-FSL	VFSL

Pedon Calculations

Calculation Name	Result	Units of Measure
Weighted Particles, 0.1-75mm, 75 mm Base	40	% wt
Volume, >2mm, Weighted Average	0	% vol
Clay, total, Weighted Average	12	% wt
Clay, carbonate free, Weighted Average	12	% wt
CEC Activity, CEC7/Clay, Weighted Average, CECd, Set 1	0.12	(NA)
LE, Whole Soil, Summed to 1m	Depth error	cm/m

Weighted averages based on control section: 0-18 cm

PSDA & Rock Fragments	-1-	-2-	-3-	-4-	-5-	-6-	-7-	-8-	-9-	-10-	-11-	-12-	-13-	-14-	-15-	-16-	-17-
	(- - - - - Total - - - - - -)			(- - Clay - - -)		(- - - - Silt - - - - -)		(- - - - - - - - - - - - Sand - - - - - - - - - - - - -)					(Rock Fragments (mm))				
	Clay	Silt	Sand	Fine	CO_3	Fine	Coarse	VF	F	M	C	VC	(- - - - - - - - Weight - - - - - - - -)				>2 mm
	<	.002	.05	<	<	.002	.02	.05	.10	.25	.5	1	2	5	20	.1-	wt %
Depth	.002	-.05	-2	.0002	.002	-.02	-.05	-.10	-.25	-.50	-1	-2	-5	-20	-75	75	whole

Layer	(cm)	Horz	Prep	(- % of <2mm Mineral Soil -)												(- - - - - - - % of <75mm - - - - - -)				soil
				3A1a1a			3A1a1a	3A1a1a		3A1a1a	3A1a1a	3A1a1a	3A1a1a	3A1a1a					
04N04374	0-1	A	S	11.3	39.4	49.3	1.2	16.2	23.2	28.7	18.6	1.4	0.3	0.3	--	--	--	21	--
04N04375	1-18	Bky	S	11.5	23.8	64.7	--	10.4	13.4	23.1	23.1	12.4	3.0	3.1	--	--	--	42	--
04N04376	18-47	Bym1	S	15.5	26.3	58.2	--	8.9	17.4	19.0	25.8	11.0	2.4	--	--	--	--	39	--
04N04377	47-90	Bym2	S	7.7	43.1	49.2	--	16.3	26.8	20.5	18.7	6.2	3.7	0.1	--	--	--	29	--
04N04378	90-151	By1	S	13.8	41.7	44.5		12.4	29.3	23.2	19.3	1.7	0.2	0.1	--	--	--	21	--
04N04379	151-178	By2	S	15.1	27.4	57.5		9.5	17.9	25.1	23.9	7.6	0.9	--	--	--	--	32	--

*** Primary Characterization Data ***

Pedon ID: S04NV-003-001 (Clark, Nevada) Print Date: May 19 2010 6:12PM

Sampled As : Drygyp Loamy, gypsic, hyperthermic, shallow Typic Petrogypsid

USDA-NRCS-NSSC-Soil Survey Laboratory ; Pedon No. 04N0770

Water Dispersible PSDA -1- -2- -3- -4- -5- -6- -7- -8- -9- -10- -11- -12-

(- Water Dispersible -)

				(- - - - - Total - - - - - -)			(- - Clay - - -)		(- - - - Silt - - - - -)		(- - - - - - - - - - - - Sand - - - - - - - - - - - -)				
				Clay	Silt	Sand	F	CO_3	F	C	VF	F	M	C	VC
				<	.002	.05	<	<	.002	.02	.05	.10	.25	.5	1
	Depth			.002	-.05	-2	.0002	.002	-.02	-.05	-.10	-.25	-.50	-1	-2
Layer	(cm)	Horz	Prep	(- % of <2mm -)											
				3A1a6a				3A1a6a	3A1a6a		3A1a6a	3A1a6a	3A1a6a	3A1a6a	3A1a6a
04N04374	0-1	A	S	7.5	40.4	52.1		0.7	21.9	18.5	24.7	18.8	3.5	3.1	2.0
04N04375	1-18	Bky	S	27.4	65.1	7.5		--	47.3	17.8	6.3	0.9	0.2	0.1	tr

Bulk Density & Moisture				-1-	-2-	-3-	-4-	-5-	-6-	-7-	-8-	-9-	-10-	-11-	-12-	-13-
				(Bulk Density)		Cole	(- - - - - - - - - - - Water Content - - - - - - - - - - -)						WRD	Aggst		
				33	Oven	Whole	6	10	33	1500	1500 kPa	Ratio	Whole	Stabl	(- - Ratio/Clay - -)	
	Depth			kPa	Dry	Soil	kPa	kPa	kPa	kPa	Moist	AD/OD	Soil	2-0.5mm	CEC7	1500 kPa
Layer	(cm)	Horz	Prep	(- - - g cm^{-3} - - -)			(- - - - - - - - - - - - % of < 2mm - - - - - - - - - - - -)						cm^3 cm^{-3}	%		
				DbWR1	DbWR1				DbWR1	3C2a1a		3D1		3F1a1a		

04N04374	0-1	A	S					4.5	1.040		53	0.74	0.40
04N04374	0-1	A	S_SK						1.127				
04N04375	1-18	Bky	S	1.08	1.08	--	6.8	1.4	1.224	0.06	62	0.08	0.12
04N04375	1-18	Bky	S_SK						1.199				
04N04376	18-47	Bym1	S	1.36	1.37	0.002	3.0	3.3	1.211	--		0.06	0.21
04N04376	18-47	Bym1	S_SK						1.188				
04N04377	47-90	Bym2	S	1.25	1.28	0.008	7.1	3.2	1.215	0.05		0.13	0.42
04N04377	47-90	Bym2	S_SK						1.195				
04N04378	90-151	By1	S	1.20	1.20	--	12.7	3.8	1.204	0.11		0.09	0.28
04N04378	90-151	By1	S_SK						1.195				
04N04379	151-178	By2	S	1.37	1.42	0.012	10.4	5.4	1.149	0.07		0.34	0.36
04N04379	151-178	By2	S_SK						1.134				

*** Primary Characterization Data ***

Pedon ID: S04NV-003-001 (Clark, Nevada) Print Date: May 19 2010 6:12PM

Sampled As : Drygyp Loamy, gypsic, hyperthermic, shallow Typic Petrogypsid

USDA-NRCS-NSSC-Soil Survey Laboratory ; Pedon No. 04N0770

Water Content

Layer	Depth (cm)	Horz	Prep	-1- LL	-2- PI	-3- Field	-4- Recon 33 kPa	-5- Recon Oven Dry	-6- Field	-7- Recon 33 kPa	-8- 6 kPa	-9- 10 kPa	-10- 33 kPa	-11- 100 kPa	-12- 200 kPa	-13- 500 kPa
				(- - Atterberg - -)		(- - - - - Bulk Density - - - - -)			(- Water Content -)							
				(- - - Limits - - -)							(- - - - - - - - - - - - - - Sieved Samples - - - - - - - - - - - - -)					
				pct <0.4mm		(- - - - - - - - g cm^{-3} - - - - - - -)			(- % of < 2mm -)							
												3C1b1a	3C1c1a	3C1d1a	3C1e1a	
04N04374	0-1	A	S									25.5	15.7	9.8	8.7	
04N04375	1-18	Bky	S									20.3	13.4	2.6	1.7	
04N04376	18-47	Bym1	S									18.1	14.1	4.9	4.1	
04N04377	47-90	Bym2	S									19.3	11.9	3.6	3.3	
04N04378	90-151	By1	S									27.4	17.3	4.6	3.8	
04N04379	151-178	By2	S									23.1	20.4	9.0	7.0	

Carbon & Extractions

-1-	-2-	-3-	-4-	-5-	-6-	-7-	-8-	-9-	-10-	-11-	-12-	-13-	-14-	-15-	-16-	-17-	-18-

				(- - - - - Total - - - - -)			Org	C/N	(- - - Dith-Cit Ext - - -)			(- - - - - - Ammonium Oxalate Extraction - - - - - -)						(- - - Na Pyro-Phosphate - - -)		
	Depth			C	N	S	C	Ratio	Fe	Al	Mn	Al+½Fe	ODOE	Fe	Al	Si	Mn	C	Fe	Al	Mn
Layer	(cm)	Horz	Prep	(- - - - - - % of <2 mm - - - - - -)					(- - - - - - - - - - - - - - - - - - - % of < 2mm - - - - - - - - - - - - - - - - - -)								mg kg^{-1}	(- - - - - - % of < 2mm - - - - -)		
				4H2a	4H2a	4H2a			4G1	4G1	4G1		4G2a	4G2a	4G2a	4G2a	4G2a		4G3	4G3	4G3
04N04374	0-1	A	S	2.39	0.07	2.64		7	0.4	tr	--	0.10	tr	0.04	0.08	0.07	62.1		--	--	--
04N04374	0-1	A	O	3.29	0.12	1.86															
04N04374[1]	0-1		O	1.75	0.07	3.23															
04N04375	1-18	Bky	S	0.40	0.03	16.30		4	--	--	--	0.02	--	0.01	0.02	0.03	--		--	--	--
04N04375	1-18	Bky	O	0.78	0.03	19.64															
04N04375[2]	1-18		O	0.46	0.11	19.20															
04N04376	18-47	Bym1	S	0.60	0.06	15.72		2	--	--	--	0.02	0.02	0.01	0.02	0.03	--		--	--	--
04N04376	18-47	Bym1	O	0.71	0.06																
04N04376[3]	18-47		O	0.55	0.03																
04N04377	47-90	Bym2	S	0.20	0.01	16.96		8	--	--	--	0.02	--	0.01	0.02	0.03	--		--	--	--
04N04377	47-90	Bym2	O	0.32	0.08	21.59															
04N04377[4]	47-90		O	0.12	0.03	21.86															
04N04378	90-151	By1	S	0.09	0.02	17.22		4	--	--	--	0.02	--	0.01	0.02	0.03	--		--	--	--

04N04378	90-151	By1	O	0.16	0.02	15.71															
04N04378[5]	90-151		O	0.34	0.11	21.28															
04N04379	151-178	By2	S	0.04	0.04	11.79	1	--	--	--	0.03	--	0.02	0.03	0.04	--	--	--	--
04N04379	151-178	By2	O	0.11	0.03	15.68															
04N04379[6]	151-178		O	0.06	0.01	13.64															

[1,2,3,4,5,6] Analyzed size fraction = <80 Mesh

*** Primary Characterization Data ***

Pedon ID: S04NV-003-001 (Clark, Nevada) Print Date: May 19 2010 6:12PM

Sampled As : Drygyp Loamy, gypsic, hyperthermic, shallow Typic Petrogypsid

USDA-NRCS-NSSC-Soil Survey Laboratory ; Pedon No. 04N0770

CEC & Bases				-1-	-2-	-3-	-4-	-5-	-6-	-7-	-8-	-9-	-10-	-11-	-12-	-13-	-14-
				(- - - - - - NH_4OAC Extractable Bases - - - - -)								CEC8	CEC7	ECEC		(- - - - Base - - - -)	
								Sum	Acid-	Extr	KCl	Sum	NH_4	Bases	Al	(- Saturation -)	
	Depth			Ca	Mg	Na	K	Bases	ity	Al	Mn	Cats	OAC	+Al	Sat	Sum	NH_4OAC
Layer	(cm)	Horz	Prep	(- - - - - - - - - - - - - - - - - cmol(+) kg^{-1} -)							mg kg^{-1}	(- - - - cmol(+) kg^{-1} - - -)			(- - - - - - - - % - - - - - - - -)		

				4B1a1a	4B1a1a	4B1a1a	4B1a1a											4B1a1a				
04N04374	0-1	A	S	171.9*	0.6	tr	0.3	172.8										8.4			100	
04N04375	1-18	Bky	S	288.1*	0.2	tr	tr	288.3										0.9			100	
04N04376	18-47	Bym1	S	303.8*	0.8	0.3	tr	304.9										0.9			100	
04N04377	47-90	Bym2	S	294.8*	0.4	0.2	tr	295.4										1.0			100	
04N04378	90-151	By1	S	300.1*	--	0.7	0.1	300.9										1.3			100	
04N04379	151-178	By2	S	298.5*	--	2.6	0.4	301.5										5.2			100	

*Extractable Ca may contain Ca from calcium carbonate or gypsum., CEC7 base saturation set to 100.

Salt				-1-	-2-	-3-	-4-	-5-	-6-	-7-	-8-	-9-	-10-	-11-	-12-	-13-	-14-	-15-	-16-	-17-	-18-	-19-	-20-
				(- Water Extracted From Saturated Paste -)																	Pred		
																			Total	Elec	Elec	Exch	
	Depth			Ca	Mg	Na	K	CO_3	HCO_3	F	Cl	PO_4	Br	OAC	SO_4	NO_2	NO_3	H_2O	Salts	Cond	Cond	Na	SAR
Layer	(cm)	Horz	Prep	(- - - - - mmol(+) L^{-1} - - - - -)				(- mmol(-) L^{-1} -)										(- - - - % - - - -)		(- - dS m^{-1} - -)		%	
				4F2	4F2	4F2	4F2	4F2	4F2	4F2	4F2	4F2	4F2	4F2	4F2	4F2	4F2	4F2		4F2	4F1a1a1		

04N04374	0-1	A	S	33.2	0.7	0.3	0.2	--	3.5	0.4	1.0	--	--	--	30.9	--	--	45.2	0.1	2.40	2.12	tr	tr
04N04375	1-18	Bky	S	30.4	0.6	0.2	0.2	--	1.0	--	0.8	--	--	--	30.1	--	0.5	54.1	0.1	2.23	2.06	4	--
04N04376	18-47	Bym1	S	29.7	3.8	3.7	0.4	--	0.6	--	5.2	--	--	--	30.1	--	1.1	56.5	0.1	2.88	2.14	5	1
04N04376[1]	18-47		S																				
04N04377	47-90	Bym2	S	28.1	1.6	2.7	0.5	--	0.4	--	3.3	--	--	--	29.9	--	--	55.4	0.1	2.50	2.12	4	1
04N04377[2]	47-90		S																				
04N04378	90-151	By1	S	23.7	5.3	12.6	0.8	--	0.4	--	8.0	--	--	--	37.1	--	--	55.3	0.1	3.60	2.37	1	3
04N04379	151-178	By2	S	24.7	15.7	45.0	1.6	--	0.4	--	22.4	--	--	--	58.5	--	--	47.2	0.2	6.60	3.09	9	10

[1,2] Multiple values present due to instrumentation or analyzed size fraction. See laboratory for more information.

*** Primary Characterization Data ***

Pedon ID: S04NV-003-001 (Clark, Nevada) Print Date: May 19 2010 6:12PM

Sampled As : Drygyp Loamy, gypsic, hyperthermic, shallow Typic Petrogypsid

USDA-NRCS-NSSC-Soil Survey Laboratory ; Pedon No. 04N0770

---

pH & Carbonates -1- -2- -3- -4- -5- -6- -7- -8- -9- -10- -11-

(- - - - - - - - - - - - - - - - - - pH - - - - - - - - - - - - - - - - - -) (- - Carbonate - -) (- - Gypsum - - -)

$CaCl_2$ As $CaCO_3$ As $CaSO_4*2H_2O$ Resist

Layer	Depth (cm)	Horz	Prep	KCl	0.01M 1:2	H_2O 1:1	Sat Paste	Sulf	NaF	<2mm	<20mm	<2mm	<20mm	ohms
										(- - - - - - - - - - - -	%	- - - - - - - - - - - -)		cm^{-1}
					4C1a2a	4C1a2a	4F2			4E1a1a1a1		4E2a1a1a1		
04N04374	0-1	A	S		7.7	7.7	7.5			16		13		
04N04375	1-18	Bky	S		7.7	7.8	7.7			2		96	96	
04N04376	18-47	Bym1	S		7.9	8.0	7.8			4		88	88	
04N04377	47-90	Bym2	S		7.8	7.8	8.0			1		89	89	
04N04378	90-151	By1	S		7.7	7.8	8.0			tr		86	86	
04N04379	151-178	By2	S		7.7	7.8	7.8			tr		60	60	

Phosphorous

Layer	Depth (cm)	Horz	Prep	-1- Melanic Index	-2- NZ %	-3- Acid Oxal	-4- Bray 1	-5- Bray 2	-6- Olsen	-7- H_2O	-8- Citric Acid	-9- Mehlich III	-10- Extr NO_3
					(- Phosphorous - - - - - - - - - - - - - - - - - -)								
						(- - - - - - - - - - - - - - - - - - - -mg kg^{-1} - - - - - - - - - - - - - - - - -)							mg kg^{-1}
					4D8a1	4G2a			4D5a1			4D6a1	

04N04374	0-1	A	S	69	186.3	27.1	48.2
04N04375	1-18	Bky	S	1	--		6.2
04N04376	18-47	Bym1	S	4	--		3.3
04N04377	47-90	Bym2	S	0	--		1.7
04N04378	90-151	By1	S	0	--		1.6
04N04379	151-178	By2	S	0	--		2.4

*** Primary Characterization Data ***

Pedon ID: S04NV-003-001 (Clark, Nevada) Print Date: May 19 2010 6:12PM

Sampled As : Drygyp Loamy, gypsic, hyperthermic, shallow Typic Petrogypsid

USDA-NRCS-NSSC-Soil Survey Laboratory ; Pedon No. 04N0770

Trace Elements Tier 1

				-1-	-2-	-3-	-4-	-5-	-6-	-7-	-8-	-9-	-10-	-11-	-12-
	Depth			Ag	As	Ba	Be	Cd	Co	Cr	Cu	Mn	Mo		Hg
Layer	(cm)	Horz	Prep	mg/kg	mg/kg	mg/kg	mg/kg	mg/kg	mg/kg	mg/kg	mg/kg	mg/kg	mg/kg		ug/kg
				4H1a	4H1a	4H1a	4H1a	4H1a	4H1a	4H1a	4H1a	4H1a	4H1a		4H1a

04N04374	0-1	A	HM	0.49	9.21	165.85	0.50	0.50	4.48	15.53	14.46	295.21	--	25
04N04375	1-18	Bky	HM	0.57	1.69	17.49	0.04	0.23	0.46	0.99	11.64	12.46	--	7
04N04376	18-47	Bym1	HM	0.58	5.20	17.08	0.06	0.23	0.53	1.05	8.49	18.62	--	1
04N04377	47-90	Bym2	HM	0.60	3.41	20.84	0.06	0.23	0.48	1.69	9.60	8.63	--	--
04N04378	90-151	By1	HM	0.59	2.22	21.86	0.09	0.20	0.74	2.30	8.92	12.40	--	--
04N04379	151-178	By2	HM	0.57	4.75	98.69	0.17	0.17	1.35	8.56	6.78	22.76	0.06	--

Trace Elements Tier 2

				-1-	-2-	-3-	-4-	-5-	-6-	-7-	-8-	-9-	-10-	-11-
	Depth			Ni	P	Pb	Sb	Se	Sn	Sr	Tl	V	W	Zn
Layer	(cm)	Horz	Prep	mg/kg	mg/kg	mg/kg	mg/kg	ug/kg	mg/kg	mg/kg	mg/kg	mg/kg	mg/kg	mg/kg
				4H1a	4H1a	4H1a	4H1a	4H1a	4H1a	4H1a		4H1a	4H1a	4H1a
04N04374	0-1	A	HM	10.54	591.45	10.42	--	154.00	--	515.01		29.22	0.68	50.10
04N04375	1-18	Bky	HM	1.61	43.92	0.23	--	124.57	--	1170.82		3.29	--	6.50
04N04376	18-47	Bym1	HM	1.63	42.25	0.05	--	158.57	--	1865.77		4.12	--	4.16
04N04377	47-90	Bym2	HM	1.30	31.38	0.05	--	101.24	--	2189.41		4.14	--	6.21

04N04378	90-151	By1	HM	1.69	29.81	0.38	--	125.64	--	2034.46	5.27	--	6.34
04N04379	151-178	By2	HM	2.99	22.69	1.62	--	66.26	--	1518.47	13.82	--	14.73

*** Primary Characterization Data ***

Pedon ID: S04NV-003-001 (Clark, Nevada) Print Date: May 19 2010 6:12PM

Sampled As : Drygyp Loamy, gypsic, hyperthermic, shallow Typic Petrogypsid

USDA-NRCS-NSSC-Soil Survey Laboratory ; Pedon No. 04N0770

Major Elements -1- -2- -3- -4- -5- -6- -7- -8- -9- -10- -11- -12-

Layer	Depth (cm)	Horz	Prep	Al mg/kg 4H1b	Ca mg/kg 4H1b	Fe mg/kg 4H1b	K mg/kg 4H1b	Mg mg/kg 4H1b	Mn mg/kg 4H1b	Na mg/kg 4H1b	P mg/kg 4H1b	Si mg/kg 4H1b	Sr mg/kg 4H1b	Ti mg/kg 4H1b	Zr mg/kg 4H1b
04N04374	0-1	A	HM	30742	89827	13961	11999	9568	320	5500	564	246133	328	2084	110
04N04375	1-18	Bky	HM	2372	213389	1006	996	819	14	466	48	25415	651	126	12
04N04376	18-47	Bym1	HM	2350	216029	1106	1049	1766	20	538	31	20743	1116	139	14
04N04377	47-90	Bym2	HM	3178	205167	1252	1386	659	11	692	17	23645	1251	181	14
04N04378	90-151	By1	HM	4556	211230	1546	1945	776	15	1113	16	30199	1205	270	18

04N04379	151-178	By2	HM	17408	148223	5444	7806	2756	34	4036	18	131072	895	961	48

*** Primary Characterization Data ***

Pedon ID: S04NV-003-001 (Clark, Nevada) Print Date: May 19 2010 6:12PM

Sampled As : Drygyp Loamy, gypsic, hyperthermic, shallow Typic Petrogypsid

USDA-NRCS-NSSC-Soil Survey Laboratory ; Pedon No. 04N0770

Clay Mineralogy (<.002 mm)

				-1-	-2-	-3-	-4-	-5-	-6-	-7-	-8-	-9-	-10-	-11-	-12-	-13-	-14-	-15-	-16-	-17-	-18-
						X-Ray				Thermal						Elemental				EGME	Inter
													SiO_2	Al_2O_3	Fe_2O_3	MgO	CaO	K_2O	Na_2O	Retn	preta
	Depth		Fract			7A1a1															tion
Layer	(cm)	Horz	ion	(- - - - - - - - - peak size - - - - - - - - - -)					(- - - - - - - - - % - - - - - - - - - -)				(- - - - - - - - - - - - - - - - - - - % - - - - - - - - - - - - - - - - - - -)							mg g^{-1}	
04N04374	0-1	A	tcly	KK 2	MT 2	GY 1	MI 1	CA 1													CMIX
				QZ 1	VR 1																
04N04375	1-18	Bky	tcly	GY 1																	CMIX
04N04376	18-47	Bym1	tcly	GY 1	CA 1																CMIX
04N04377	47-90	Bym2	tcly	GY 2	CA 1																CMIX
04N04378	90-151	By1	tcly	GY 2	MI 1	CA 1	KK 1	QZ 1													CMIX

04N04379	151-178	By2	tcly	MM 3	MI 3	KK 2	GY 1	QZ 1													CMIX

FRACTION INTERPRETATION:

tcly - Total Clay, <0.002 mm

MINERAL INTERPRETATION:

CA - Calcite GY - Gypsum KK - Kaolinite MI - Mica MM - Montmorillonite-Mica

MT - Montmorillonite QZ - Quartz VR - Vermiculite

RELATIVE PEAK SIZE: 5 Very Large 4 Large 3 Medium 2 Small 1 Very Small 6 No Peaks

*** Primary Characterization Data ***

Pedon ID: S04NV-003-001 (Clark, Nevada) Print Date: May 19 2010 6:12PM

Sampled As : Drygyp Loamy, gypsic, hyperthermic, shallow Typic Petrogypsid

USDA-NRCS-NSSC-Soil Survey Laboratory ; Pedon No. 04N0770

Sand - Silt Mineralogy (2.0-0.002 mm)	-1-	-2-	-3-	-4-	-5-	-6-	-7-	-8-	-9-	-10-	-11-	-12-	-13-	-14-	-15-	-16-	-17-	-18-
			X-Ray				Thermal						Optical				EGME	Inter
										Tot Re			Grain Count				Retn	preta

Layer	Depth (cm)	Horz	Fraction	(- - - - - - - - peak size - - - - - - - - -)					(- - - - - - - - % - - - - - - - - - -)				(- % - - - - - - - - - - - - - - - - - -)							mg g^{-1}	7B1a2 tion
04N04374	0-1	A	vfs										65	QZ 61	FK 17	CB 6	CA 5	CD 3	PR 2		SMIX
														BT 1	OP 1	FP 1	GY 1	HN 1	FE tr		
														MS tr	GN tr	GS tr	BY tr	TM tr			
04N04375	1-18	Bky	vfs										8	GY 85	QZ 8	FK 3	CB 2	CA 1	BT tr		SMIX
														CD tr	HN tr	MS tr	FP tr	PR tr			
04N04376	18-47	Bym1	fs										2	GY 96	QZ 2	BT 1	CA tr	CB tr	HN tr		SMIX
														MS tr	FP tr	FK tr	PR tr				
04N04377	47-90	Bym2	csi										33	GY 48	QZ 31	FK 12	CA 3	PR 2	OP 1		SMIX
														CB 1	CD 1	HN 1	MZ tr	MS tr	GN tr		
														FP tr	BY tr	BT tr	TM tr	ZR tr			
04N04378	90-151	By1	csi										48	QZ 45	GY 28	FK 17	PR 3	HN 2	OP 2		SMIX
														FP 1	CD 1	CL tr	GN tr	GS tr	BY tr		
														BT tr	CA tr	CB tr	PO tr	MS tr	RU tr		
														TM tr	ZE tr	ZR tr					
04N04379	151-178	By2	vfs										52	QZ 52	GY 29	FK 15	FP 2	PR 1	MS 1		SMIX
														OP tr	HN tr	FE tr	BY tr	BT tr	GN tr		
														ZR tr							

*** Primary Characterization Data ***

Pedon ID: S04NV-003-001 (Clark, Nevada) Print Date: May 19 2010 6:12PM

Sampled As : Drygyp Loamy, gypsic, hyperthermic, shallow Typic Petrogypsid

USDA-NRCS-NSSC-Soil Survey Laboratory ; Pedon No. 04N0770

FRACTION INTERPRETATION:

csi - Coarse Silt, 0.02-0.05 mm vfs - Very Fine Sand, 0.05-0.1 mm fs - Fine Sand, 0.1-0.25 mm

MINERAL INTERPRETATION:

BT - Biotite	BY - Beryl	CA - Calcite	CB - Carbonate Aggregates	CD - Chert (Chalcedony
CL - Chlorite	FE - Iron Oxides (Goethite	FK - Potassium Feldspar	FP - Plagioclase Feldspar	GN - Garnet
GS - Glass	GY - Gypsum	HN - Hornblende	MS - Muscovite	MZ - Monazite
OP - Opaques	PO - Plant Opal	PR - Pyroxene	QZ - Quartz	RU - Rutile
TM - Tourmaline	ZE - Zeolite	ZR - Zircon		

INTERPRETATION (BY HORIZON):

SMIX - Mixed Sand

*** Supplementary Characterization Data ***

Pedon ID: S04NV-003-001 (Clark, Nevada) Print Date: May 19 2010 6:14PM

Sampled as on Apr 13, 2004 : Drygyp ; Loamy, gypsic, hyperthermic, shallow Typic Petrogypsid

Revised to SSL on Mar 09, 2006 : Drygyp ; Loamy, gypsic, hyperthermic, shallow Typic Petrogypsid

United States Department of Agriculture

SSL - Project C2004USNV132 IUSS Tour

Natural Resources Conservation Service

- Site ID S04NV608069-DM Lat: 36° 23' 10.60" north Long: 114° 25' 43.50" west NAD83 MLRA: 30

National Soil Survey Center

- Pedon No. 04N0770

Soil Survey Laboratory

- General Methods 1B1A, 2A1, 2B

Lincoln, Nebraska 68508-3866

Tier 1

				-1-	-2-	-3-	-4-	-5-	-6-	-7-	-8-	-9-	-10-	-11-	-12-	-13-	-14-	-15-	-16-	-17-	-18-	-19-	-20-	-21-	-22-	-23-	-24-	-25-
				(- Engineering PSDA -)													(- - - - - Cumulative Curve Fractions - - - - -)							(<75mm)		(Atter-)		(Gradation)	
				Percentage Passing Sieve													USDA Less Than Diameters (mm) at							berg		Uni-		Cur-
	Depth			3	2	3/2	1	3/4	3/8	4	10	40	200	20	5	2	1.	.5	.25	.10	.05	60	50	10	LL	PI	fmty	vtur
Layer	(cm)	Horz	Prep	(----------Inches----------)						(---------Number---------)				(------Microns----)			(---------Millimeter----------)					(-----Percentile---)			(----%----)		CU	CC

04N04374	0-1	A	S	100	100	100	100	100	100	100	100	99	68	28	18	11	100	99	98	79	51	0.06	0.049	0.002			40.8	5.1
04N04375	1-18	Bky	S	100	100	100	100	100	100	100	100	91	49	22	16	12	97	94	82	58	35	0.11	0.078	0.001			71.9	7.7
04N04376	18-47	Bym1	S	100	100	100	100	100	100	100	100	95	52	24	19	16	100	98	87	61	42	0.10	0.067	0.001			>100	8.4
04N04377	47-90	Bym2	S	100	100	100	100	100	100	100	100	95	63	24	14	8	100	96	90	71	51	0.07	0.049	0.003			24.7	3.2
04N04378	90-151	By1	S	100	100	100	100	100	100	100	100	99	70	26	19	14	100	100	98	79	56	0.06	0.042	0.001			53.9	8.4
04N04379	151-178	By2	S	100	100	100	100	100	100	100	100	97	57	25	19	15	100	99	92	68	43	0.08	0.062	0.001			88.2	9.3

Tier 2				-26-	-27-	-28-	-29-	-30-	-31-	-32-	-33-	-34-	-35-	-36-	-37-	-38-	-39-	-40-	-41-	-42-	-43-	-44-	-45-	-46-	-47-	-48-	-49-	-50-
				(- Weight Fractions -)														(- - - - - - - - - - - Weight Per Unit Volume (g cm^{-3})- - - - - - - -)									(- - Void - -)	
				Whole Soil (mm)								<75 mm Fraction						Whole Soil					<2 mm Fraction				Ratios	
				>2	250	250	75	75	20	5		75	75	20	5			Soil Sur		Engineering		Soil Survey			Engineering		At 33 kPa	
	Depth				-UP	-75	-2	-20	-5	-2	<2	-2	-20	-5	-2	<2		33	Oven	Moist	Satur	33	1500	Oven	Moist	Satur	Whole	<2
Layer	(cm)	Horz	Prep	(---------- % of Whole Soil ----------)								(--------- % of <75 mm ---------)						kPa	-dry		-ated	kPa	kPa	-dry		-ated	Soil	mm
																						DbWR1		DbWR1				
04N04374	0-1	A	S	--			--	--	--	--	100	--	--	--	--	100		1.45			1.90							

04N04375	1-18	Bky	S	--	--	--	--	--	100	--	--	--	--	100	1.08	1.08	1.16	1.67	1.08	1.08	1.08	1.15	1.67	1.45	1.45
04N04376	18-47	Bym1	S	--	--	--	--	--	100	--	--	--	--	100	1.36	1.37	1.40	1.85	1.36	1.36	1.37	1.40	1.85	0.95	0.95
04N04377	47-90	Bym2	S	--	--	--	--	--	100	--	--	--	--	100	1.25	1.28	1.34	1.78	1.25	1.24	1.28	1.34	1.78	1.12	1.12
04N04378	90-151	By1	S	--	--	--	--	--	100	--	--	--	--	100	1.20	1.20	1.36	1.75	1.20	1.20	1.20	1.35	1.75	1.21	1.21
04N04379	151-178	By2	S	--	--	--	--	--	100	--	--	--	--	100	1.37	1.42	1.51	1.85	1.37	1.31	1.42	1.51	1.85	0.93	0.93

*** Supplementary Characterization Data ***

Pedon ID: S04NV-003-001 (Clark, Nevada) Print Date: May 19 2010 6:14PM

Sampled As : Drygyp Loamy, gypsic, hyperthermic, shallow Typic Petrogypsid

USDA-NRCS-NSSC-Soil Survey Laboratory ; Pedon No. 04N0770

Tier 3 -51- -52- -53- -54- -55- -56- -57- -58- -59- -60- -61- -62- -63- -64- -65- -66- -67- -68- -69- -70- -71- -72- -73- -74- -75-

				(- - - - - - - - - - - - - - - - - Volume Fractions - - - - - - - - - - - - - - - -)											C	(- - - - - - Ratios To Clay - - - - - -)					(- - Linear Extensiblity - -)			(- - WRD - -)
				Whole Soil (mm) At 33 kPa											/N	<2 mm Fraction					Whole Soil	<2 mm	Whole	<2
				>2	250	250	75	75	20	5	2-	.05-	LT	Pores	Rat	Fine	CEC	1500	LEP	33 kPa	to %	Soil	mm
	Depth				-UP	-75	-2	-20	-5	-2	<2	.05	.002	.002	D F	-io	Clay	Sum	NH_4-	kPa	33	1500	Oven	1500	Oven
Layer	(cm)	Horz	Prep	(---------- % of Whole Soil ----------)														Cats	OAC	H_2O	kPa	kPa	-dry	kPa	-dry	(---in^3/in^3---)

04N04374	0-1	A	S	--	--	--	--	--	--	--	100	27	22	6			7			0.40								
04N04375	1-18	Bky	S	--	--	--	--	--	--	--	100	26	10	5	51	8	4			0.12	--	--	--	--	--	0.06	0.06
04N04376	18-47	Bym1	S	--	--	--	--	--	--	--	100	30	13	8	45	4	2			0.21	0.013	--	0.2	--	0.2	--	--
04N04377	47-90	Bym2	S	--	--	--	--	--	--	--	100	23	20	4	44	9	8			0.42	0.104	--	0.8	--	0.8	0.05	0.05
04N04378	90-151	By1	S	--	--	--	--	--	--	--	100	20	19	6	39	16	4			0.28	--	--	--	--	--	0.11	0.11
04N04379	151-178	By2	S	--	--	--	--	--	--	--	100	30	14	8	34	14	1			0.36	0.079	--	1.2	--	1.2	0.07	0.07

Tier 4				-76-	-77-	-78-	-79-	-80-	-81-	-82-	-83-	-84-	-85-	-86-	-87-	-88-	-89-	-90-	-91-	-92-	-93-	-94-	-95-	-96-	-97-	-98-
				(- - - - - - - - - - - - - - - - - - - Weight Fractions - Clay Free - - - - - - - - - - - - - - - - - - -)																Text	PSDA (mm)			pH	Elect.	Part-
				(---------- Whole Soil ----------)						(---------- <2 mm Fraction ----------)										-ure	Sand	Silt	Clay	Ca	Res-	Con-	-icle
				>2	75	20	2-	.05-	<	(---------- Sands ----------)					(--- Silts ---)		Cl			by	2-	.05-	<	Cl_2	ist.	duct	Den-
	Depth				-20	-2	.05	.002	.002	VC	C	M	F	VF	C	F	ay			PSDA	.05	.002	.002	.01M	ohms	dS m^{-1}	sity
Layer	(cm)	Horz	Prep	(- % of >2 mm Sand and Silt -)						(----------% of Sand and Silt ----------)										<2 mm	(---- % of 2 mm ----)			(-------- <2 mm --------)			g cm^{-3}
																						3A1a1a	4C1a2a			4F2		

04N04374	0-1	A	S	--	--	--	56	44	13	tr	tr	2	21	32	26	18	13	l	49.3	39.4	11.3	7.7	2.40
04N04375	1-18	Bky	S	--	--	--	73	27	13	4	3	14	26	26	15	12	13	fsl	64.7	23.8	11.5	7.7	2.23
04N04376	18-47	Bym1	S	--	--	--	69	31	18	--	3	13	31	22	21	11	18	fsl	58.2	26.3	15.5	7.9	2.88
04N04377	47-90	Bym2	S	--	--	--	53	47	8	tr	4	7	20	22	29	18	8	l	49.2	43.1	7.7	7.8	2.50
04N04378	90-151	By1	S	--	--	--	52	48	16	tr	tr	2	22	27	34	14	16	l	44.5	41.7	13.8	7.7	3.60
04N04379	151-178	By2	S	--	--	--	68	32	18	--	1	9	28	30	21	11	18	vfsl	57.5	27.4	15.1	7.7	6.60

Drygyp Soil Series: Interpretation of Lab Data and Micromorphology

Rebecca Burt
Research Soil Scientist, Soil Survey Investigations, NSSL

DRYGYP S04NV-003-001

The soil material for Drygyp that further hardened upon air-drying during sample preparation and initially recorded as particles >2-mm was nulled, i.e., no chemical analysis (e.g., % gypsum) are reported on this material. Carbonates range from 16% in the surface to trace with depth. Unlike carbonates, gypsum increases dramatically with depth, ranging from 14% in the surface to 90% within <20 cm, with these large amounts generally maintained with depth. Gypsum and carbonates are in nearly equal amounts in the surface horizon of the Drygyp pedon. Soil pH of the surface horizon is 7.7. The solubility diagram (Lindsay, 1979) shows the solubility of gypsum is not pH dependent, whereas calcite is. With the presence of competing species such as gypsum and calcite in a soil system, calcite formation is favored at a higher pH. Gypsum is rarely present in soils if pH > 8.2 (Nelson, 1982). Shifts in the dynamics of a system can result in a predominating mineral species (calcite versus gypsum), i.e., shifts in system inputs, (e.g., Ca^{2+}, SO_4^{2-}, acidity, water content), will ultimately affect system outputs,(e.g., calcite and/or gypsum).

It is a relatively small window in which these two minerals can co-exist, and an even smaller window in which these minerals could possibly exist in equal amounts. The use of gypsum in sodic soils is an example of this equilibria between the two mineral species. If gypsum is introduced, naturally or anthropogenically, into a soil system with a pH of 8.5 or higher, the soluble Ca^{2+} is raised above calcite equilibria and leads to the precipitation of calcite. This calcite reaction releases H^+ ions. Over time, the pH will drop from 8.5 to 7.5 to 8.0 which is the pH range that gypsum and calcite can co-exist. In addition, soluble Ca^{2+} is restored to approximately $10^{-2.5}$M, keeping colloids flocculated and predominately Ca^{2+} saturated. Displaced Na^+ is then leached from the system. Water soluble Na is relatively low throughout the profile of the Drygyp pedon (0.2 to 3.7 mmol(+)/L), increasing only at the lower depths, e.g., 45 mmol(+)/L in the By2 horizon (151-178 cm).

In the FAO document about gypsiferous soils specifically the chapter related to laboratory methods for analyzing these kinds of soils, there is a statement that the method developed at the U.S. Salinity Laboratory (Richards, 1954) and later adopted and currently used at the SSL, "is used by many laboratories where accurate figures of the gypsum content are not required". I do not agree with this statement. The SSL has verified its gypsum results by conducting some methods testing over a period of time. The SSL recently analyzed a number of samples for gypsum, primarily from the Western Region. Samples with very high amounts of gypsum (e.g., >90%), as with the Drygyp pedon, pose some complexity as related to appropriate sample size and resulting reproducibility of data. In 2002 we conducted a comparative study with the U.S. Salinity Laboratory for gypsum content in soil. The U.S Salinity Laboratory determines gypsum by the multiple dilutions method. The standard SSL procedure is by acetone precipitation followed by an EC reading (semi-quantitative). Our testing indicated that the SSL gypsum data closely parallels data by the U.S. Salinity Laboratory. These data were on the low end for gypsum content, with comparative results for the U.S. Soil Salinity Laboratory gypsum standard of 7.08 to 7.27% versus 7.82 to 7.85% (SSL and U.S. Salinity Laboratory,

respectively). Additionally, on the high-end for gypsum content, we also generated comparative gypsum values between the SSL standard procedure and thermal analysis (54 versus 56%, respectively, for a New Mexico soil; 91 versus 93%, respectively for an Arizona soil; and 12 versus 13% , respectively, for the SSL gypsum standard). Gypsum determination in soils by the acetone method and by total SO_4^{2-} in aqueous extracts was recently compared in an article entitled "Occurrence, formation, and micromorphology of gypsum in soils from the Central-German Chernozem region" by Dultz and Kuhn (2005). In addition to chemical tests, optical analysis and x-ray diffraction (XRD) are useful tools for the identification and semi-quantification (XRD) of gypsum. If gypsum is present in soils, XRD shows the characteristic peak at 7.61 Angstroms. These XRD and optical data are located on the SSL data sheets for Drygyp.

The field and laboratory textures for the Drygyp pedon differ some throughout the soil profile. These discrepancies were not unexpected. As I mentioned in my trip report, in the standard SSL method for particle-size distribution analysis (PSDA), gypsum is considered an "interference" (as do many labs), i.e., gypsum interferes with PSDA by causing flocculation of particles and therefore is removed by stirring and washing the soil with water. The SSL considers this procedure effective if the soil contains <25% gypsum. Interestingly, while carbonates are sometimes destroyed in the process of PSDA, the generally accepted procedure is to consider calcium carbonate particles as contributing to the texture of a soil. In April 2004, I forwarded a method for PSDA of gypsiferous soils (Hesse, 1976), using a barium sulfate solution. There are other methods for PSDA in gypsiferous soils (FAO, 2005). Knowledge of these methods may be useful background information. Field textures for gypsiferous soils can serve as useful alternatives to laboratory-determined textures. Typically, depending on such factors as particle size of gypsum and form of gypsum (well-crystallized, powder, cemented crust, etc), field textures are coarser than laboratory data. With gypsum identified by XRD (clay fraction), optical analysis (CSI to FS), and by thin section analysis, there appears to be a range of gypsum particle sizes in the Drygyp pedon. The adverse effect of gypsum upon dispersion during PSDA increases with decreasing particle-size, related to increased solubility.

Bulk density ranges from 1.08 g/cm^3 in the surface to 1.37 g/cm^3 in the By2 horizon (151-178 cm). Poch and Verplancke (1997) found the general physical and chemical characteristics of some gypsiferous soils show much variation in gypsum content (none to 90%) as well as bulk density and particle-size distribution (analyses done without gypsum dissolution (Hesse, 1976; Viellefon, 1979). In general, it appears that those soils with increasing amounts of gypsum show decreasing bulk density, e.g., 89% gypsum with 1.33 g/cm^3 bulk density (Poch and Verplancke, 1997). This compares to the Bym1 horizon of the Drygyp pedon with 90% gypsum and 1.36 g/cm^3 bulk density. The WRD values appear higher than one would expect in these kinds of soils, ranging from 0.27 to 0.40 cm^3/cm^3. The properties of gypsiferous soils such as 1500-kPa water content that are reported on an oven-dry weight basis are converted to include the weight of crystal water in gypsum. The 1500-kPa water content is corrected when the gypsum content of the soil is >1%, whereas the 33-kPa water content is not. This may need to be adjusted as well. If the 33-kPa data are adjusted, these data will also be reflected in any updates of the laboratory data that will be forwarded to you or available on the web at a later date.

Micromorphology:

The matrix of the Bky horizon (04N04375a-d) of the Drygyp pedon is primarily composed of gypsum. Lab data show 96% gypsum in the Bky horizon. Small amounts of carbonates are also visible in thin section (04N04375a). Lab data show 2% carbonates in the Bky horizon. Gypsum varies in shape (some lenticular and some not) and in particle-size and does not appear to have any particular orientation within the matrix (04N04375b-d). Similar to the Bky horizon, the Bym1 (04N04376a-e) is primarily composed of gypsum. Lab data show 90% gypsum in the Bym1. A localized feature of the Bym1 horizon (04N04376c) is a carbonate aggregate with skeletal grains embedded. This carbonate aggregate is segregated from the gypsum matrix. The Bym1 horizon (04N04376d) shows little void space except for a few channels, nearly filled with gypsum. A pore in the Bym1 horizon (04N04376e) appears to show no active processes of gypsum crystallization. Similar to the Bym1 horizon, the Bym2 (04N04377a) shows few void spaces, but unlike the Bym1 there appears to be some pattern or organization of the gypsum crystals. The By1 horizon is shown in photomicrographs (04N04378a-c). In some parts of the fabric of the By1, sand-sized gypsum crystals show a unidirectional orientation (04N04378a), whereas in other parts, the gypsum appears to show no particular orientation with a range of particle-sizes. The By2 horizon is shown in 04N04379a-c. The By2 (04N0437c) shows "swirls" of gypsum precipitated in the voids.

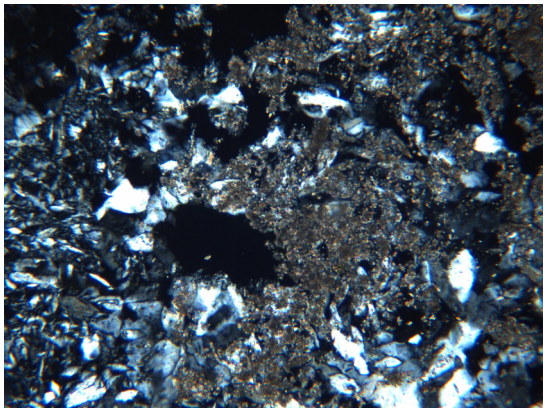

Drygyp_04N0770_04N04375a_XPL_10X

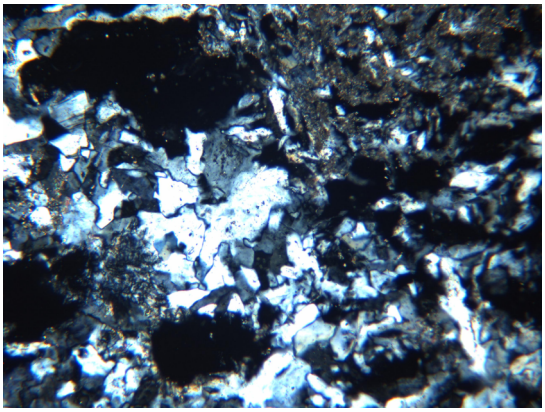

Drygyp_04N0770_04N04375b_XPL_10X

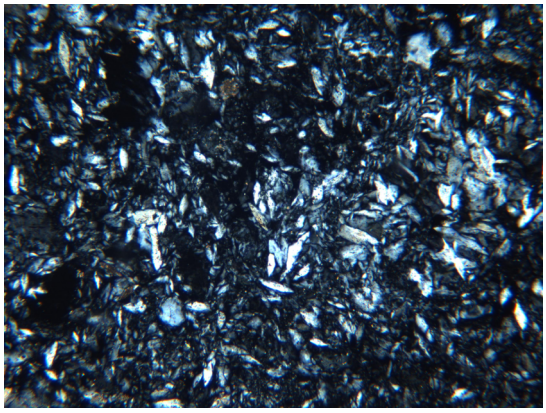

Drygyp_04N0770_04N04375c_XPL_10X

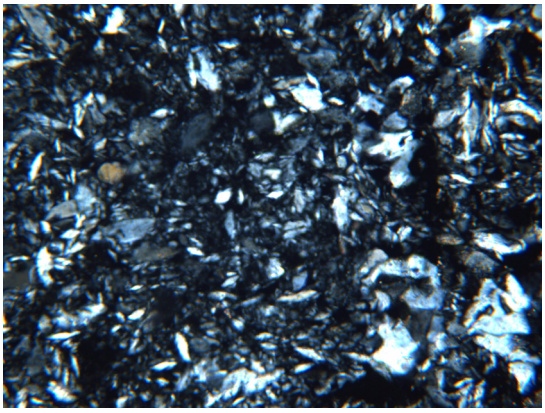

Drygyp_04N0770_04N04375d_XPL_10X

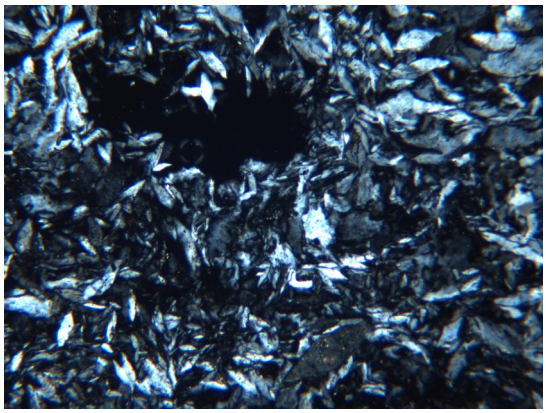

Drygyp_04N0770_04N04376a_XPL_10X

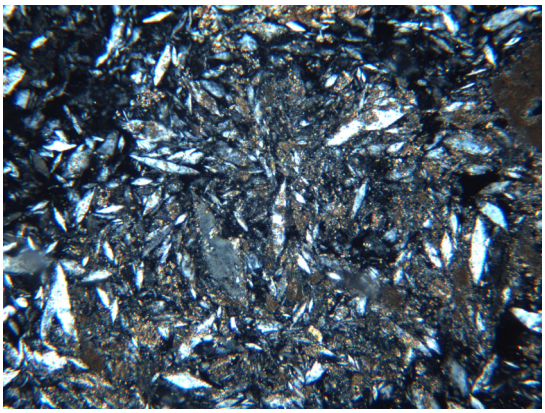

Drygyp_04N0770_04N04376b_XPL_10X

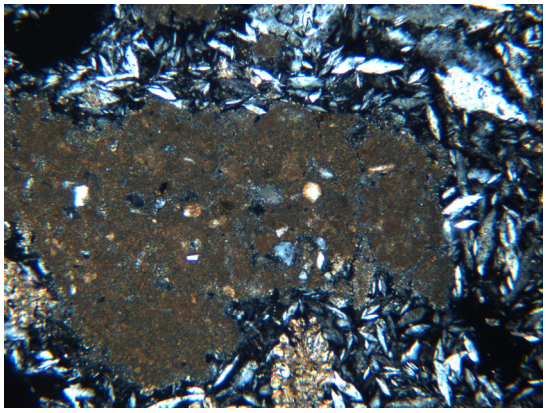

Drygyp_04N0770_04N04376c_XPL_10X

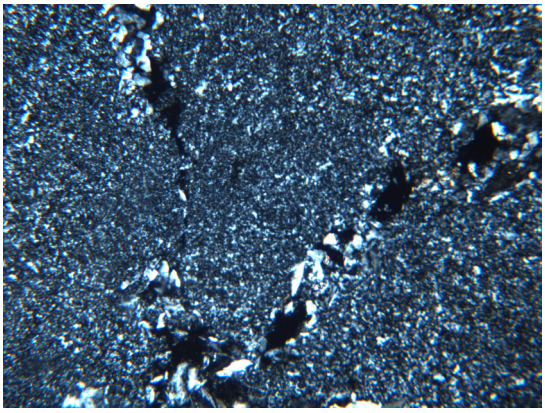

Drygyp_04N0770_04N04376d_XPL_4X

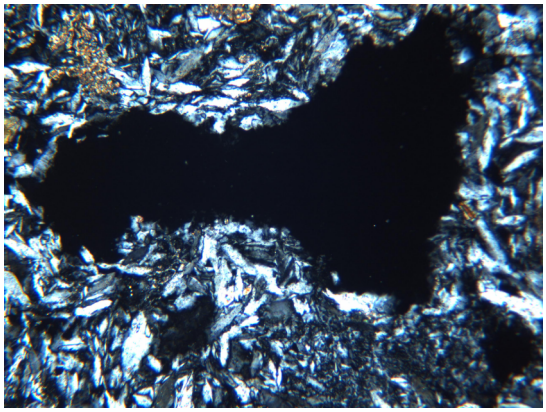

Drygyp_04N0770_04N04376e_XPL_10X

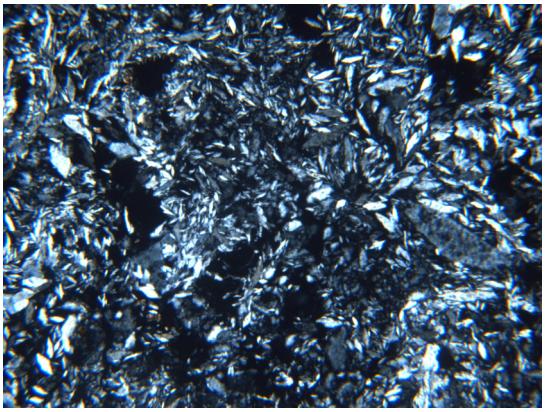

Drygyp_04N0770_04N04377a_XPL_4X

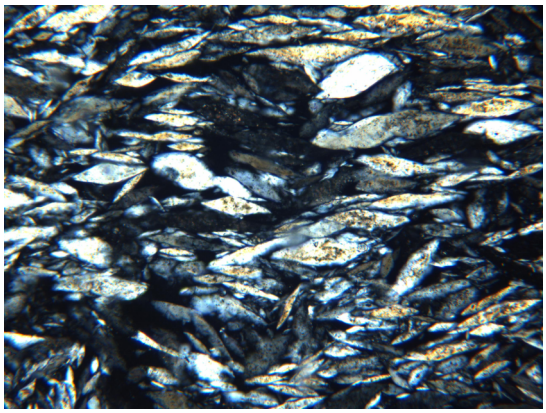

Drygyp_04N0770_04N04378a_XPL_10X

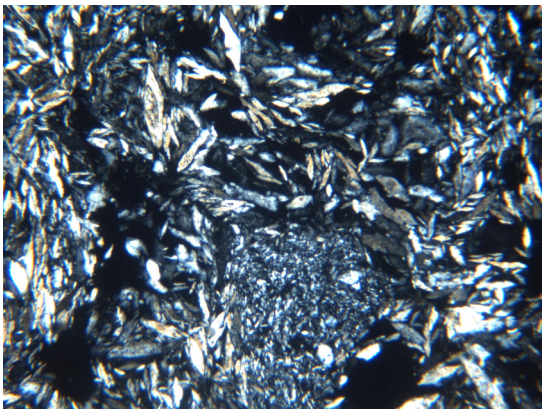

Drygyp_04N0770_04N04378b_XPL_4X

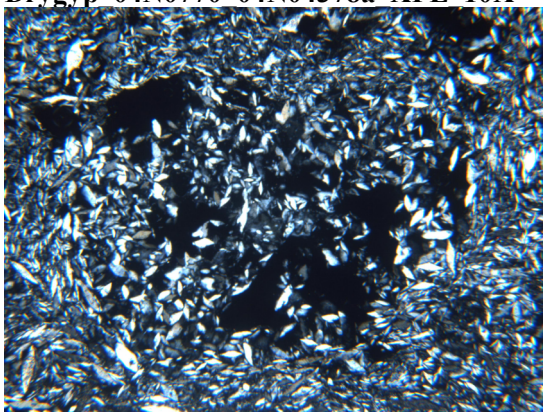

Drygyp_04N0770_04N04378c_XPL_4X

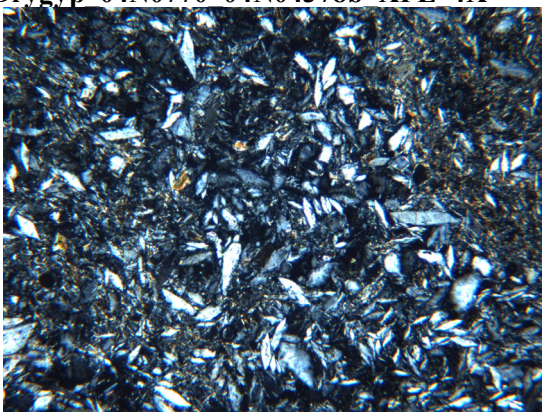

Drygyp_04N0770_04N04379a_XPL_10X

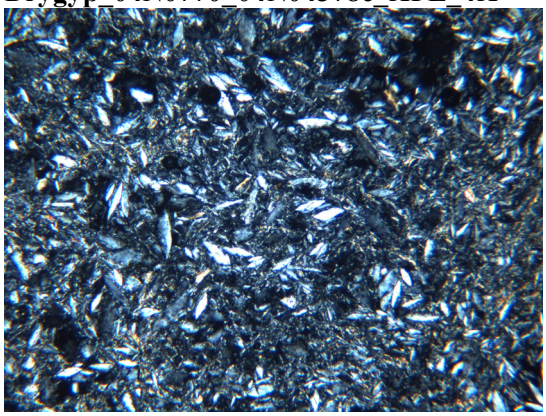

Drygyp_04N0770_04N04379b_XPL_10X

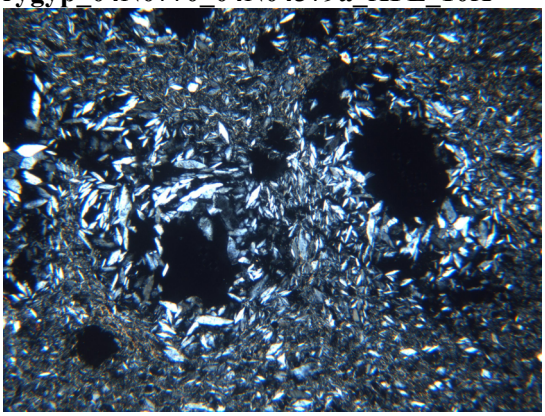

Drygyp_04N0770_04N04379c_XPL_4X

References

Dultz, S., and P. Kuhn. 2005. Occurrence, formation, and micromorphology of gypsum in soils from the Central-German Chernozem region. Geoderma 2005.01.022.

Hess, P.R. 1976. Particle size distribution in gypsic soils. Plant and Soil. 44:241-247.

Lindsay, W.L. 1979. Chemical equilibria in soils. John Wiley & Sons, Inc., NY. 6

Nelson, R.E. 1982. Carbonate and gypsum. In: A.L. Page, R.H. Miller, and D.R. Keeney (eds.) Methods of soil analysis. Part 2. Chemical and microbiological properties. 2nd ed. Agron. 9:159-165.

Poch, R.M.,and H. Verplancke. 1997. Penetration resistance of gypsiferous horizons. Euro. J. Soil Sci. 48:535-543.

Richards L. A., U.S. Salinity Lab. Staff. Diagnosis and Improvement of Saline and Alkali soils, USDA Handbook 60 (1954)

Vieillefon, J. 1979. Contribution to the improvement of analysis of gypsiferous soils. Cahiers/ORSTOM, Série Pédologie 17:195-223. Translated from Food and Agriculture Organization of the United Nations. 1990. Management of gypsiferous soils. FAO Soils Bulletin 62. Rome.

Edaphic Relationships of the Drygyp Soil Series: Las Vegas bearpoppy and Relict Leopard frog

Douglas Merkler[1] and Shawnalea Thai[2]

[1]Nevada State Resource Soil Scientist, Natural Resource Conservation Service, USDA, Las Vegas NV, doug.merkler@nv.usda.gov; [2]Volunteer, UNLV & Natural Resource Conservation Service, USDA, Las Vegas NV

Edaphic factors includes the physical, chemical, and biological properties of soil that result from biologic and geologic phenomena or anthropogenic activities. Discontinuities in the edaphic factors contribute to the intriguing patterns of diversity we see in the biotic world. Chemical and physical features of soil greatly influence the ecology and evolution of plants and their associated biota. Extreme soil conditions, such as those found on serpentine outcrops, limestone, gypsum deposits, and even mine tailings, have led to the formation of unique plant and animal communities characterized by rarity and endemism.

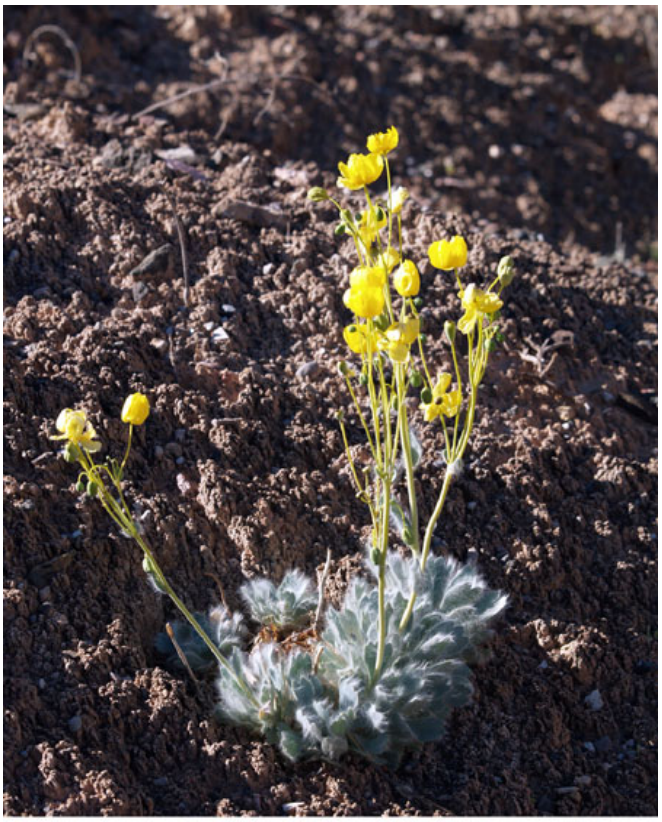

Las Vegas bearpoppy, *Arctomecon californica*

"Arctomecon californica was first discovered in 1844 near Las Vegas, Clark County, Nevada, by John Charles Frémont on his second expedition through the American West, and was described as a new species the following year by John Torrey and Frémont, who named it for the Mexican territory where it was found. All three known species of this distinctive genus of the poppy family are endemic to the northern Mojave Desert." (Orlando M. et al., 1996)

Las Vegas bearpoppy, *Arctomecon californica* is a species of interest which is associated with the Drygyp soil series. Noted as an endemic to gypsic soils in the Lake Mead National Recreation Area's sensitive plant, animal and community field guide (Moore, et al. 1993), recent work by (Drohan and Merkler 2009) shows that with respect to the *Arctomecon californica,* gypsum is but one part of the explanation for *A. californica* habitat differentiation and in fact is not an obligate gypsophile but more likely is a species adapted to extreme environments.

Relict Leopard Frog
Lithobates onca (formally *Rana onca)*

The environment of the Roger and Blue Point Springs complex responsible for the deposition of the soluble salts that the Drygyp series formed in provides a refuge for the endangered species *Lithobates onca*, the Relict Leopard frog. This frog was listed as endangered in 2004 because its area of occupancy is less than 500 km^2, all individuals are in fewer than five locations, and no subpopulation contains more than 250 mature individuals. In the 1990's seven populations of *Lithobates onca* in three locations were known to exist. Twenty years later, there are only five known populations remaining, estimated population sizes for the five groups range from as few as 36 adults in the smallest population to about 600 adults in the largest population. Studies have shown that the species has likely existed here since the origins of the springs and certainly have been present for the last 5 million years.

The Blue Point and Roger Springs are fast moving springs. The swift current places a limitation on vegetative growth, specifically *Scirpus,* and promotes *Lithobates onca* habitat. The Colorado River area south of Lake Mead includes three streams and is about 5.1 km long respectively. This area harbors another population of *Lithobates onca*, because the aquatic habitat here is not too crowded with emergent vegetation. Habitat destruction and redirecting of water as well as the introduction of the American Bull frog (*Lithobates catesbeiana),* game fishes, and crayfish are all threatening the survival of this species.

Lithobates onca is not alone; amphibians are going extinct faster than any other group of organisms. Since 1980, 122 species may have disappeared. Of the roughly 6,000 species of amphibians remaining, up to half are threatened; some 500 could go extinct in the next 50 years. Another of the suspected causes of extinction is a "chytrid" type of fungus (Phylum Chytridiomycota). There are approximately 1,000 different chytrid species that live exclusively in water or moist environments. In 1999, a new species of chytrid was described that infects the skin of amphibians and was named *Batrachochytrium dendrobatidis* or "Bd" for short (Longcore et al., 1999). Bd is a very important chytrid fungus because it appears to be capable of infecting most of the world's approximately 6,000 amphibian species; many of those species develop the disease chytridiomycosis which is linked to devastating population declines and species extinctions (Berger et al., 1998; Skerratt et al., 2007; Fisher et al., 2009).

Disease ecologist Jason Rohr of the University of South Florida in Tampa, stated that none of the amphibian extinction theories were quite right—and the parts that were correct were correct for the wrong reasons. To illustrate his point, he showed that frog extinctions were more closely correlated to beer and banana production than to air temperature. One of Rohr's conclusions in this article is that he suspects that the frogs' ability to secrete fungus-fighting skin secretions is temperature-sensitive. In addition, the presence on the skin of specific types of symbiotic bacteria discourage the growth of chytrid fungus. Amphibians or amphibian populations that normally have large numbers of these bacteria on the skin might be more resistant to developing chytridiomycosis. Also, the production by the poison glands in amphibian skin of chemicals called "antimicrobial proteins" seem to discourage the growth of chytrid fungus. Specific types, combinations, or amounts of antimicrobial proteins might help some species to be more resistant to chytridiomycosis.

These five remaining populations have been red-listed as endangered by the IUCN as of 2010. Collaborative efforts by federal, state, and local government agencies are currently promoting conservation. It is interesting that the habitat provided by the streams that are responsible the genesis of the hyperthermic Drygyp soil series continue to provide one of the safe havens for this relict species.

References:

Berger, L., R. Speare, P Dazsak, D.E. Green, A.A. Cunningham, C.L. Goggin, R. Slocombe, M.A. Ragan, A.D. Hyatt, K.R. McDonald, H.B. Hines, K.R. Lips, G. Marantelli and H. Parkes, 1998. Chytridiomycosis causes amphibian mortality associated with population declines in the rain forests of Australia and Central America. Proceedings of the National Academy of Sciences of the United States of America 95: 9031-9036.

Drohan, P.J. and D.J. Merkler 2009. How do we find a true gypsophile? Geoderma 150 96–105

Fisher, M.C., T.W.J. Garner, and S.F. Walker. 2009. Global emergence of *Batrachochytrium dendrobatidis* and amphibian chytridiomycosis in space, time, and host. Annual Review of Microbiology 63:291–310.

Longcore, J.E., A.P. Pessier and D.K. Nichols. 1999. *Batrachochytrium dendrobatidis* gen. et sp. nov., a chytrid pathogenic to amphibians. Mycologia 91:219-227.

Moore, B. C., J.S. Sealove, and T.A. Knight. 1993. Lake Mead National Recreation Area Sensitive Plant, Animal and Community Field Guide, Barrick Museum of Natural History.

Orlando, M., R. Pant, T.S. Ross, J.M. Porter, and J.D. Morefield. 1996. Current Knowledge and Conservation Status of *Arctomecon californica* Torrey & Frémont (Papaveraceae), the Las Vegas bearpoppy. Nevada Natural Heritage Program and U.S. Fish & Wildlife Service status report.

Skerratt, L.F., L. Berger, R. Speare, S. Cashins, K.R. Mcdonald, A. Phillott, H.Hines, and N. Kenyon. 2007. Spread of chytridiomycosis has caused the rapid global decline and extinction of frogs. EcoHealth 4:125-134.

Endolithic Cyanobacteria in Soil Gypsum: Applications for Extraterrestrial Life

Laura Eaton[1], Amanda Williams[1], Brenda J. Buck[1], Sa'eb A. Khresat[2], Z. Rawajfih[2], and Robyn Howley[1]

[1]Dept. Geoscience, University of Nevada Las Vegas, Las Vegas NV, lmzeaton@gmail.com
[2]Jordan University of Science and Technology, Irbid 22110 Jordan

Soil sulfates are present in arid and hyperarid soils around the world, including the Mojave Desert. Gypsum and other salt minerals at the soil surface can harbor microbial life because they are hygroscopic, thus retaining water from the atmosphere and providing habitats in climates that might otherwise be too harsh (Buck et al., 2008) (Fig 1). Additionally, the minerals provide protection from UV, but are translucent, thus allowing photosynthesis (Dong et al., 2007).

SEM (scanning electron microscope) analyses of gypsum from A horizons in Atacama Desert, Chile, the Mojave Desert (Drygyp soil series, Lake Mead NV), USA, the Al-Jafr and Badia basins, Jordan, and Chihuahuan Desert, Mexico were analyzed (Dong et al., 2007; Buck et al., 2008). Within the upper few millimeters of the surface in all samples, a wide variety of taxa and metabolic types were observed (Figs 2-11). Among the most striking images are the unicellular and filamentous cyanobacteria with and without exopolymer polysaccharides (EPS). The exopolymer polysaccharides (EPS) are common in the Mojave Desert sample, less common in the Chihuanhuan Desert sample, rare in the Jordan Desert, and not present in the Atacama Desert samples (Buck et al., 2008). Coccoid and rod-shaped bacteria were also present in the Jordan, Mojave, and Chihuahuan deserts but absent in the Atacama (Buck et al., 2008). SEM analyses indicate that growth of cyanobacteria has caused dissolution of tabular pseudohexagonal gypsum crystals (Buck et al., 2008). Microscopic and 16S rRNA gene analyses identified the dominant cyanobacteria as *Chroococcidiopsis* (Dong et al., 2007). Additionally, samples from snowballs in Av horizons in the Badia Desert, Jordan and were found to contain endolithic lichen.

In addition to tremendous biological diversity, the study reveals relationships between crystal morphology and microbial metabolism. The moisture levels dictate the species richness (i.e., the driest sites have the lowest species richness, and the wettest have the greatest). In some cases, the biological activity has resulted in the dissolution of gypsum crystals (Figs. 5,7, and 8). In other cases, gypsum crystals have precipitated on the biological materials (Figs. 2 and 9).

The identification of diverse biota in gypsum soils shows life is possible in Earth's most extreme environments and highlights potential microbial habitats for life on other planets and on early Earth.

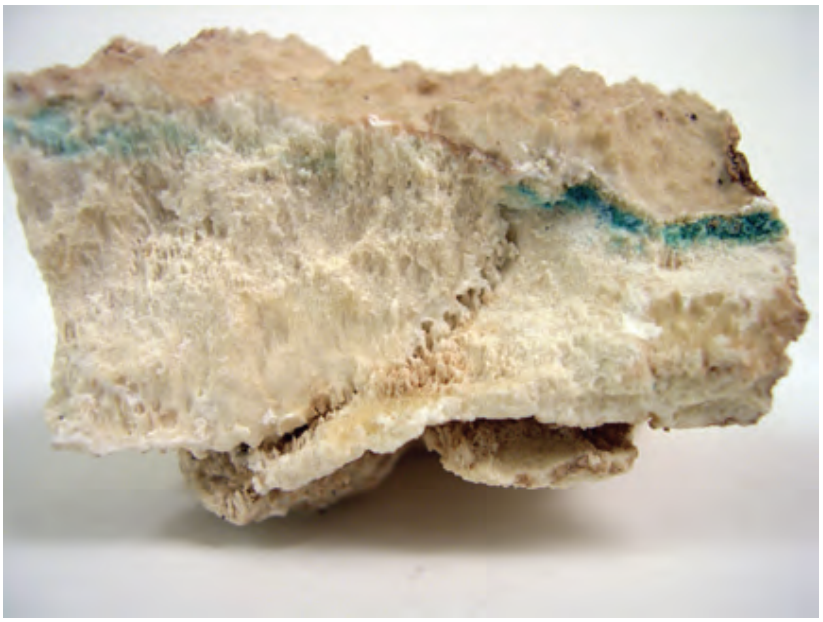

Figure 1. Example of endolithic cyanobacteria communities (green) just below the soil surface within a gypsum crust from the Atacama Desert, Chile (from Dong et al, 2007).

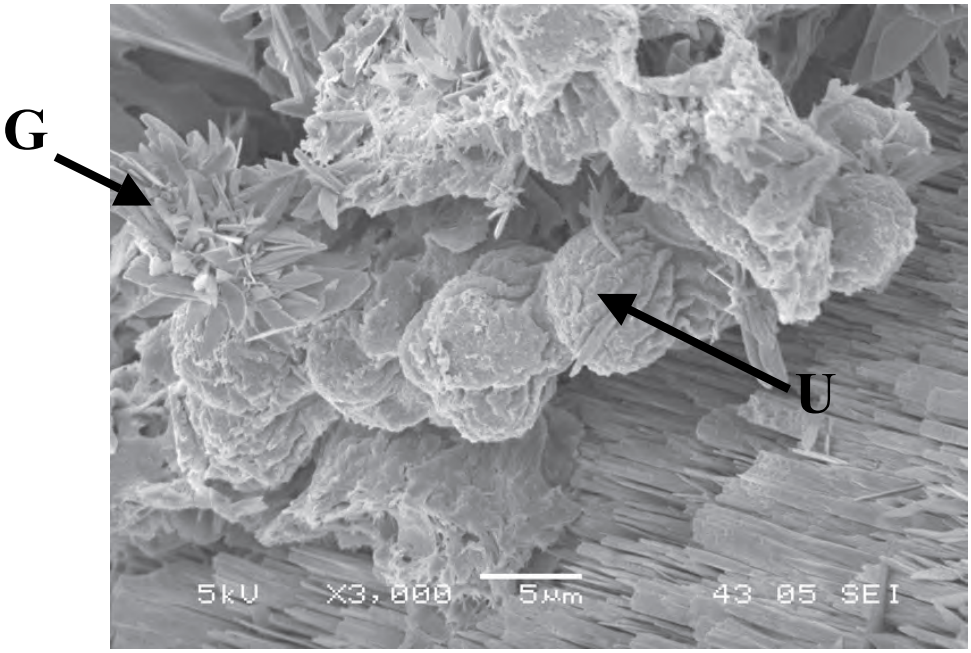

Figure 2. Mojave Desert (United States: Drygyp NV): unicellular cyanobacteria (U) covered in exopolymer polysaccharides. Gypsum crystals growing on cyanobacteria (G) (unpublished image from data collected for Dong et al., 2007).

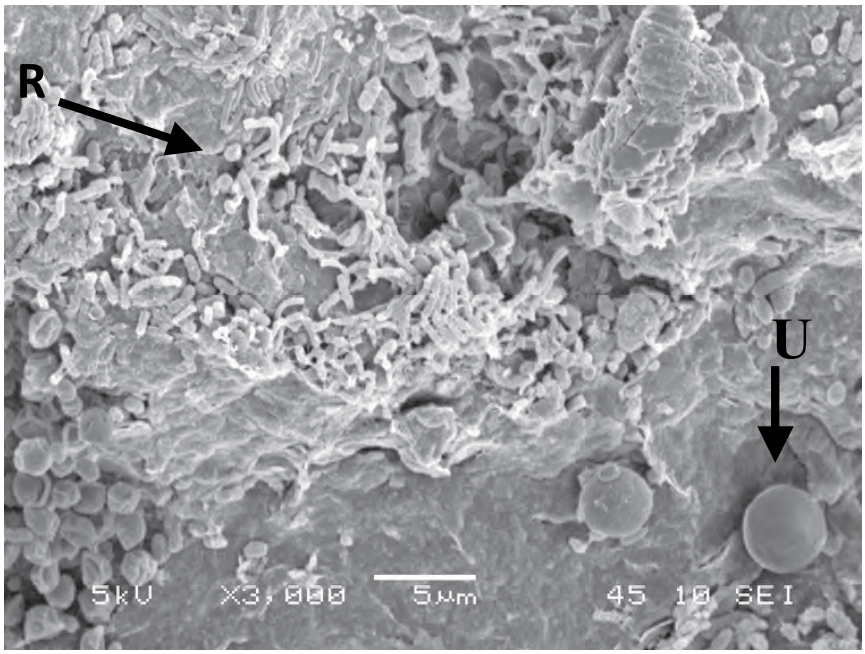

Figure 3. Al-Jafr Desert (Jordan): A dense population of rod-shaped bacteria (R) and a few unicellular cyanobacteria (U) cover smooth gypsum surfaces (unpublished image from data collected for Dong et al., 2007).

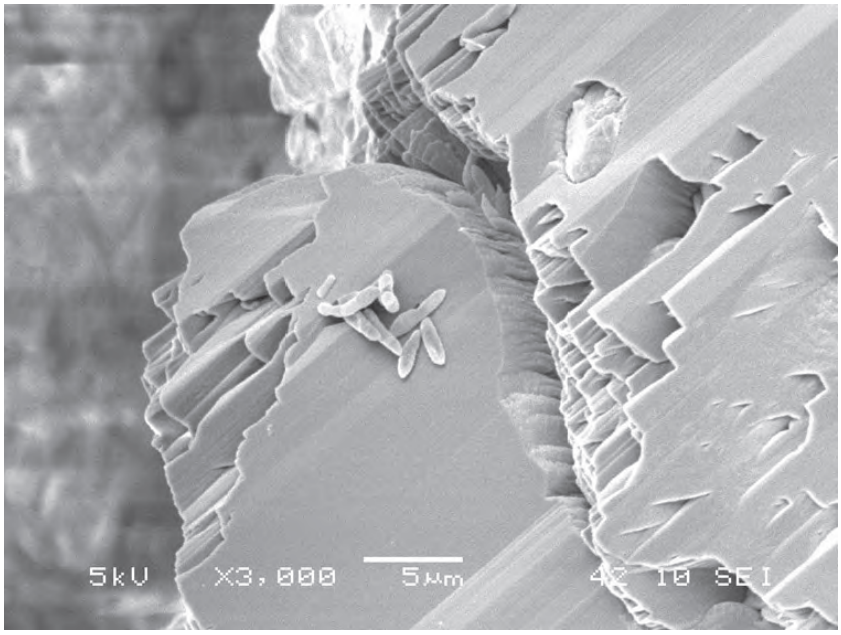

Figure 4. El Papolote (Mexico): Rod-shaped bacteria cluster on smooth gypsum crystal surface.

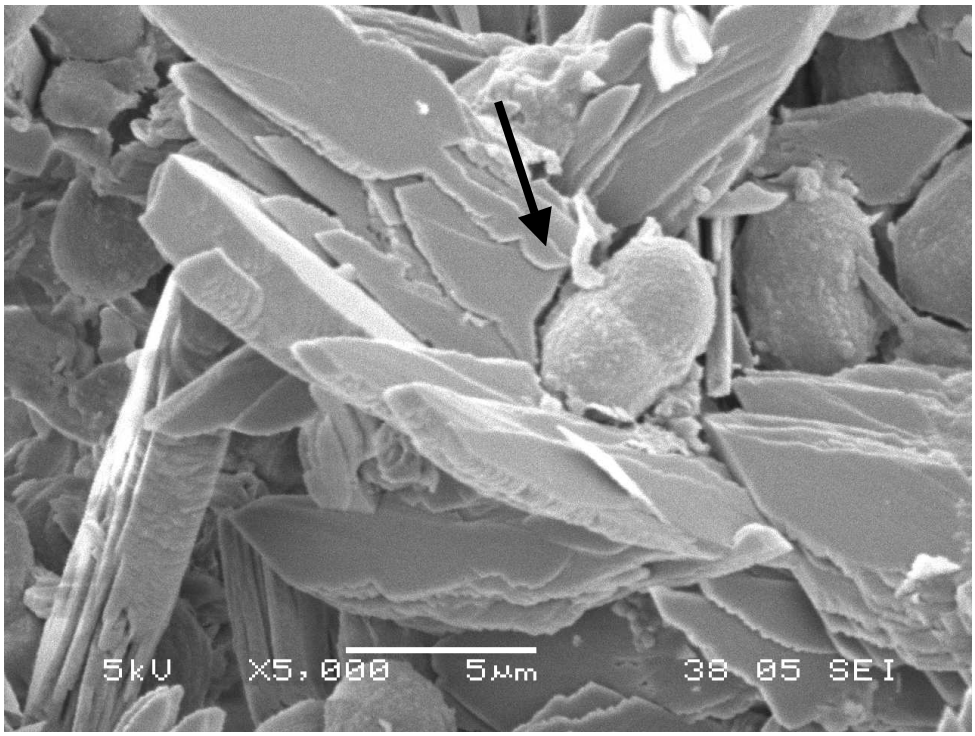

Figure 5. Atacama Desert (Chile): Euhedral gypsum crystal dissolved by unicellular cyanobacteria (displaying cell division)(From for Dong et al., 2007).

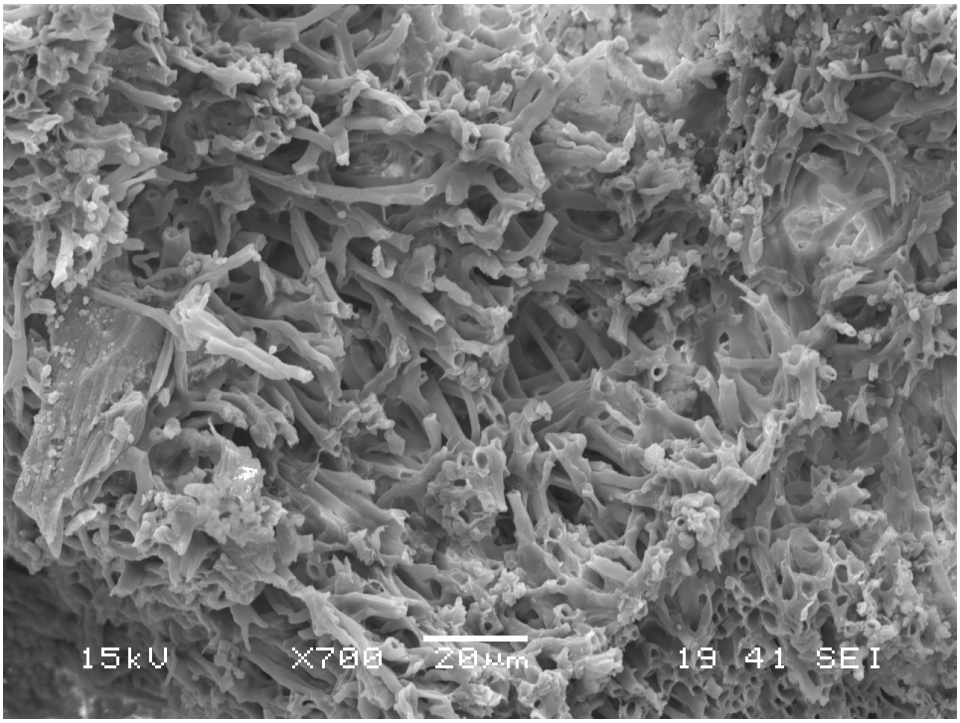

Figure 6. Badia Desert (Jordan): Endolithic lichen inhabiting gypsum snowballs at the surface of an Av horizon.

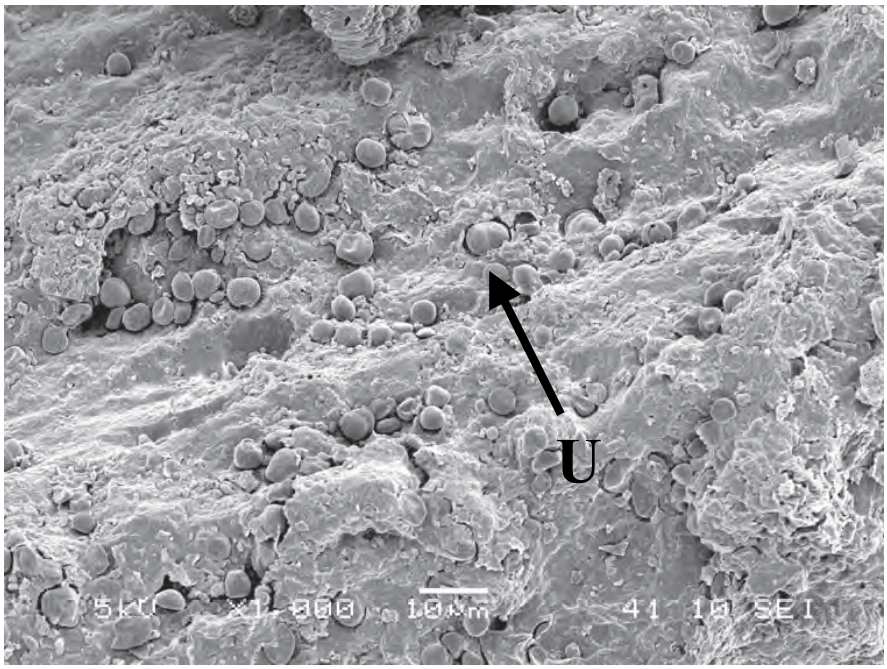

Figure 7. Al-Jafr Desert (Jordan): Unicellular cyanobacteria (U) in depressions in gypsum (note some biologically-driven gypsum dissolution)(unpublished image from data collected for Dong et al., 2007).

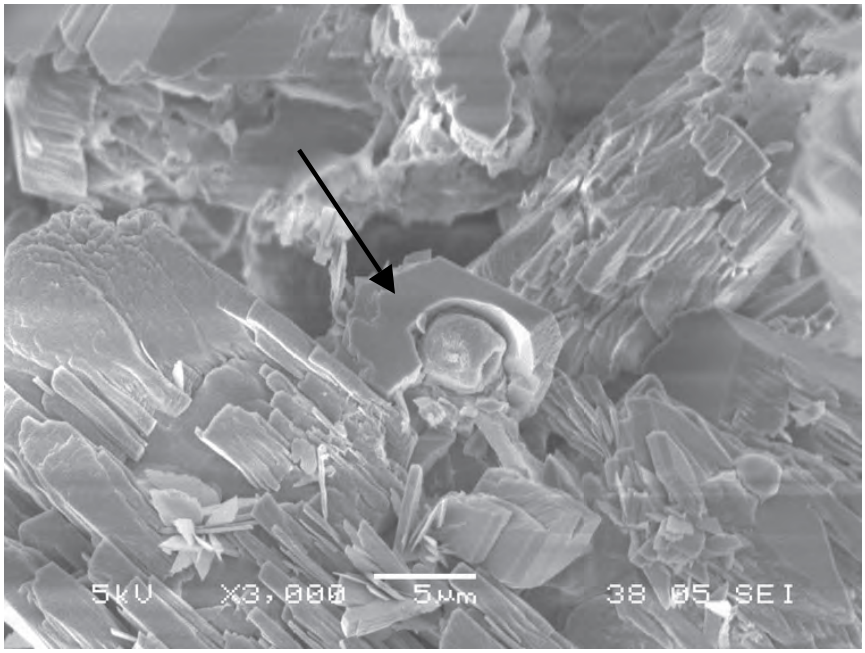

Figure 8. Atacama Desert (Chile): Unicellular cyanobacterium dissolving pseudohexagonal gypsum crystal (arrow)(unpublished image from data collected for Dong et al., 2007).

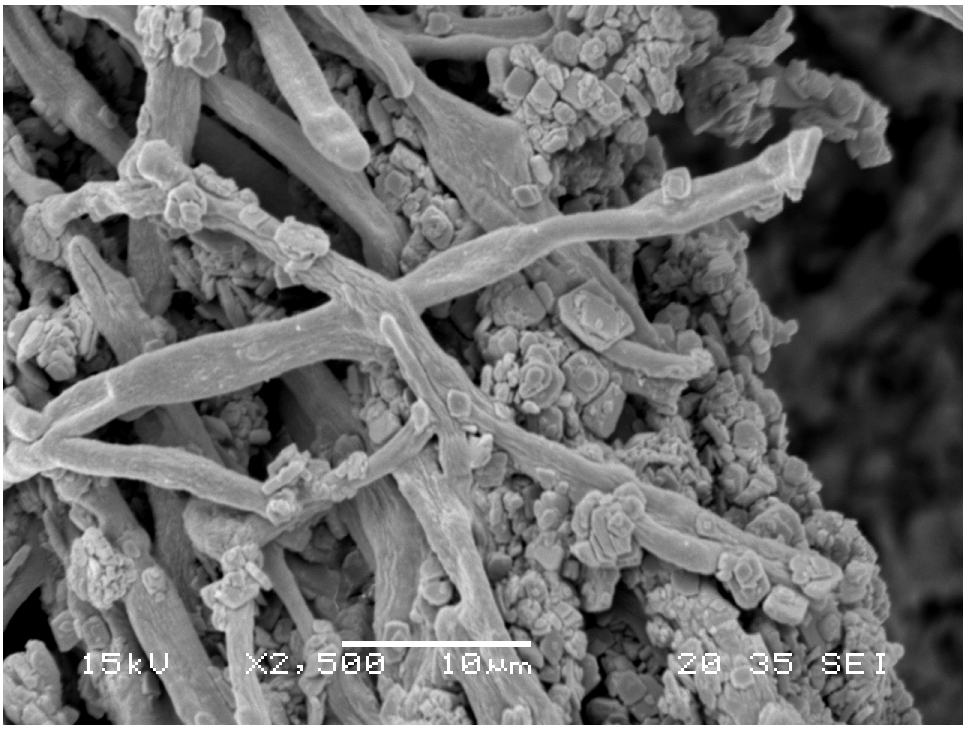

Figure 9. Badia Desert (Jordan): Gypsum crystals precipitate along microbial filaments.

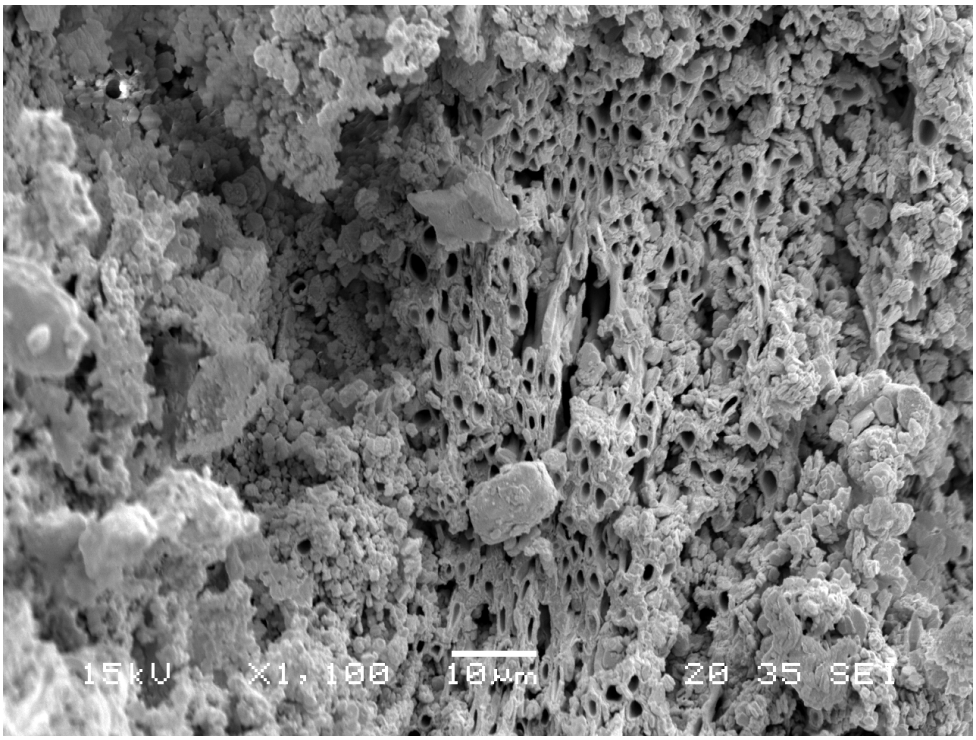

Figure 10. Badia Desert (Jordan): Gypsum crystals precipitate along microbial filaments.

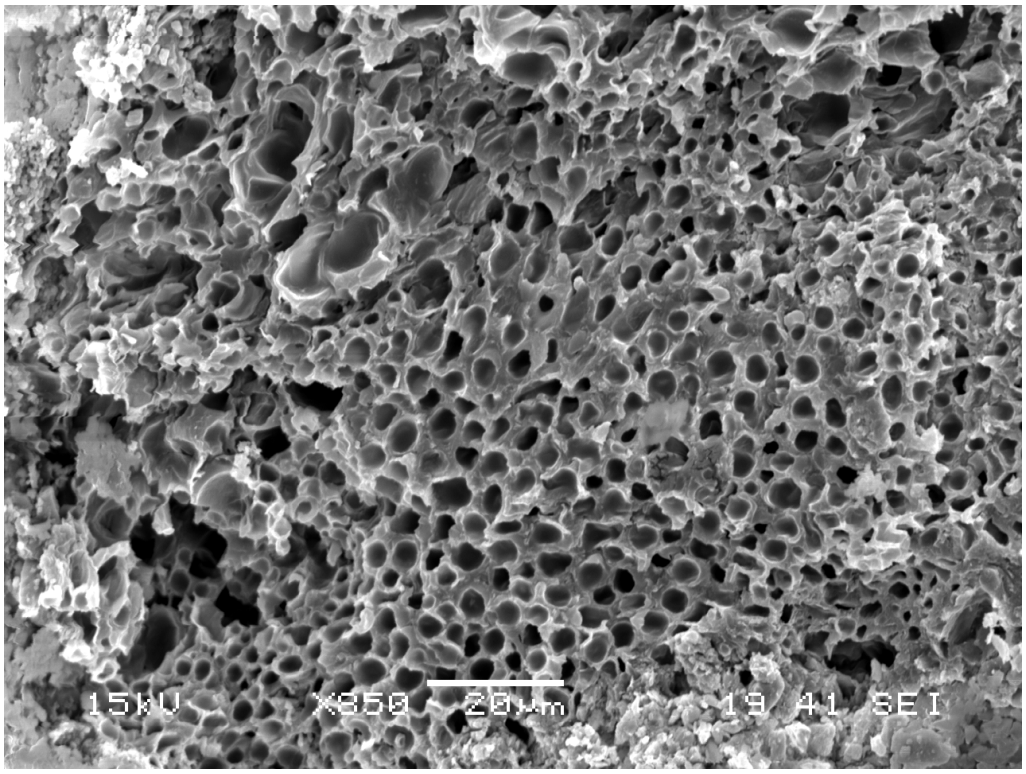

Figure 11. Badia Desert (Jordan): Cross section of probable endolithic lichen.

Acknowledgements
We thank all the authors in the previous studies (Dong et al., 2007 & Buck et al., 2008): Hailiang Done, Jason Rech, Hongchen Jiang, Henry Sun, and Judy Costa. Additionally, we thank Henry Sun, who identified the lichens in the Badia Desert, Jordan samples. We greatly appreciate the help of Doug Merkler, who obtained permits and assisted B. Buck with field sample collection on the Drygyp soil, Lake Mead, NV. We thank Lake Mead National Recreation Area personnel who have graciously helped us gain access to the site. Additional field assistance with soil characterization and laboratory analyses of the Drygyp pedon were provided by Joe Chiaretti and Rebecca Burt. Thanks also to Tim Lawton who assisted with obtaining samples from Mexico.

References

Buck, B.J., Sun, H., Williams, A., Costa, J., Hailiang, D., Rech, J., Hongchen, J., 2008, Micromorphology of endolithic cyanobacteria in soil gypsum: Applications for life on Mars, Abstracts of the 13th International Conference on Soil Micromorphology, Sept. 11-16, Chengdu China, p. 46.

Dong, H., J. A. Rech, H. Jiang, H. Sun, and B. J. Buck, 2007, Endolithic cyanobacteria in soil gypsum: Occurrences in Atacama (Chile), Mojave (United States), and Al-Jafr Basin (Jordan) Deserts, *J. Geophys. Res.,* 112, G02030, doi:10.1029/2006JG000385.

Field Trip Schedule

2:00 p.m.	Depart	
2:00 p.m.	Drive north on Hw169, turn left at Valley of Fire	
2:35 p.m.	Stop at Valley of Fire Visitor Center	Go straight through exhibits to back door, take the marked path uphill to lecture area for **Stop 4**
2:40 p.m.	**Stop 4: *Biologic Soil Crusts***	

Logistical Notes

Exit bus. Enter the Valley of Fire State Park Visitor Center, go straight through exhibits to back door, take the marked path uphill to lecture area for 10 min presentation on soil biological crusts. Following talk, return to Visitor Center to view exhibits and purchase gifts.

3:15 p.m.	Return to Buses & Depart	Take I-15 south to Las Vegas	
5:00 p.m.	Arrive	Embassy Suites	

Stop 4. Valley of Fire

Biological Soil Crusts in the Mojave

Amanda Williams[1], Brenda Buck[1], Mengesha Beyene[1], Douglas Merkler[2], and Debbie Soukup[1]

[1]Dept. Geoscience, University of Nevada Las Vegas, Las Vegas NV willamje@unlv.nevada.edu;
[2]Natural Resource Conservation Service, USDA, Las Vegas NV

Biological soil crusts (BSCs) are critical features in arid ecosystems. These crusts are complex matrices of soil particles intermingled with algae, cyanobacteria, lichen, mosses, microfungi, and bacteria (Friedmann and Galun, 1974)(Figure 1). Microbial filaments grow around soil sediments, fusing into a desert skin that resists erosion (Belnap, 1995). BSC organisms are ecosystem engineers that contribute soil organic matter and nutrients, manage soil moisture and temperature, influence vascular plant germination and prevent desertification (Eldridge and Greene, 1994; Jones et al., 1997). The ecological impacts of BSCs are potentially enormous, as these crusts can cover up to 70 percent of arid landscapes (Belnap, 1994)(Figure 2a).

BSCs come in a variety of forms, in both species composition and surface morphology. Early succession crusts (smooth crusts) are primarily composed of cyanobacteria (Belnap et al., 2003)(Figure 1a). Later succession crusts (pinnacled crusts) are colonized by moss, lichen, cyanobacteria, and algal communities (Figure 1b). While the exact age of these crusts is unknown, some estimate the succession of these crusts may take 10s to 1000s of years (Belnap et al., 2001). Several potential factors may influence BSC distribution and species composition, including elevation, precipitation, topography, soil texture, soil chemistry, soil depth, vascular plant competition, time, and disturbance (Belnap et al., 2001) (Figure 1). Recent research has attempted to understand these environmental controls of BSCs within the Mojave Desert (Figure 3)(i.e., Williams et al., 2010).

(a) (b)

Figure 1: (a) Smooth crusts are dominated by filamentous cyanobacteria; (b) Pinnacled crusts are dominated by lichen and short mosses.

BSCs are easily destroyed by physical impacts (off-road vehicular use, foot traffic, grazing, and horseback riding), making them key elements to protect in recreational areas (Belnap, 1995)(Figure 2b). Despite their important ecological roles in arid systems, BSCs are often overlooked or excluded from arid land management plans (Belnap et al., 2001). Many of these oversights may be due to the organisms' size and difficulty identifying individual species (Belnap et al., 2001). Even if land managers are able to identify BSC types, mapping their distribution on large tracts of land is usually unfeasible because of the crusts' patchy growth nature. Understanding BSC ecology and growth potential would help predict their distribution across the landscape and would provide reference conditions for ecological restoration.

Ongoing research has shown important relationships among BSCs, pedogenesis, landscape evolution, and soil fertility. Micromorphological investigations suggest moss-lichen BSCs play important roles in dust capture at the organism- and pinnacle-scale. BSC dust capture increases soil water, nutrient, and surface area availability. Greater crust growth leads to higher dust capture, thus creating a positive feedback mechanism that enhances continued moss-lichen propagation (Williams et al., 2010). Because crust distribution is tied to dust capture, stable landforms with high surface roughness show the highest BSC growth potential. In the Mojave, sandy-skeletal, mid-Holocene alluvial surfaces (i.e., Arizo soil series) have the most extensive moss-lichen growth (Williams et al., 2010). These soil-geomorphic and micromorphological investigations suggest BSCs are key factors in the development of arid soils and potentially affect surface stability and landform development (Williams et al., 2010).

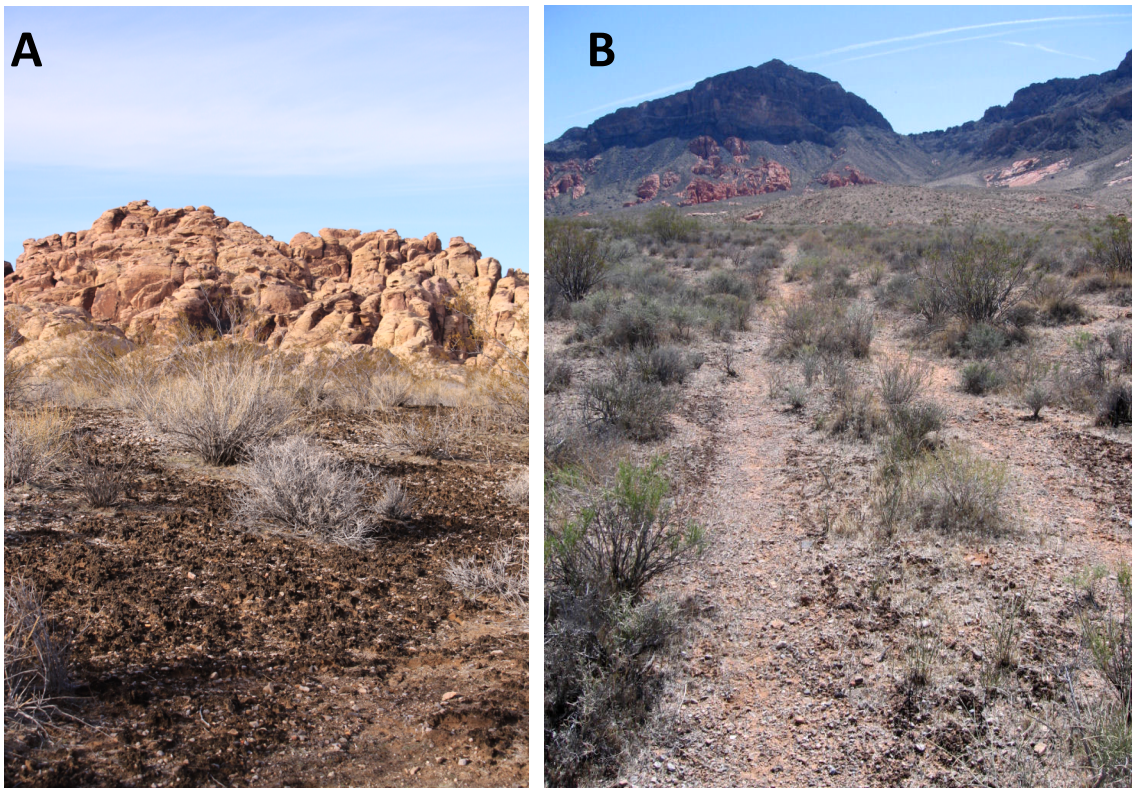

Figure 2: (a) Moss-lichen (pinnacled) crusts fill shrub interspaces; (b) Tracks left by motorized vehicles scar the landscape within Hidden Valley (MMWA) Nevada.

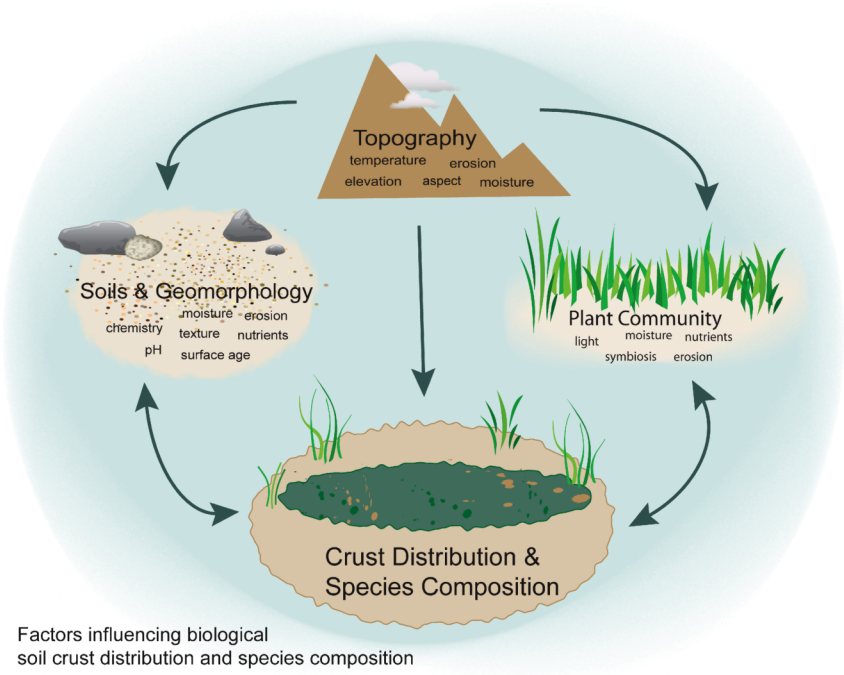

Figure 3: Potential factors that may influence the distribution, density, morphology, and species composition of BSCs in the Mojave Desert.

Acknowledgements
Thanks to the Bureau of Land Management, Cooperative Ecosystems Studies Unit (CESU) for generously funding and supporting this research. We especially appreciate Sarah Peterson's contributions and assistance with this project. We are grateful for funding provided by the UNLV Urban Sustainability Initiative (Graduate Fellowship), NSF-EPSCoR (SEPHAS Fellowship Program), NASA-EPSCoR, the Geological Society of America Student Grant Award Program, the Farouk El-Baz Student Research Program, the ExxonMobil Student Research Program, UNLV Geoscience Scholarship Fund, and UNLV Graduate & Professional Student Association. Thanks to the UNLV Environmental Soil Analysis Laboratory (especially Yuanxin Teng), the UNLV EMIL Lab (Sean Mulcahy), Lloyd Stark, and Andrew Hanson for lab support. We also thank Jon Egelin, John Brinda, Scott Abella, Bruce Lund, Seth Page, Ben Williams, Craig Westenberg, Colin Robins, Peg Rees, Steve Rowland, Jayne Belnap, Roger Rosentreter, Becki Huntoon, Crystal Erickson, Anton Westenveld, Clay Crow, and David Charlet for their assistance and scientific advice on this project.

References

Belnap, J., 1994, Potential role of cryptobiotic soil crust in semiarid rangelands, in: Monsen, S.B., Kitchen S.G., eds., Proceedings – Ecology and Management of Annual Rangelands: Ogden, UT, USDA Forest Service, Intermountain Research Station, p. 179-185.

Belnap, J., 1995, Surface disturbances: their role in accelerating desertification: Environmental Monitoring and Assessment, v. 37, p. 39-57.

Belnap, J., Budel, B., Lange, O.L., 2003, Biological soil crusts: characteristics and distribution, in: Belnap, J., and Lange, O.L., eds., Biological Soil Crusts: Structure, Function, and Management, v.150: Berlin, Springer, p. 3-30.

Belnap, J., Kaltenecker, J., Rosentreter, R., Williams, J., Leonard, Eldridge, D., 2001, Biological Soil Crusts: Ecology and Management, Technical Reference 1730-2: Denver, CO, U.S. Department of the Interior, 118 p.

Eldridge, D.J., Greene, R.S.B., 1994, Microbiotic soil crusts: A review of their roles in soil and ecological processes in the rangelands of Australia: Australian Journal of Soil Research, v. 32, p. 389-415.

Friedmann, E.I. and Galun, M., 1974, Desert algae, lichens and fungi, in: Brown, G.W., ed., Desert Biology: New York, Academic Press, p. 165-212.

Jones, C.G., Lawton, J.H., Shachack, M., 1997, Positive and negative effects of organisms as physical ecosystem engineers, Ecology, v. 78, p. 1946-1957.

Williams, A., Buck, B., Soukup, D., Merkler, D., 2010, Geomorphic controls of biological soil crust distribution, Mojave Desert (USA), Proceedings from the 19th World Congress of Soil Science, 1-6 August, 2010, Brisbane, Australia.

Field Trip Schedule

3:00 p.m.	Return to Buses & Depart	Take I-15 south to Las Vegas
4:30 p.m.	Arrive	Embassy Suites

Acknowledgments

Special thanks to Jack de Golia for formatting assistance and advice on guidebook layout.